CHARACTERISATION AND PALEOCLIMATIC SIGNALS WITHIN TEPHRIC LOESS DEPOSITS AGED BETWEEN C. 33 TO 9.5 CAL KA IN THE ROTORUA AREA, NORTHERN NEW ZEALAND

A thesis
submitted in partial fulfillment
of the requirements for the degree
of
Master of Science in Earth Science
at
The University of Waikato
by
KERRI LANIGAN

KO TE TANGATA

THE UNIVERSITY OF
WAIKATO
Te Whare Wānanga o Waikato

The University of Waikato
2012

Abstract

I studied tephric loess deposits aged between c. 33 and 9.5 cal ka in the Rotorua region, north-east central North Island. I produced a stratigraphic framework for the loess deposits and characterised them using a range of field and laboratory methods to develop a multi-proxy paleoclimatic reconstruction for the region. A number of key tephra marker layers, including Kawakawa (c. 25.4 cal ka), Te Rere (c. 25.2 cal ka), Okareka (c. 21.9 cal ka), Rerewhakaaitu (c. 17.5 cal ka), Rotorua (c. 15.6 cal ka), Waiohau (c. 13.6 cal ka) and Rotoma (c. 9.5 cal ka) tephras, were used as isochronous tie-points within the loess deposits and to provide ages within the loess. In contrast to those of previous studies, the findings from my study suggest that loess deposition continued at some sites in the Rotorua region until c. 9.5 cal ka. The average rate of loess accumulation was about 2.3 cm per century. The thickest loess sequence deposited between c. 33 and 9.5 cal ka was about 4.3 metres (tephra-free thickness) at Dansey Rd. In general, the tephric loess deposits are largely massive, silty and often yellowish brown, dull yellowish brown or dull yellow orange in colour (Munsell colour codes 10YR 5/4, 5/6, 5/8 or 6/4). Paleoclimate proxy analyses of the loess included grain size, accumulation rates, phytolith analysis, magnetic susceptibility, total carbon content, carbon isotopes and potassium content.

The results from my study suggest that the Rotorua region underwent a change from relatively warm, wet and less windy interstadial conditions to relatively cold, dry and more windy stadial conditions (indicative of the beginning of the extended-last glacial maximum) at c. 25.4 cal ka (about the time of deposition of the Kawakawa Tephra). Between c. 25.4 and 18.4 cal ka, stadial conditions likely dominated, although climate was also variable, and results suggest that two short-lived interstadials, centred around c. 23 cal ka and c. 21 cal ka, may have occurred. Stadial conditions appear to have ended at c. 18.4 cal ka when conditions became relatively warmer, wetter and less windy (likely indicative of last glacial – interglacial transition conditions). However, during these

warming conditions, between c. 13.8—12.8 cal ka, results suggest that conditions became temporarily relatively cooler and drier (indicative of the late glacial reversal). In general, there is good support from the New Zealand climate event stratigraphy (CES) (D.J. Barrell and others in preparation. “The sequence of climatic events in New Zealand over the past 30 000 years – a composite stratotype for regional correlation and comparison.” *Quaternary Science Reviews* [Australasian INTIMATE issue]) and other North Island paleoclimate records for these three broad changes in climate from interstadial to stadial and back to interstadial (and possibly interglacial) conditions during this time. However, the exact timing of these broad changes as well as that of the shorter-lived climatic variations are not perfectly synchronised with the timing of similar changes in the CES and other North Island records.

Acknowledgments

I would like to express my thanks and appreciation to my chief supervisor Professor David Lowe for his constant support, guidance and enthusiasm throughout this project. I have really appreciated his thoughtful encouragement and his willingness to make time for me and to reply to my many emails, even while abroad. I am also grateful for his immense help with revision and editing of this thesis. He has been a wonderful supervisor and it has been my privilege to study under him.

I would like to acknowledge the support that Will Esler, co-supervisor, has provided me with during this project. Will selflessly put many, many hours into assisting with field work, help with scouting out field sites, scraping down soil profiles, scaling ladders and sharing interesting stories! I would also like to thank Will and his family for the very generous hospitality they extended to me during my field work. Will also shared and allowed me to use some of his unpublished work and knowledge of Rotorua geology. My thanks also go to Will for all his help with the revision and editing of this thesis.

I would also like to thank Dr Adrian Pittari, co-supervisor, for his help, guidance and time he has given to this project. In particular, I would like to acknowledge his help with field work and thesis revision and editing.

Many technicians have generously assisted me during this project. I would like to thank Janine Ryburn for her advice in sample preparation, general use of the soil laboratory and friendly chats. I thank Anjana Rajendram and the Waikato Stable Isotope Unit for total carbon and nitrogen analysis and carbon and nitrogen isotope analysis. I thank Annette Rogers for help with grain size and XRF analysis. I thank Chris McKinnon for help with grain size analysis. I also thank Associate Professor Roger Briggs for his input into XRF analysis. I thank Helen Turner for her assistance with the Scanning Electron Microscope to obtain phytolith images.

I am grateful to Dr John Carter for his enormous help with the phytolith analyses, including laboratory work, guidance in interpretation of results and logistical support whilst in Wellington. I would also like to thank Dr Peter Almond for his helpful comments and guidance with interpretation of the phytolith results.

I thank Dr Karyne Rogers and Associate Professor Chris Hendy for comments and discussion regarding carbon and nitrogen isotope results.

I also thank Associate Professor Louis Schipper for discussion regarding total carbon and nitrogen results.

I would like to acknowledge Drs David Barrell and Peter Almond for allowing me to use the unpublished “New Zealand Climate Event Stratigraphy” paper, the writing of which they are leading coordinating and leading.

I would like to acknowledge finical support which I have received during this project, including a University of Waikato Masters Research Scholarship, monetary contribution from the Broad Memorial Fund, Study Link Bonded Merit Scholarship, funding from Professor David Lowe, University of Waikato Earth and Ocean Sciences department funding towards total carbon and nitrogen analysis and carbon and nitrogen isotope analysis and purchase of a MagRock magnetic susceptibility meter. Thanks are due to Dr Dave Campbell for facilitating this department funding.

My thanks go to Mrs Sydney Wright for all her administrative help during my time at university.

I would also like to thank friends and colleagues who have supported me during this project. I thank Kirsty for the privilege of her great friendship, support and baking and knowing the answer to (just about) anything! I thank Danielle for her loyal friendship and support throughout Master's and the outdoor lunch days! I also thank my office buddies: Serena, David and Alice – I have appreciated their willingness to help and friendly and caring natures. All the very best to you all.

I would also like to thank David and Robyn Denny for their generous and friendly hospitality while under taking field work in Rotorua.

My thanks and love go to my family for the huge amount of support they have given me throughout this project and all my university study. I appreciate the belief my family has in me, and their encouragement with gems of wisdom. I am also grateful for the help of Dad, Mum, Aaron and Monique with field work as well as the use of a vehicle and other gear for field work. I would also like to thank Dad for his time to help out with editing. To my whole family…thank you very, very much!!

Aroha nui and God's blessings to you all.

Table of Contents

Chapter 1 Introduction

1.1 Introduction to topic

This thesis focuses on reconstructing the paleoclimate of the last glaciation in the Rotorua region of New Zealand, though detailed analysis and characterisation of tephric loess. This study is the first detailed laboratory-based work on Rotorua tephric loess of this age to be carried out since Benny *et al.* (1988). Investigation for climatic signals in tephric loess was performed using a range of paleoclimatic proxies.

This chapter includes a summary of loess in New Zealand and an outline of the geology and geomorphology of the Rotorua area. An introduction to paleoclimatic studies in New Zealand spanning the past c. 30 calibrated (cal) ka, the role of tephras in such studies and a summary of paleoclimatic reconstructions in the wider Rotorua area is given. Following this is an outline of the field area for this study. The aims of this study are also outlined followed by a summary of the structure of this thesis and a list of abbreviations.

1.2 Loess and pedogenesis

Loess can be defined as “any fine-textured deposit of aeolian origin other than sand dunes or tephra” (Eden & Hammond, 2003). Loess was first documented in New Zealand by Julius von Haast in 1878 at Banks Peninsula, Christchurch (Lowe *et al.*, 2008a). Extensive loess deposits occur in the southern and eastern South Island and in the southern North Island of New Zealand (Figure 1.1) (Eden & Hammond, 2003). It is estimated that at least 10% of New Zealand’s land surface is covered by loess deposits of at least 1 m in thickness (Eden & Hammond, 2003).

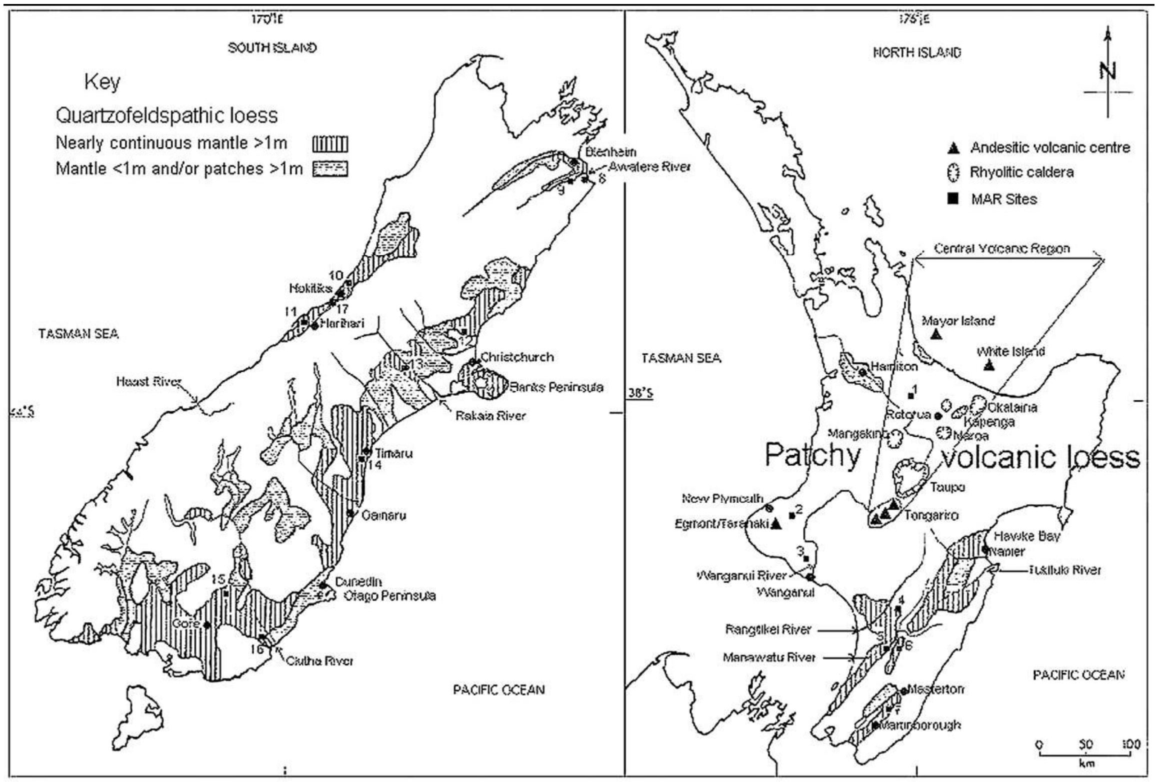

Figure 1.1 Loess distribution in New Zealand (Eden & Hammond, 2003).

In general terms, two main types of loess occur in New Zealand: mountain loess and tephric/volcanic loess (Eden & Hammond, 2003). Mountain loess has formed mostly as a result of dust produced mainly during river aggradation by abrasion as well as freeze/thaw and possibly grinding by glacial activity (Eden & Hammond, 2003; Lowe *et al.*, 2008a). The sources for tephric loess in the central North Island have mostly been produced from the erosion of volcanoes within the Taupo Volcanic Zone and Taranaki area and the re-working of tephras (Lowe *et al.*, 2008a). Benny *et al.* (1988) suggested that re-worked tephra has been the main source of these loess deposits. Vucetich & Pullar (1969) were probably the first to document tephra-related loess deposits in the central North Island region. Benny *et al.* (1988) showed that grain-size and sorting characteristics of some tephric loess deposits in the North Island were largely controlled by the grain-size of the main source-tephra of the loess. Hill (1999) presented a revised stratigraphy of the cover bed sequence on the Mamaku Plateau which included a number of tephra marker beds as well as tephric loess deposits. In general, loess accumulation in New Zealand increased around the time of the Last Glacial Maximum possibly as a result of an increase in sediment supply due to increased erosion of sparsely vegetated landscapes, aggrading river flood plains and a lowered sea level; drier climatic conditions; and possibly an enhanced southerly/south-westerly wind system (Lorrey *et al.*, in press). The degree to which loess deposits are influenced by post-depositional alteration can be viewed as “competition” between the rate of loess accumulation and pedogenesis governed by prevailing climatic and other conditions under which the loess was deposited (Verosub *et al.*, 1993; Almond & Tonkin, 1999; Lowe & Tonkin, 2010). For example, loess deposited during cold glacial conditions (i.e. MOIS (marine oxygen isotope stage) 2, 6, 8) when loess accumulation rates were relatively high will show only weakly altered/developed soil features (Figure 1.2) (Lowe & Tonkin, 2010). This is because the constant but slow accumulation of loess at the soil surface restricts the affects of topdown pedogenesis so that the loess, at any point in time, is not exposed long enough to surface-dominated pedogenic processes for strong soil horizon development to occur before being buried by further loess accumulation (Lowe & Tonkin, 2010). In this situation the land surface is slowly rising with loess accumulation and so with time deeper loess deposits gradually become increasingly isolated from surface process, in particular the organic cycle (Lowe & Tonkin, 2010). However, a change to less glacial climatic conditions (i.e. MOIS 1, 5, 7), during which loess deposition is minimal or stops altogether, will result in loess deposits which have more strongly developed soil features because the effects of topdown pedogenesis are not hindered as much by the gradual burial by loess and hence rising land surface and climatic and other conditions are more favourable for soil development (Figure 1.2) (Lowe & Tonkin, 2010). The land surface elevation in this situation stays constant. A characteristic feature of loess deposits is that every part of the sequence has been an A horizon at one time and so has pedogenic features throughout the sequence to a greater or lesser extent (Figure 1.2) (Lowe & Tonkin, 2010).

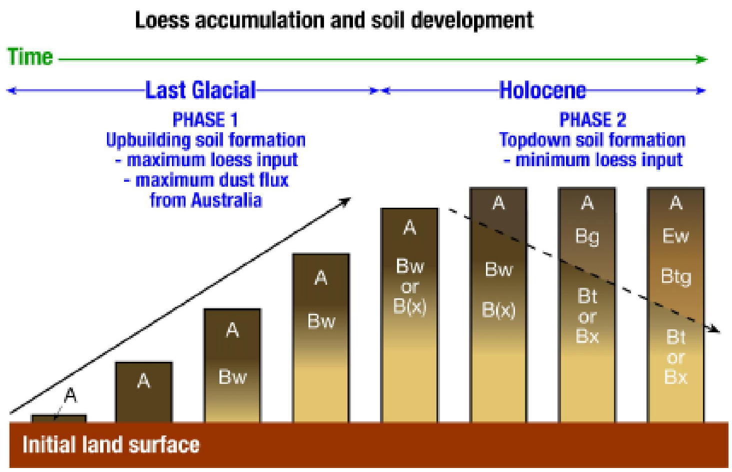

Figure 1.2 Model contrasting upbuilding pedogenesis (dominant during the Last Glacial) resulting in weakly developed soil features with topdown pedogenesis (dominant during Holocene) resulting in more strongly developed soil features (Lowe & Tonkin, 2010).

1.3 Geology and geomorphology of the Rotorua area

1.3.1 Introduction

In the North Island a blanket of younger volcanic and sedimentary rocks has mostly covered greywacke basement rocks (Mortimer, 2008). For the most part, the volcanic cover rocks and deposits of the North Island have been produced by volcanism in response to subduction of the Pacific Plate beneath the Australian Plate (Cole *et al.*, 2008). Subduction-related volcanism has been responsible for producing the Northland Arc, Coromandel Volcanic Zone, Kiwitahi Volcanics, Mangatatari Volcanics, Alexandra Volcanic Group, Taranaki Volcanic Lineament and the Taupo Volcanic Zone (Cole *et al.*, 2008). Features of the Taupo Volcanic Zone are summarised below.

1.3.2 Taupo Volcanic Zone (TVZ)

The TVZ has been the dominant source of young (c. 2 Ma—present) volcanic activity in New Zealand (Wilson et al., 1995) and noted as "the most productive and frequently active Quaternary silicic volcanic area on Earth" (Wilson *et al.*, 2009) . The TVZ is oriented northeast-southwest and extends from White Island in the Bay of Plenty to Ohakune in the central North Island. The dominant fault set of the TVZ strikes northeast-southwest (Milner *et al.*, 2002). The TVZ includes 9 rhyolite calderas (Taupo, Whakamaru, Ohakuri, Maroa, Mangakino, Kapenga, Reporoa, Okataina and Rotorua) (Figure 1.3) and multiple andesite centres (Tongariro Volcanic Centre, White Island, Mt Edgecumbe, Whale Island and Manawahe) (Lowe, 2010), many of which form prominent landforms in the central North Island. Taupo and Okataina volcanic centres account for most of the rhyolitic eruptions from TVZ which have occurred in the last 65 cal ka (59 out of 64 eruptions) (Wilson & Leonard, 2008; Wilson *et al.*, 2009; Leonard *et al.*, 2010). Figure 1.4 shows a summary of tephras erupted from these two centres during the last c. 61 cal ka. No large-volume eruptions have been generated from the Rotorua Volcanic Centre during the last 65 cal ka, but it was responsible for producing at least one widespread ignimbrite deposit in the vicinity of the field area (Wilson et al., 1984) c. 230—220 cal ka (Milner *et al.*, 2003). The activities of the Taupo, Okataina, and Rotorua volcanic centres are summarised below.

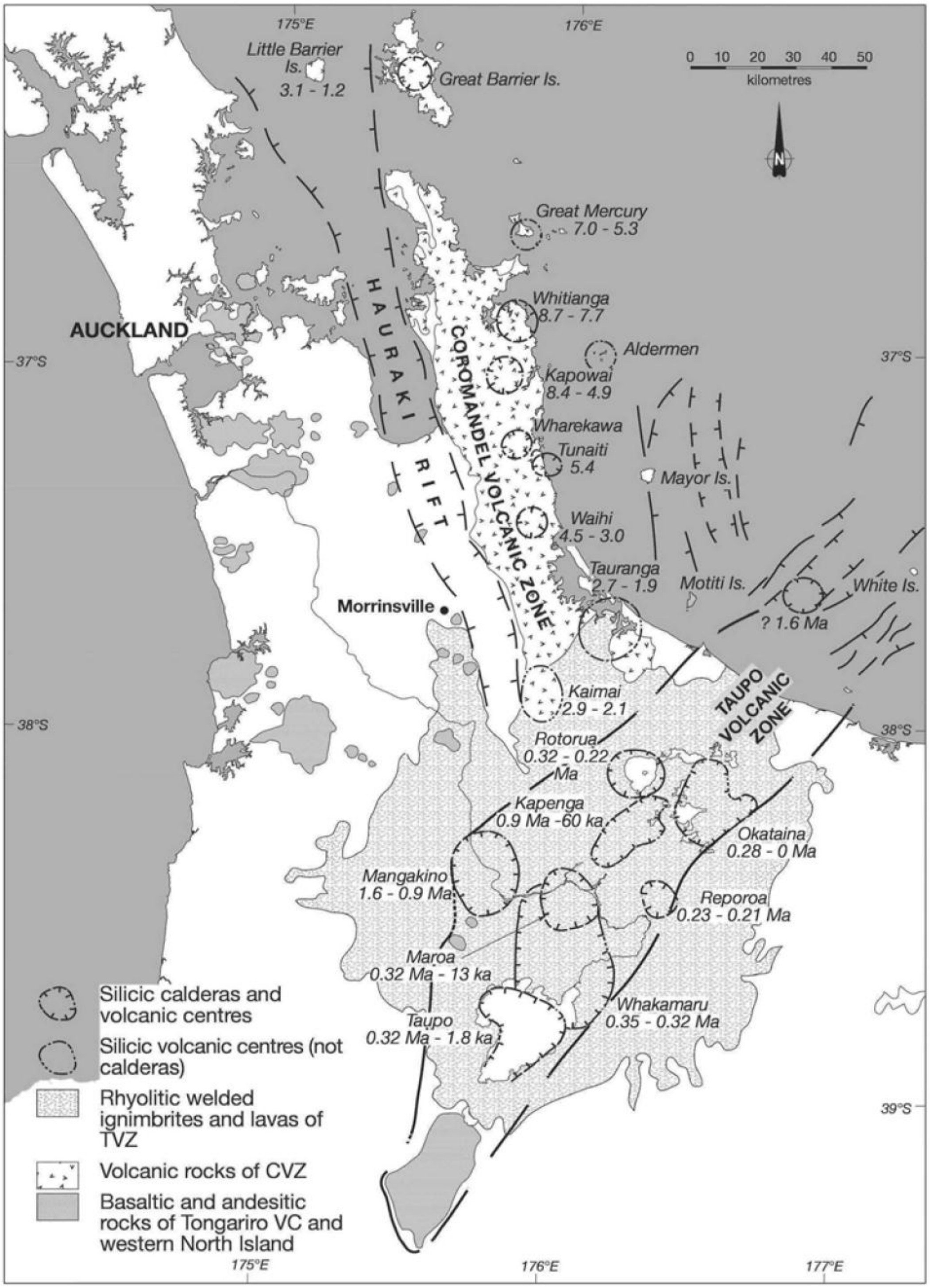

Figure 1.3 Map showing location and age of activity of 8 of the 9 rhyolite calderas of the Taupo Volcanic Zone (TVZ). Ohakuri caldera not shown (Briggs *et al.*, 2005).

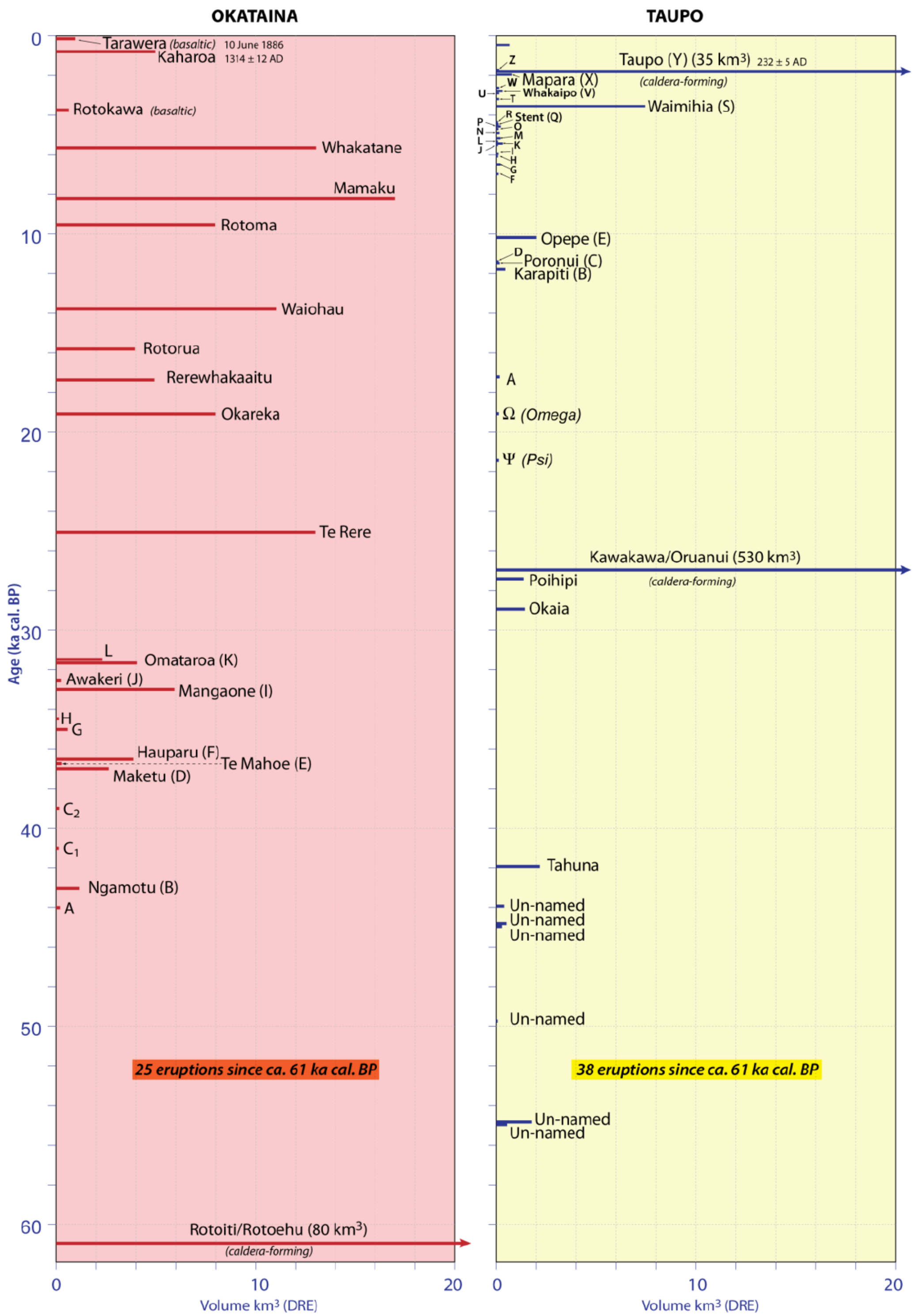

Figure 1.4 Summary of tephras, by age and volume, erupted from Okataina and Taupo volcanic centres during the last c. 61 cal ka (DRE = dense-rock equivalent) (from Lowe 2011, after Wilson et al., 2009).

1.3.3 Taupo Volcanic Centre (TVC)

The TVC located at the southern end of the TVZ, has been active since c. 320 cal ka (Wilson *et al.*, 1995) and since c. 61 cal ka has produced at least 38 eruptions (Lowe *et al.*, 2011). The largest eruption from the TVC since c. 61 cal ka has been the Kawakawa eruption (c. 25.4 cal ka (Vandergoes *et al.*, 2011)) which was responsible for the formation of the caldera in which modern Lake Taupo now partially occupies (Wilson, 2001a). The super-eruption also generated significant fall and pyroclastic density current deposits (Wilson, 2001a). Kawakawa Tephra is widespread throughout the North Island (Wilson, 2001a) and much of the South Island (Lowe *et al.*, 2008b) and has been found as far as Chatham Islands (Holt *et al.*, 2010). Another significant caldera-forming eruption from the TVC was the Taupo eruption which occurred c. 232 ± 5 AD (Hogg *et al.*, in press). Multiple smaller eruptions have also been generated by the TVZ (Figure 1.4).

1.3.3.1 Okataina Volcanic Centre (OVC)

The OVC, located at the north east end of the TVZ, has been active since c. 280 cal ka (Wilson *et al.*, 1995) and since c. 61 cal ka has produced 25 eruptions (Lowe, 2011). Of these 25 eruptions, the largest caldera forming and ignimbrite producing event was the Rotoiti/Rotoehu eruption (Wilson *et al.*, 1984) which occurred c. 61 cal ka (Lowe, 2011). Multiple smaller-volume eruptions from the OVC, of interest to this study, include Te Rere, Okareka, Rerewhakaaitu and Rotorua (Figure 1.4). The most recent eruption from OVC was the basaltic eruption of Mt Tarawera in 1886. The OVC has two linear vent zones where magma erupted as lava has built up to produce Mt Tarawera and Mt Haroharo (Wilson & Leonard, 2008). Another notable geomorphic feature of the OVC is the multiple lakes which have developed within and around the centre mostly in response to landscape changes associated with volcanic activity (Lowe & Green, 1992)

1.3.3.2 Other geomorphic features of the Rotorua area

A notable lake terrace at c. 380 m asl occurs around Lake Rotorua and is thought to have formed some time between the deposition of the Mangaone Tephra and Unit L, although there is also strong stratigraphic evidence for at least five other previous high-stands; the highest of which is at about 420 m asl (Esler, 2010, W. Esler, pers. comm., 2012, and unpublished data). The Mamaku plateau, underlain by the Mamaku Ignimbrite and earlier ignimbrites, is a very prominent geomorphic feature west of Lake Rotorua that covers an area of c. 1,800 km^2 and has a peak elevation of c. 600 m (Kennedy, 1994). The plateau ends abruptly in the south forming the Horohoro Bluffs. In the east the plateau is dissected by a number of paleolake terraces and it has shallow sloping sides at its northern and western boundaries (Kennedy, 1994). Prominent features of the plateau include deeply incised valleys, especially on the plateau's western side, and remnant ignimbrite "tors" up to 10 m high around the plateau summit (Kennedy, 1994; Esler, 2010).

1.3.4 Cover beds of the Rotorua area

Eruptions from the TVZ have been responsible for producing tephras which, along with tephric loess deposits and some lake sediments (W. Esler pers. comm., 2010) form most of the coverbed sequence in the Rotorua area (Vucetich & Pullar, 1969). In the Rotorua area, tephric loess deposits commonly occur stratigraphically between the Okaia and Rerewhakaaitu tephras (Newnham *et al.*, 2003) indicating an age of c. 30—17.5 cal ka (Lowe *et al.*, 2008b) (i.e. during MOIS 2). During this time it appears glacial conditions prevailed in the Rotorua area as indicated by the presence of the tephric loess and stratigraphic evidence of erosion and weak soil development (McGlone *et al.*, 1984; Newnham *et al.*, 2003). The Rerewhakaaitu Tephra appears to approximately mark the boundary where post-eLGM climatic warming began in the Rotorua area and elsewhere, indicated stratigraphically by increased landscape stability and enhanced soil development and by data from pollen percentage curves etc. (Newnham *et al.*, 2003).

Lake sediments, subaerially deposited between Unit L and pre-Kawakawa tephric loess have been noted in the Rotorua basin (W. Esler, pers. comm., 2012) indicating a rise of Lake Rotorua to >30 metres above present level. This rise was apparently due to impeded subsurface drainage by the Unit L pyroclastic flow. Between the interval of Unit K and Unit L, Lake Rotorua fell from 380 m asl to below 280 m asl (and possibly drained completely) as a result of surface drainage through the present Lake Rotoiti (Okere Arm) and groundwater seepage. Okaia Tephra and Poihipi Tephra were deposited during the deposition of the post-Unit L lake sediments, however, these lake sediments were mostly eroded soon after the breakout and drainage of the lake eastward into the “Rotoiti River” (W. Esler pers. comm., 2012, and unpublished data).

Various tephras of late Pleistocene and Holocene age, including the Taupo Tephra and, close to source often conspicuous, Rotorua Tephra, form the upper part of the coverbed sequence in the Rotorua area (Vucetich & Pullar, 1969).

1.4 Introduction to paleoclimatic reconstruction

Climatic information from instrumental data is limited to about the past ~200 yrs and so it is necessary to use other records to recover climatic information from the deeper past (Carter, 2008). A variety of ‘stand-in’ records otherwise known as ‘proxies’, including diatoms, pollen, position of glacial deposits, isotope composition of speleothems, various chemical and physical properties of lake sediments and many more, have been used in place of instrumental data to reconstruct paleoclimatic information greater than ~200 yrs old (Alloway *et al.*, 2007).

In New Zealand, new paleoenvironmental reconstructions spanning the past c. 30 cal ka have been undertaken recently as part of the NZ-INTIMATE project (Alloway *et al.*, 2007). NZ-INTIMATE ("INTegration of Ice-core, Marine and Terrestrial records") is a subgroup, along with OZ-INTIMATE, of the Australasian-INTIMATE group, which in turn is part of the wider INQUA Paleoclimate Commission (Alloway *et al.*, 2007). The focus of NZ-INTIMATE and OZ-INTIMATE is to bring together high-resolution paleoclimatic data from New Zealand and Australia, respectively, and subsequently form a "Climate Event Stratigraphy" (CES) spanning ~30—8 cal ka (Alloway *et al.*, 2007; Newnham *et al.*, 2007a; Lowe *et al.*, 2008b; Barrell *et al.*, in prep.). The latest provisional CES for New Zealand spanning the past c. 30, 000 yrs based on multiple paleoclimatic reconstructions is presented in (Barrell *et al.*, in prep.)(Figure 1.5). Within this CES, four key climatic divisions have been recognised: 1) *Preceding interstadial*, 2) *Last Glacial Coldest Period (LGCP) or extended Last Glacial Maximum (eLGM)* (Newnham *et al.*, 2007b), 3) *Last Glacial-Interglacial Transition (LGIT),* and 4) *Holocene Interglacial*. Type records for most of these key divisions are outlined in (Barrell *et al.*, in prep.). Climatic variability (events) within most of these divisions has also been recognised.

The first climate division of the CES, 1) *preceding interstadial*, is characterised by warm climatic conditions (event 10w). The base of this division is not defined. The transition from the first division (*preceding interstadial)* into the second division (*LGCP/eLGM)* occurs at c. 28.9 cal ka.

The second division of the CES, *LGCP/eLGM,* spans c. 28.9—18.4 cal ka and is mainly dominated by cold climatic conditions, (events 9c, 7c and 5c), with two relatively warmer events (events 8w and 6w). Division two includes the Last Glacial Maximum (LGM) *stricto sensu,* defined as 21 ± 2 or 3 cal ka (Mix *et al.*, 2001) and later re-defined as 26.5—20/19 cal ka (Clark et al., 2009) based predominantly on Northern Hemisphere records. Regarding the cause of the difference in timing of LGM onset and duration between the Northern and Southern hemispheres, Vandergoes *et al.* (2005) suggested "that Southern

Hemisphere insolation may have been responsible for these differences in timing”. Termination 1 occurs at c. 18.4 cal ka and marks the change from division two to division three of the CES.

The third division of the CES, *LGIT*, spans c. 18.4—11.8 cal ka and includes a time of transitional climate conditions (event 4t), followed by warmer conditions (event 3w), and then a switch to cooler conditions for a short time (event 2c) before changing to transitional conditions again (event 2t).

The final climatic division recognised in the CES is the *Holocene Interglacial* division which begins at c. 11.8 and continues until at least c. 8 cal ka, the younger limit of the CES time window. The *Holocene Interglacial* division is characterised by warm climatic conditions (event 1w) with at least two optimums (times of greatest warmth) recognised: the Early Holocene Optimum and the Mid-Holocene Optimum (outside the CES time window).

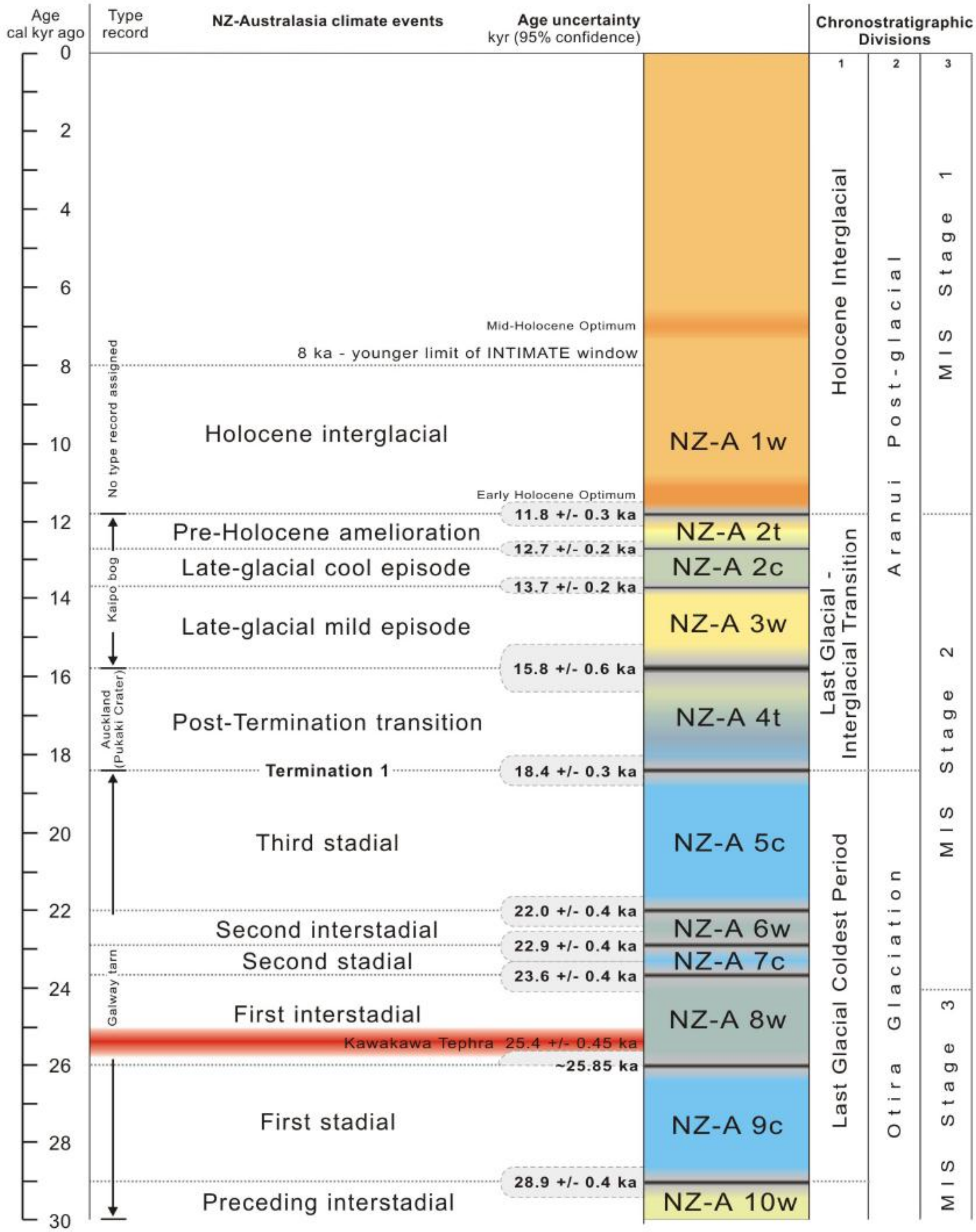

Figure 1.5 New Zealand provisional climate event stratigraphy (CES) for last c. 30, 000 yrs (Barrell *et al.*, in prep.).

1.4.1 Role of tephras in paleoclimatic reconstructions

Tephra is defined as “all the explosively-erupted, unconsolidated pyroclastic products of a volcanic eruption” (Lowe, 2011). The presence of tephra beds within paleoclimatic records can act as “time-parallel” marker beds, know as isochrons, allowing records from different locations to be linked and their ages constrained (Lowe *et al.*, 2008b). Such linkages can potentially aid in identifying and quantifying any differences in timing of paleoclimatic events between records (Lowe *et al.*, 2008b). The NZ-INTIMATE project draws on 22 marker tephras erupted from various North Island locations and generally occurring as widespread deposits (Table 1.1) (Lowe *et al.*, 2008b). In particular, the Kawakawa tephra, the result of a super-eruption from the Taupo Volcanic Centre, has been an important isochron in paleoclimatic studies as it is the only tephra which has been identified in both North and South Island paleoclimatic records as well as offshore records (Alloway *et al.*, 2007).

Table 1.1 Summary of the 22 marker tephras used in the NZ-INTIMATE project (adapted from Lowe *et al.,* (2008b)).

Tephra name	**Source**	**Age** **(Mid-point 2σ range) (cal. yr BP)**	**Magma volume** **(km^3)**	**References for proximal stratigraphy and Isopach maps** (see Lowe *et al.*, 2008b for references)
Taupo Volcanic Centre (rhyolitic)				
Taupo (Unit Y)	Taupo volcano	1718 ± 5^	13.4	Wilson and Walker (1985), Wilson (1993)
Whakaipo (Unit V)	Taupo volcano	2960 ± 190	0.24	Wilson (1993)
Waimihia (Unit S)	Taupo volcano	3410 ± 40	5.10	Wilson (1993)
Unit K	Taupo volcano	5120 ± 150	0.12	Wilson (1993)
Opepe (Unit E)	Taupo volcano	10,075 ± 155	1.40	Wilson (1993)
Poronui (Unit C)	Taupo volcano	11,190 ± 80	0.23	Wilson (1993)
Karapiti (Unit B)	Taupo volcano	11,140 ± 190	0.42	Wilson (1993)
Kawakawa/Oruanui	Taupo volcano	25,384 ± 220#	530	Wilson (2001), Manville and Wilson (2004), Wilson et al. (2006)
Poihipi	Taupo volcano	28,181 ± 383	0.5	

Okaia	Taupo volcano	29,713 ± 484#	3.0	Vucetich and Howorth (1976b)
Okataina Volcanic Centre (rhyolitic)				
Kaharoa	Tarawera linear vent zone	636 ± 12	5.0	Nairn (1989, 2002), Nairn et al. (2001), Shane et al. (2007b)
Whakatane	Haroharo linear vent zone	5530 ± 60	11.3	Nairn (2002), Kobayashi et al. (2005), Smith et al. (2006), Shane et al. (2007b)
Mamaku	Haroharo linear vent zone	8005 ± 45	13.0	Nairn (2002), Smith et al. (2006)
Rotoma	Haroharo linear vent zone	9,498 ± 48 #	8.0	Nairn (2002), Smith et al. (2006)
Waiohau	Tarawera linear vent zone	13,635 ± 165	3.3	Nairn (1989, 2002), Speed et al. (2002), Shane et al. (2002b)
Rotorua	Okareka basin	15,588 ± 435#	1.0	Nairn (2002), Smith et al. (2004), Shane et al. (2007b)
Rerewhakaaitu	Tarawera linear vent zone	17,461 ± 435#	5.0	Nairn (1989, 2002), Newnham et al. (2003), Darragh et al. (2006), Shane et al. (2007a)
Okareka	Tarawera linear vent zone	21,850 ± 360#	3.6	Nairn (1989, 1992, 2002), Darragh et al. (2006), Shane et al. (2007b)
Te Rere	Haroharo linear vent zone/Okareka basin	25,240 ± 900#	13.0	Nairn (1992, 2002)
Tuhua Volcanic Centre (peralkaline rhyolitic)				
Tuhua	Mayor Island	7005 ± 155	0.48	Houghton et al. (1992), Manighetti et al. (2003)
Tongariro Volcanic Centre (andesitic)				
Okupata	Mt Ruapehu	11,620 ± 190	0.07	Donoghue et al. (1995, 1999, 2007)
Egmont Volcano (andesitic)				
Konini	Mt Taranaki	11,720 ± 220	>0.003	Alloway et al. (2005)

^ = Hogg *et al*. (in press)

= D.J. Lowe, pers. comm., 2012 (*see Table 2.1 for details*)

1.5 Paleoclimatic reconstructions from the wider Rotorua area

A summary of previous paleoclimatic studies spanning c. 30—8 cal ka for the wider Rotorua area, although limited, is outlined below. McGlone *et al.* (1984) investigated the stratigraphy and carried out palynology studies in the Bay of Plenty to Gisborne area. They concluded that from the time of the Rotoehu Ash to Omataroa Tephra climate was dominated by cool interstadial conditions before a change at the time of the Omataroa or Kawakawa Tephra to much harsher conditions characterised by an unstable landscape which continued until the time of the Rerewhakaaitu or Waiohau Tephra. Newnham *et al.* (1989) examined the palynology from Waikato lake cores and established a climatic history for the area. For the period of time since about 20,000 years ago, they recognised three main climatic phases: (1) Last Glacial phase, where the environment was mainly unforested; (2) Late Glacial transitional phase, beginning just after Rerewhakaaitu Tephra, when forest quickly became re-established, and lasting until early Post-Glacial times, with climate continuing to become warmer and wetter; and (3) Early Post-Glacial phase, where climate reached maximum warm wet conditions. Later during this phase the occurrence of frosts and or droughts became more common and the environment became drier (Newnham *et al.*, 1989). Pickett (2008) examined Rotorua paleoclimate during the Holocene from a core from Lake Rotorua and McGlone (1983) presented Holocene-aged pollen diagrams from the Rotorua area.

1.6 Study location

The study field area is located in the wider Rotorua area in the Bay of Plenty region, North Island, New Zealand (Figure 1.6). The field area consists of thirteen main field sites distributed mostly to the north-west of the Rotorua lakes (and north-west of the OVC). Details of each of the field sites, including map references and approximate elevations, are given in Table 1.2. Field sites consist of profiles on road side cuttings, with the exception of Tapapa Rd site which is located on a farm track off Tapapa Road (Goodwin Farm). Field sites were chosen based on the presence and number of recognisable tephra layers (aged between c. 33—15 cal ka) within intervening loess deposits. Photographs of each of the field site are given in Appendix 1. Dansey Rd and Maniatutu Rd sites were the primary and secondary master field sites respectively for this study and most of the laboratory work was carried out from samples from these sites. These two sites were chosen as master sites on the basis of either all or most of the expected tephra layers being present and the intervening deposits of tephric loess being some of the thickest recorded in the field area meaning that the resolution of proxies could be maximised.

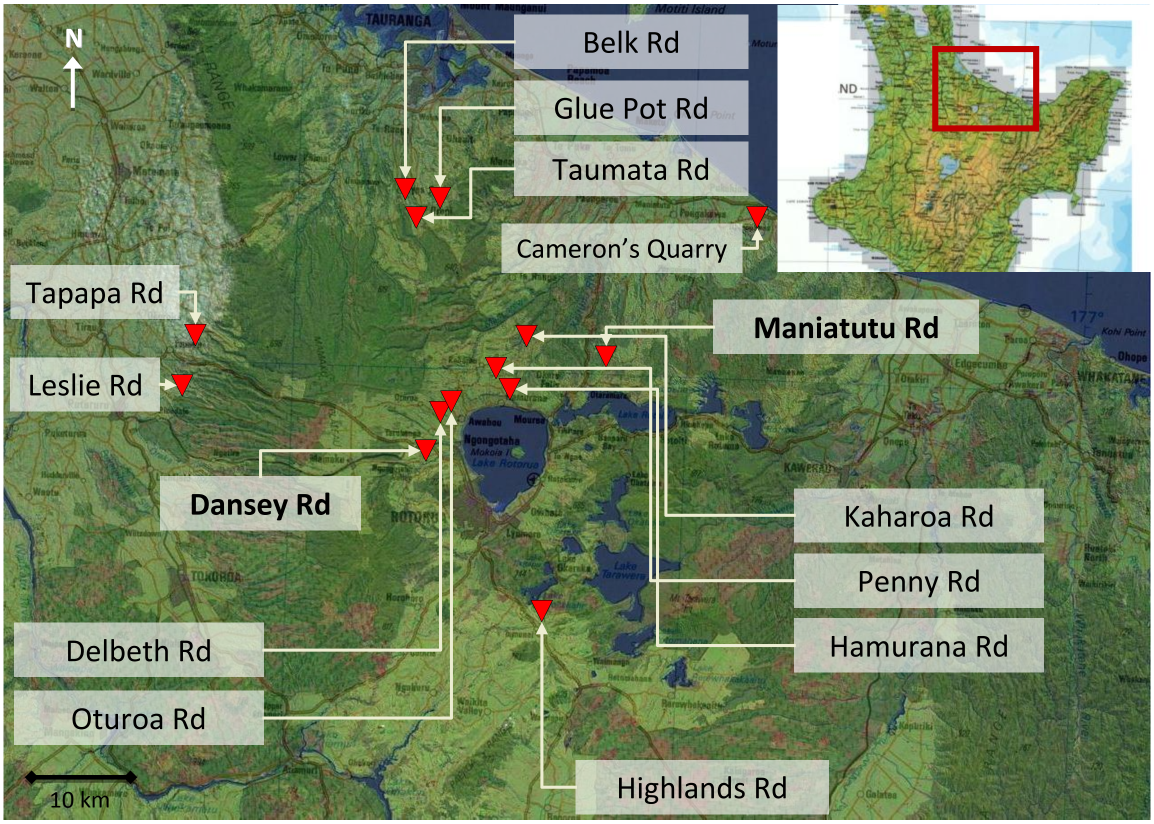

Figure 1.6 Map showing the location of the study field area and field sites (map inset shows the location of the study field area within the North Island of New Zealand)

Table 1.2 Details of field sites within this study, including map references and elevation data.

Field site details			
Site name	**Map reference** (NZMS 260)	**Approximate elevation** (nearest 10 masl)	**Notes**
Tapapa Rd	T15 524 634	250	Goodwin Farm
Leslie Rd	T15 688 453	420	
Belk Rd	U15 827 677	320	
Taumata Rd	U15 842 635	250	
Glue Pot Rd	U15 876 661	360	
Kaharoa Rd	U15 011 543	300	
Penny Rd	U15 966 498	400	
Maniatutu Rd	U15 078 496	340	Secondary master site
Hamurana Rd	U15 997 468	300	
Oturoa Rd	U15 893 462	380	
Dalbeth Rd	U15 880 435	340	
Dansey Rd	U15 858 408	410	Primary master site
Highlands Rd	U16 011 229	520	
Cameron's Quarry	V15 255 660	60	No formal stratigraphic description or analysis was carried out at this site

1.7 Aims of study

The aim of this study is to determine if there are past climate signals recorded in tephric loess spanning mainly from the eLGM to LGIT in the Rotorua region. In order to meet this aim a number of objectives have been developed:

- Characterise tephric loess and develop a tephra and tephric loess stratigraphic framework (using a tephra-based chronology) spanning c. 33—9.5 cal ka for the Rotorua region.
- Investigate tephric loess sequences spanning mainly c. 33—15 cal ka for evidence of paleoclimatic signals using a variety of biological, chemical and physical proxies:
    - Biological
        - opal phytoliths
    - Chemical
        - total carbon content of loess
        - carbon and nitrogen isotope values of loess
        - potassium and phosphorus content of loess
    - Physical
        - thickness of loess deposits
        - grain-size of loess
        - magnetic susceptibility and pedogenesis of loess

    (Note some analysis of loess deposits younger than c. 15 cal ka (i.e. up to the Rotoma Tephra aged c. 9.5 cal ka) were undertaken at Dansey Rd to investigate possible climatic amelioration following the LGIT)
- Compare any paleoclimatic signals found with other paleoclimatic records from New Zealand, including the CES of Barrell *et al*. (in prep.).

1.8 Structure of thesis

- In Chapter 1 of this thesis I have provided a broad introduction to the study topic, an overview of the geology and geomorphology of the wider study area, the location of the study area, the study aims and the structure of this thesis.
- In Chapter 2 I present the stratigraphy and chronology of the field area.
- In Chapters 3 and 4 I present and examine the results of various biological, chemical and physical paleoclimatic proxies used in this study:
    - phytoliths,
    - total carbon content of loess,
    - carbon isotope values of loess,
    - potassium and phosphors content of loess,
    - thickness of loess deposits,
    - grain-size of loess,
    - magnetic susceptibility of loess.
- In Chapter 5 I compare the results from the different proxies analysed in this study and develop a paleoclimatic stratigraphy for the study field area focusing on the timeframe between c. 33—15 cal ka although also extending to c. 9.5 cal ka. I also compare the results of this study with those of other New Zealand paleoclimatic studies including the CES of Barrell *et al*. (in prep.).
- In the final chapter, Chapter 6, I summarise the main findings of this study and suggest ideas for further study.

1.9 List of abbreviations

Table 1.3 shows a list of selected abbreviations used in this document.

Table 1.3 Selected abbreviations used in this document

c.	circa (around/about)
Kk	Kawakawa Tephra
Te	Te Rere Tephra
Ok	Okareka Tephra
Rk	Rerewhakaaitu Tephra
Rr	Rotorua Tephra
Wh	Waiohau Tephra
Rm	Rotoma Tephra
cal	calibrated (or calendar)
ka	thousand years
masl	metres above sea level
TVZ	Taupo Volcanic Zone
OVC	Okataina Volcanic Centre
DRE	dense rock equivalent
MOI	marine oxygen isotope
CES	climate event stratigraphy
eLGM	extended last glacial maximum
LGM	last glacial maximum
LGCP	last glacial coldest period
LGIT	last glacial-interglacial transition
RCES	Rotorua climate event stratigraphy
hpd	highest posterior density

Chapter 2 Stratigraphic framework and tephra-based chronology

2.1 Introduction

Tephric loess deposits in the Rotorua region aged between c. 33—9.5 cal ka include a number of rhyolitic tephra beds, mostly derived from the Okataina Volcanic Centre (OVC) (Smith *et al.*, 2002; Lowe *et al.*, 2008b). These tephras, dated elsewhere (Table 2.1), provide a chronological framework for the loess succession via tephrochronology.

In this study, 13 main sites were examined in the field and the tephric loess and intervening tephra layers of these sites were identified and described (see appendix 2 for detailed stratigraphic logs of each field site. Note that at Cameron's Quarry site the main stratigraphic units were noted but no formal stratigraphic description was undertaken. See also appendix 1 for photographs of each of the main field sites).

In this chapter I summarise the stratigraphy across the field area by firstly describing the age, source, distribution and lithology of the tephra beds, and secondly by describing the tephric loess deposits.
Figure 2.1 shows a general composite stratigraphic log for the entire field area. The individual stratigraphy of each at the thirteen field sites is shown in Figure 2.2.

Table 2.1 Summary of marker tephras present in the field area, aged between c. 33—9.5 cal ka.

Tephra name	**Tephra source** [a] (Lowe *et al.*, 2008b)	**Mid-point 2σ (^{14}C) age range** (cal yr BP) (Lowe *et al.*, 2008b)	**Mid-point 2σ (^{14}C) age range** (cal yr BP) (Augustinus *et al.*, 2011)	**This study** [c] (cal yr BP) (mid-point or mean age of 95% confidence range)
Rotoma	Okataina (HA)	9,505 ± 25	9,523 ± 11	9,498 ± 48
Waiohau	Okataina (TA)	13,635 ± 165	13,689 ± 95	13,635 ± 165[^#]
Rotorua (Rr)	Okataina (OB)	15,425 ± 325	15,824 ± 332	15,588 ± 435
Rerewhakaaitu (Rk)	Okataina (TA)	17,625 ± 425	17,913 ± 241	17,461 ± 435
Okareka (Ok)	Okataina (TA)	21,800 ± 500	21,862 ± 183	21,850 ± 360
Te Rere (Te)	Okataina (HA/OB)	25,271 ± 779	25,256 ± 446	25,240 ± 900*
Kawakawa (Kk)	Taupo (TP)	27,097 ± 957	27,282 ± 373	25,384 ± 220[□]
Okaia Tephra	Taupo (TP)	30,092 ± 340	29,435 ± 249	29,713 ± 484
Unit L	Okataina	33,000[b]		32,700 ± 1450

Notes:

a = OB: Okareka basin, TA: Tarawera linear vent zone, HA: Haroharo linear vent zone, TP: Taupo Volcano

b = Age from Allan *et al*. (2008).

c = Ages for Rotoma to Rerewhakaaitu tephras (excluding Waiohau Tephra) were derived by Bayesian age modelling using IntCal09 dataset and the age-depth modelling programme 'Bacon' (Blaauw & Christen, 2011) on the Kaipo bog sequence (Hajdas *et al.*, 2006). Ages are reported as mid-points of the 95% hpd confidence limits. Ages for Okareka to Unit-L tephras were derived by re-calibration of previous ages (terrestrial samples only) using IntCal09 (Reimer *et al.*, 2009) and OxCal4.1 (Ramsey, 2009a, 2009b) (D.J. Lowe pers comm., 2012). Ages are reported as mean ages in the 95.4% confidence range.

^ = age from Lowe *et al*. (2008b)

= Recently undertaken age modelling using IntCal09 dataset and the age-depth modelling programme 'Bacon' (Blaauw & Christen, 2011) on Kaipo bog sequence (Hajdas *et al.*, 2006) has resulted in an age for the Waiohau Tephra of 14,034 ± 143 cal BP (D. J. Lowe, pers. comm., 2012). As the modelling was undertaken near the end of this thesis preparation it has not been possible to adopt it here.

* = It is possible that this age may have been influenced by a component of "in-built" age in the sample material (wood) and hence may be too old. Note the large error.

□ = This revised age for the Kawakawa Tephra is based on re-calibration of 7 newly-dated samples pertaining to this eruption event (described by Vandergoes *et al*., 2011) using IntCal09 (Reimer *et al.*, 2009) and OxCal4.1 (Ramsey, 2009b, 2009a) (D.J. Lowe pers comm., 2012).

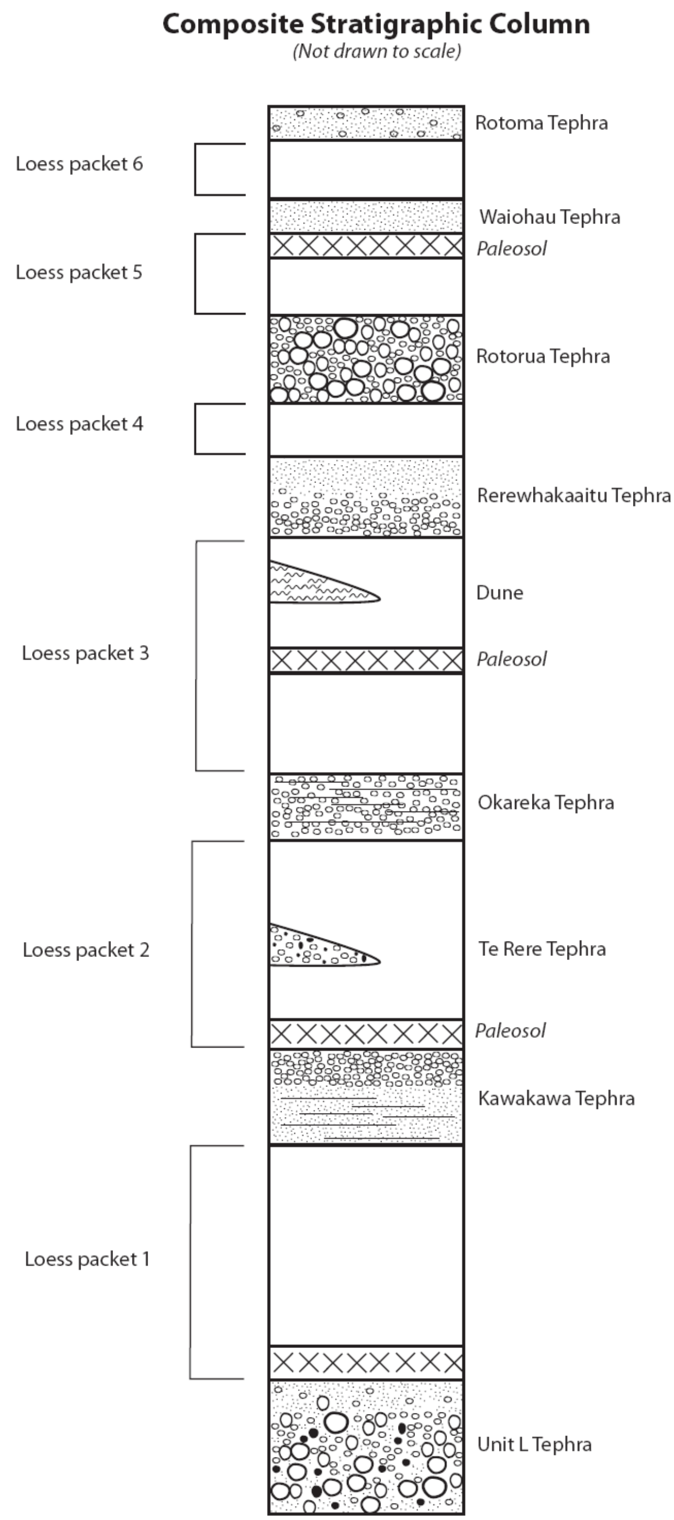

Figure 2.1 Generalised composite stratigraphic column for entire field area from Unit L to Rotoma Tephra. Note that there is a weak pedogenic imprint throughout the loess deposits but in some places enhanced imprints are recognised ("paleosols")

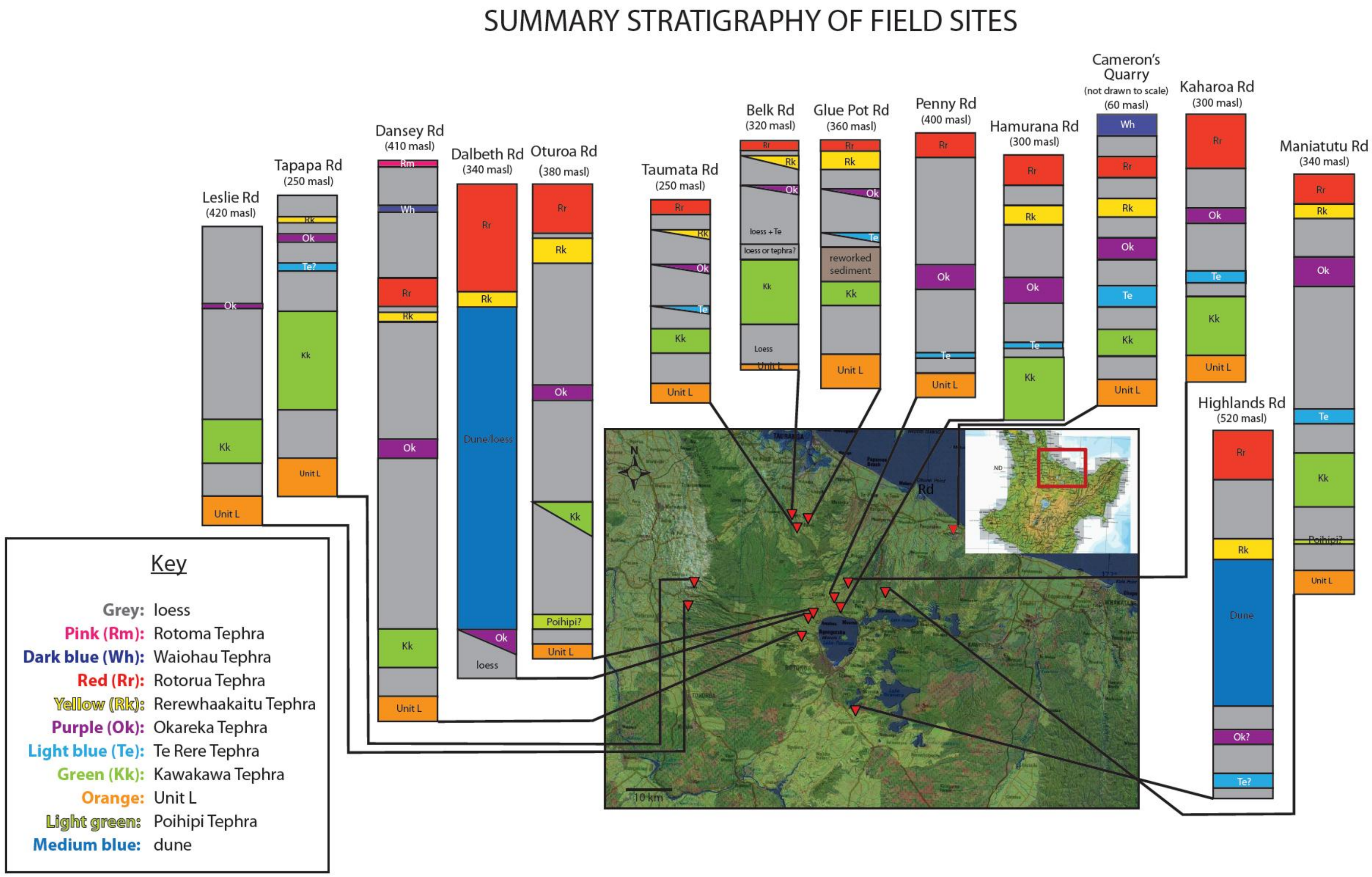

Figure 2.2 Diagram showing the location and stratigraphy of all field sites. All sites are linked via tephra marker beds. Note Unit L and Rotorua Tephra units are not drawn to scale

2.2 Unit L

2.2.1 Age, source and distribution

Smith *et al.* (2002) used the terms 'Omataroa' and 'Unit L' to describe the young Mangaone Subgroup pyroclastic fall and flow deposits (respectively) which had previously been termed 'Unit K' and 'Unit L' (respectively) by Jurado-Chichay & Walker (2000) and earlier as 'Omataroa Tephra Formation' by Howorth (1975). Jurado-Chichay & Walker (2000) suggested that the source of both Omataroa and Unit L tephras was the eastern side of the Okataina Volcanic Centre (OVC) (Puhipuhi basin). The distributions of Omataroa Tephra and Unit L are given in Figure 2.3. Omataroa Tephra was dated at c. 28,220 ± 630 yrs BP (error-weighted mean of three ^{14}C ages for the Omataroa Tephra) by Froggatt & Lowe (1990). Later, the Omataroa Tephra was dated at c. 33 ka (on the basis of the orbitally-tuned oxygen isotope age model of Ocean Drilling Programme Site 1123) by Allan *et al*. (2008). Calibration, using INTCAL09 and OxCal4.1, of the age given by Froggatt & Lowe (1990) gives an age of c. 32,700 ± 1450 yrs BP for the Omataroa Tephra (D.J. Lowe, pers. comm., 2011). This age is adopted in this study. Ages of other Mangaone Subgroup tephras are given in Froggatt & Lowe (1990). Subaqueously deposited Unit K has been noted in the Rotorua basin as 11—15 cm of vaguely stratified fine ash (W. Esler, pers. comm., 2012). In this study the distinction between the Omataroa Tephra and Unit L (of Smith *et al.* (2002)) was not made, hence the term 'Unit L' is used from here on to describe all material of upper Mangaone Subgroup origin. Unit L is present at least 11 out of the 13 field sites (the exceptions being at Dalbeth Rd, where the stratigraphic column was recorded to pre-Okareka loess only, and Hamurana Rd, where Kawakawa Tephra rests unconformably on coarse Rotoiti ignimbrite lithic lag breccia (including well-rounded clasts up to 1 m diameter) (W. Esler, pers. comm., 2010).

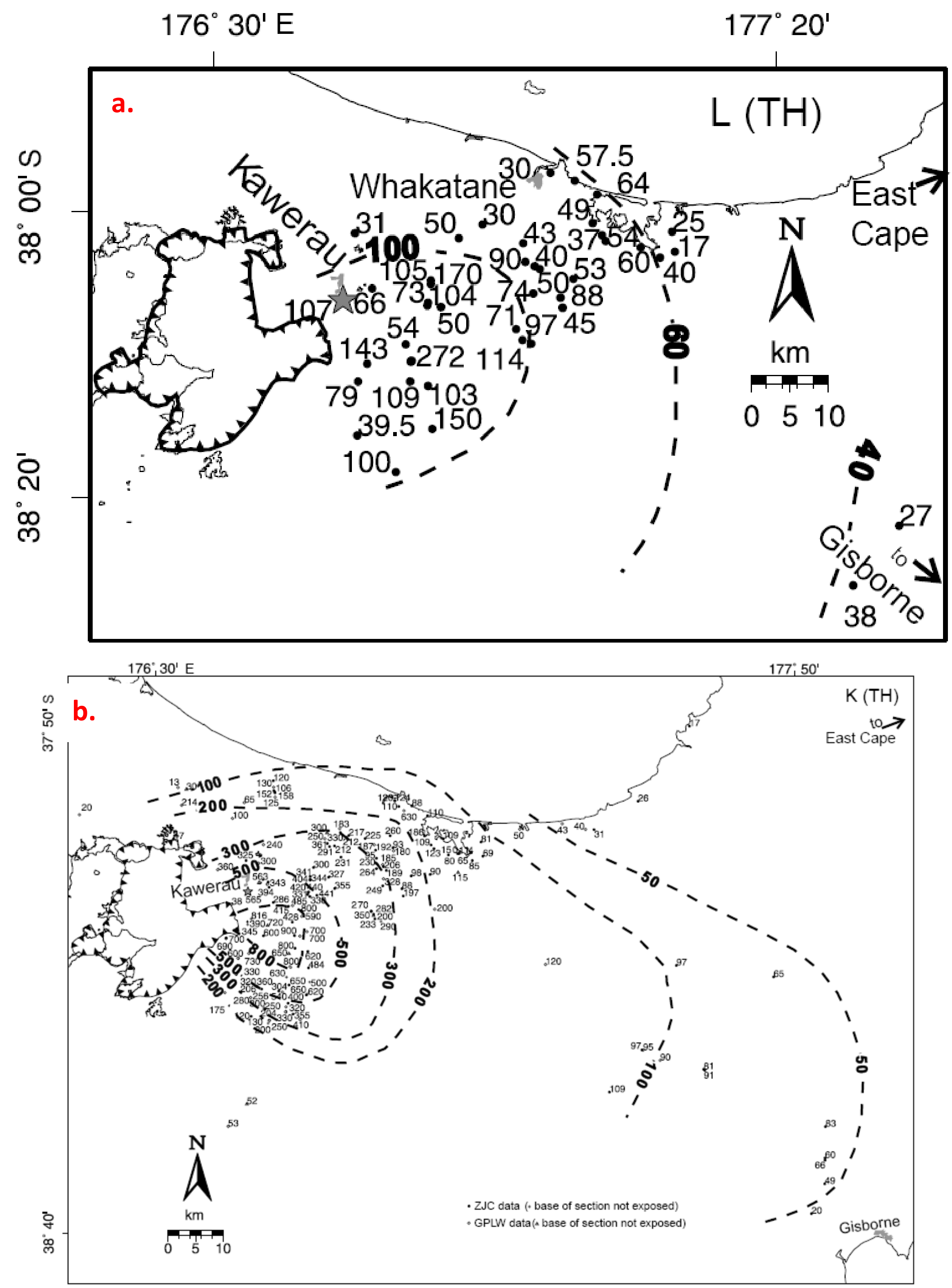

Figure 2.3 Isopach maps showing the distribution and thickness (in cm) of (a.) Unit K (Omataroa) and (b.) Unit L (Jurado-Chichay & Walker, 2000, pp. 358, 366)

2.2.2 Lithology

Unit L is well exposed at Kaharoa Rd where it grades upward from clast-supported cobble-sized clasts within a pebble-sized matrix to sand-sized grains (Figure 2.4) (grain-size based on Cas *et al.,* 2008). The unit is orange (Munsell colour 7.5YR 6/8), although variable throughout and becoming paler toward the top of the unit. Pumice clasts are soft, very fine-textured and weathered to orange on the outside and yellowish white on the inside. Hard, black lithic clasts are also present. Throughout the field area the upper matrix of Unit L tends to be clay/silt-sized. The heavy mineral assemblage of Unit L is dominated by hornblende and Fe-Ti oxides at Dansey Rd, and by hypersthene at Maniatutu Rd (Table 2.2).

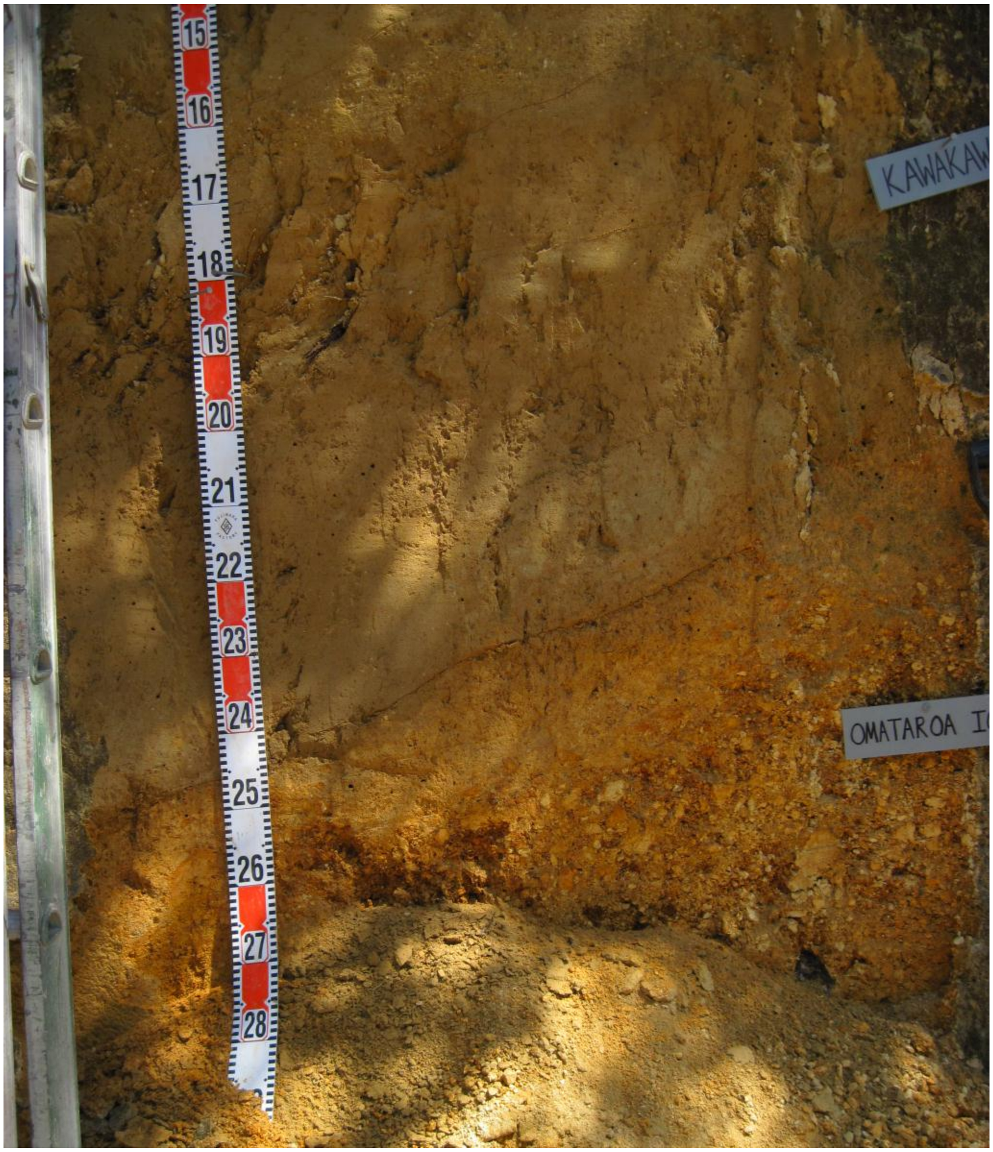

Figure 2.4 Unit L (labelled 'Omataroa' in photo) at base of profile at Kaharoa Rd. Note measuring tape numbers are decimetres; black/white ticks are centimetres.

Table 2.2 Table showing heavy mineralogy of some tephras at Dansey Rd, Maniatutu Rd and Glue Pot Rd. Heavy mineral reference data also shown. Some tephras have multiple units with differing mineralogy as shown in the reference data. An attempt to link the mineralogy of this study with specific units of the listed reference tephras has been made.

Reference data (Lowe et al., 2008)		**This study**		
Tephra	**Assemblage***	**Dansey Rd**	**Maniatutu Rd**	**Glue Pot**
Rr	Hyp>Hbl>Aug	Hyp>Hbl>Oxi>Aug>Bio		
	Bio>Hbl>Hyp		Bio>Hbl>Hyp + Aug + Oxi >Cum	
Rk	Hyp>Hbl	Hyp>Hbl + Oxi>Bio>Aug		
	Hbl + Bio>>Hyp		Bio>>Cum + Hbl + Oxi + Aug + Hyp	
	Hyp>Hbl	Hyp>Hbl + Oxi>Bio>Aug		
Ok	Hyp + Hbl>>Cum	Hyp>Bio>Hbl + Oxi>Cum	Hyp>Hbl>Oxi>Cum >Bio	
	Hbl + Bio>>Hyp			
	Hyp>Hbl			
Te	Hyp + Hbl			Hyp + Hbl +Oxi>Cum + Aug +Bio
	Hyp + Hbl + Bio>Aug		Hbl>Hyp>Cum + Oxi>Aug>Bio	
	Hyp + Hbl			Hyp + Hbl +Oxi>Cum + Aug +Bio
Kk	Hyp>Hbl	Hyp>Bio>Oxi + Hbl>>Aug	Hyp>Hbl + Oxi>Bio>Aug	
Unit L	Hyp >Hbl (also Hbl>Hyp, but less common) (Smith et al., 2002)	Hbl + Oxi>Hyp>>Aug>Cum	Hyp>Oxi + Hbl + Cum>Bio + Aug	

* = Hyp, hypersthene; Hbl, hornblende; Aug, augite; Bio, biotite; Cum, cummingtonite; Oxi, Fe-Ti oxides (mainly titanomagnetite).

2.3 Kawakawa Tephra

2.3.1 Age, source and distribution

The rhyolitic Kawakawa Tephra (Kk), also known as 'Oruanui', was erupted from the central North Island Taupo volcano within the TVZ (Figure 2.5) (Wilson, 2001b) at c. 25,384 ± 220 cal yrs BP. This multi-phased, phreatomagmatic eruption produced ~430 km^3 of fall deposits, ~320 km^3 of pyroclastic density current deposits and a ~420 km^3 intracaldera deposit (stated as deposit volumes) (Wilson, 2001b). Kk was noted as present at all thirteen field sites in this study.

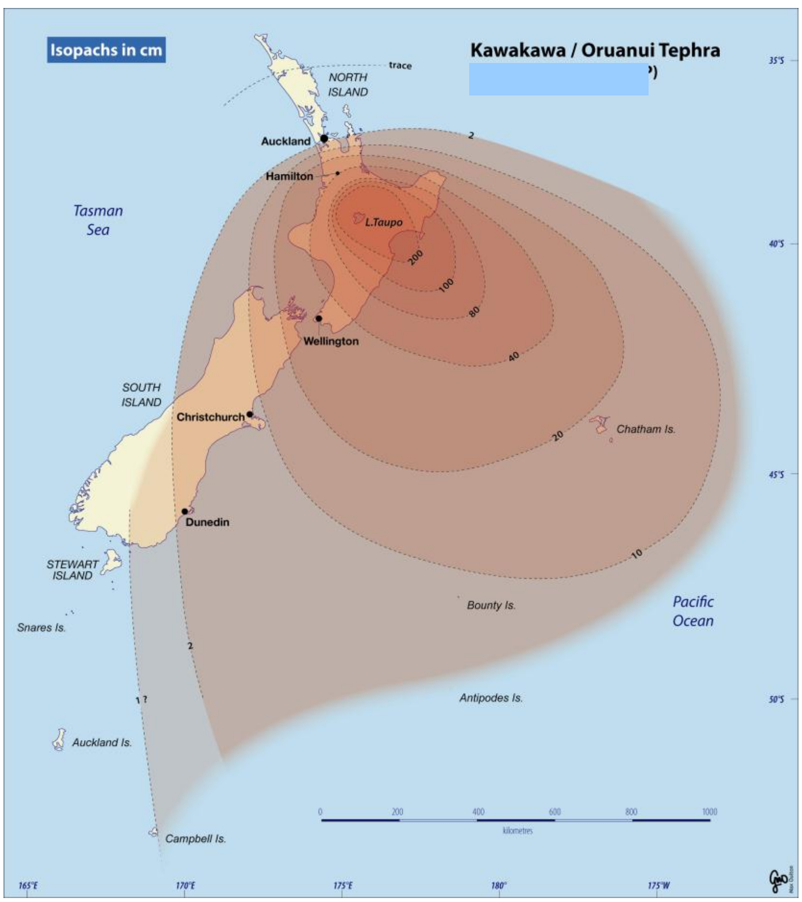

Figure 2.5 Isopach map, in centimetres, showing distribution of Kawakawa Tephra (after Lowe *et al.* (2008b)).

2.3.2 Lithology

Within the field area, Kk consists of two distinct units: an upper coarse unit and a lower finer unit (Figure 2.6). The upper unit is on average medium sand-sized sometimes including a few pebble-sized pumice clasts. The upper unit tends to be either dull yellow orange or dull yellowish brown. The boundary between the upper and lower unit is often wavy or irregular and appears to be an erosional boundary in many places. This 'lava-lamping' effect observed in the Kk may be a result of liquefaction associated with seismic activity at the time of the Kk eruption or deformation of the lower unit in response to loading by the upper courser unit. In some places complete erosion of the lower unit seems to have occurred. The lower unit is commonly clay/silt-sized and tends to be dull yellow orange (10 YR 7/3). It is often weakly stratified and may include manganese di-oxide concretions (redox segregations). At a number of field sites, this unit also has a thin coarse basal unit, sometimes composed of clast-supported accretionary lapilli (approx. 3 mm diameter). The lower boundary of the lower unit is commonly sharp or abrupt and wavy or smooth. The heavy mineral assemblage of Kk is dominated by hypersthene and biotite at Dansey Rd (the presence of biotite in this unit is not explained) and hypersthene, hornblende and Fe-Ti oxides at Maniatutu Rd (Table 2.2).

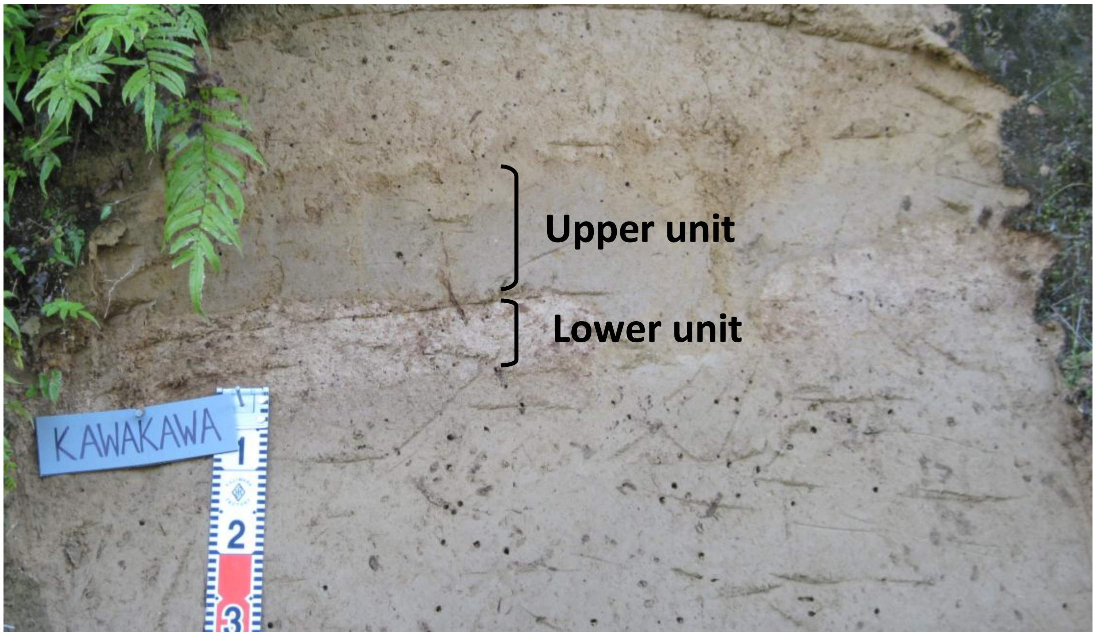

Figure 2.6 Kawakawa Tephra at Oturoa Rd. Upper and lower units separated by an erosional boundary. Note measuring tape numbers are decimetres; black/white ticks are centimetres.

2.4 Te Rere Tephra

2.4.1 Age, source and distribution

The rhyolitic Te Rere Tephra (Te) was erupted from the Haroharo linear vent zone system within the OVC (Nairn, 1992) c. 25,240 cal yrs BP (this age may have been influenced by a component of “in-built” age from the sample material comprising wood, and hence may be too old). Figure 2.7 shows the distribution of the Te (including post-Te loess) (Nairn, 1992). In this study Te was noted (often tentatively) at seven of the thirteen field sites which were confined to a band northwest of the proposed source vent of Te.

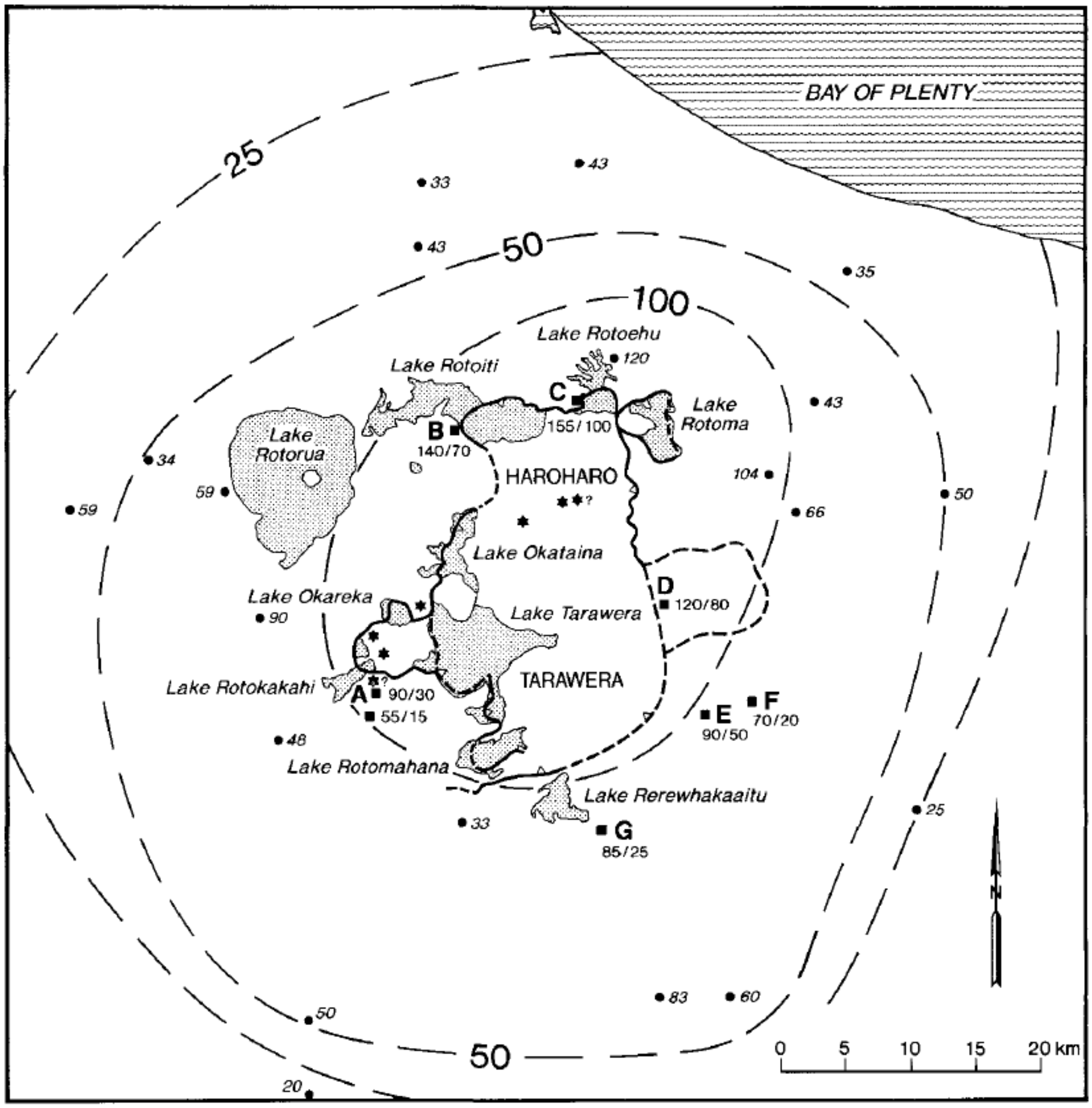

Figure 2.7 Isopach map in centimetres of Te Rere Tephra distribution (including post-Te Rere loess). The double numbers near Haroharo caldera denote thickness of total loess + Te Rere Tephra / thickness of Te Rere Tephra only. Stars denote likely active vent locations at the time of Te Rere eruption (from Nairn, 1992 (p. 95)).

2.4.2 Lithology

Te is well exposed at Maniatutu Rd (Figure 2.8) and is approximately 15 cm thick. The unit is shower bedded, composed of sand—pebble-sized clasts, variable in colour and contains pumice clasts with low vesicularity and glassy black rhyolitic lithics up to 4 cm. The unit has an abrupt lower boundary. At distal field sites (i.e. Belk Rd and Glue Pot Rd) Te appears mostly as a few dark lithics (up to 8 mm in diameter) within post-Kk loess. The heavy mineral assemblage of Te is dominated by hornblende and hypersthene at Maniatutu Rd and hypersthene, hornblende and Fe-Ti oxides at Glue Pot Rd (Table 2.2).

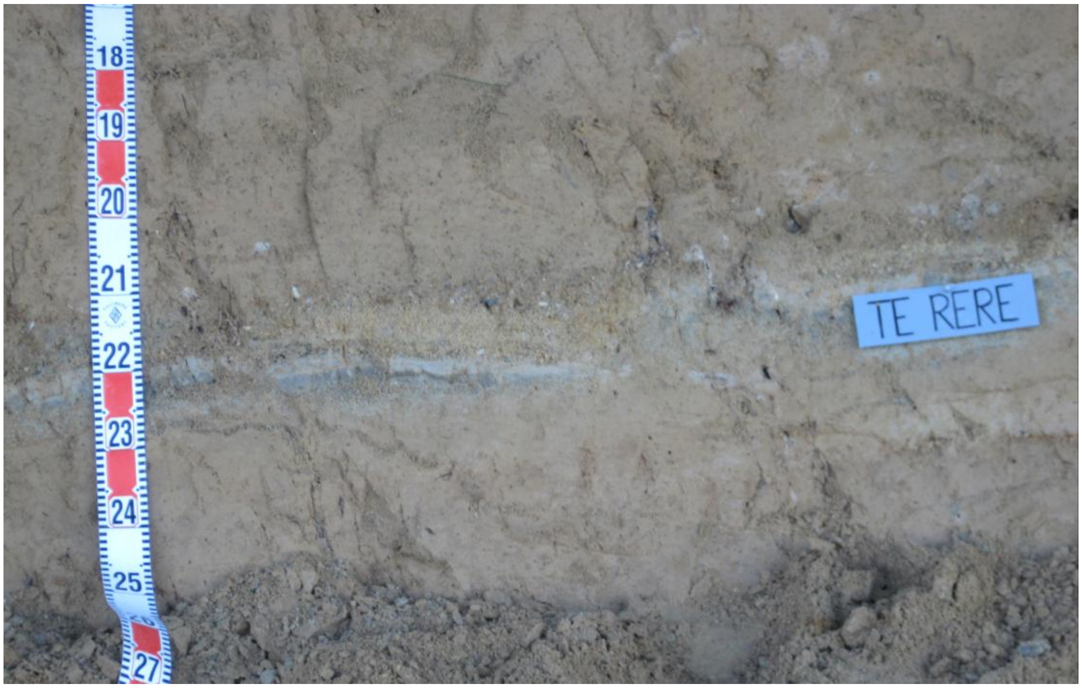

Figure 2.8 Te Rere Tephra at Maniatutu Rd. Note measuring tape numbers are decimetres; black/white ticks are centimetres.

2.5 Okareka Tephra

2.5.1 Age, source and distribution

The biotite-bearing rhyolitic, Okareka Tephra (Ok) was erupted from the OVC, probably from Tarawera linear vent zone (Nairn, 1992), c. 21,850 cal yrs BP. Ok is the oldest Last Glacial Maximum central North Island erupted tephra to contain significant amounts of biotite (Benny *et al.*, 1988). Figure 2.9 shows the distribution of Ok (including post-Ok loess). Ok was noted as present at all thirteen of the field sites in this study.

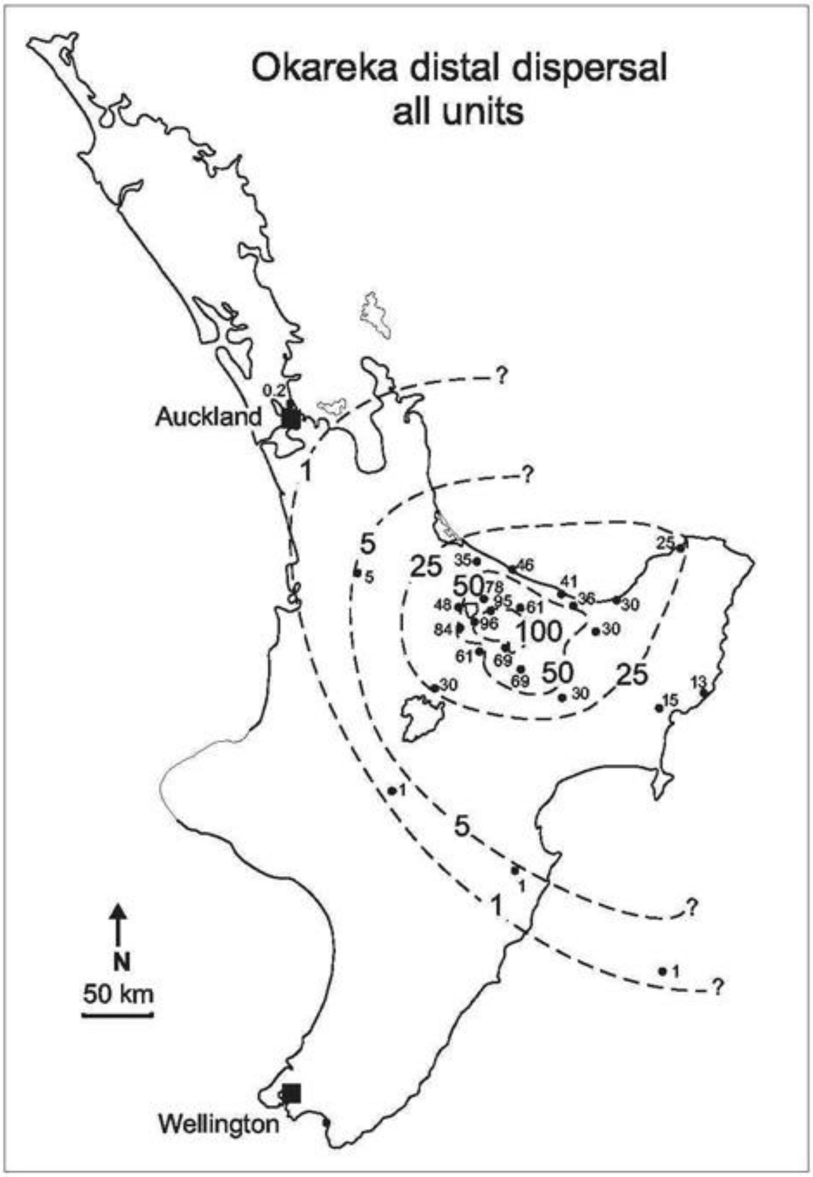

Figure 2.9 Isopach map in centimetres showing the distribution of the Okareka Tephra (Darragh *et al.*, 2006, p. 318).

2.5.2 Lithology

Most sites in this study (except distal sites to the north and also Kaharoa Rd) show Ok to be a shower bedded unit (Figure 2.10) with a medium sand-sized (on average) basal unit, a coarse sand-sized middle unit, and medium sand-sized upper unit. The individual beds may also vary in colour. For example, at Tapapa Rd and Leslie Rd, the upper and lower units are dull yellow orange and the middle coarser unit is bright yellowish brown. The maximum thickness of Ok within the field area is 30 cm (Maniatutu Rd). The lower boundary of Ok with loess is often sharp and occluded. At some distal sites and also Dalbeth Rd, Ok is discontinuous. The heavy mineral assemblage of Ok is dominated by hypersthene and biotite at Dansey Rd and hypersthene and hornblende at Maniatutu Rd (Table 2.2).

Figure 2.10 Okareka Tephra at Hamurana Rd showing shower bedding. Note measuring tape numbers are decimetres; black/white ticks are centimetres.

2.6 Rerewhakaaitu Tephra

2.6.1 Age, distribution and source

The biotite-bearing Rerewhakaaitu Tephra (Rk) was erupted from the Tarawera linear vent zone system of the OVC (DRE of about 5 km^3, Darragh *et al.*, 2006) (Newnham *et al.*, 2003) c. 17,461 cal yrs BP. Figure 2.11 shows the distribution of Rk. Rk was distributed over the entire field area (Figure 2.11), but at three sites (Leslie Rd, Kaharoa Rd and Penny Rd) Rk was not identified, perhaps due to local erosion or the tephra being too thin to discern by field techniques or mixing of the tephra into the soil. At distal sites Rk is usually discontinuous.

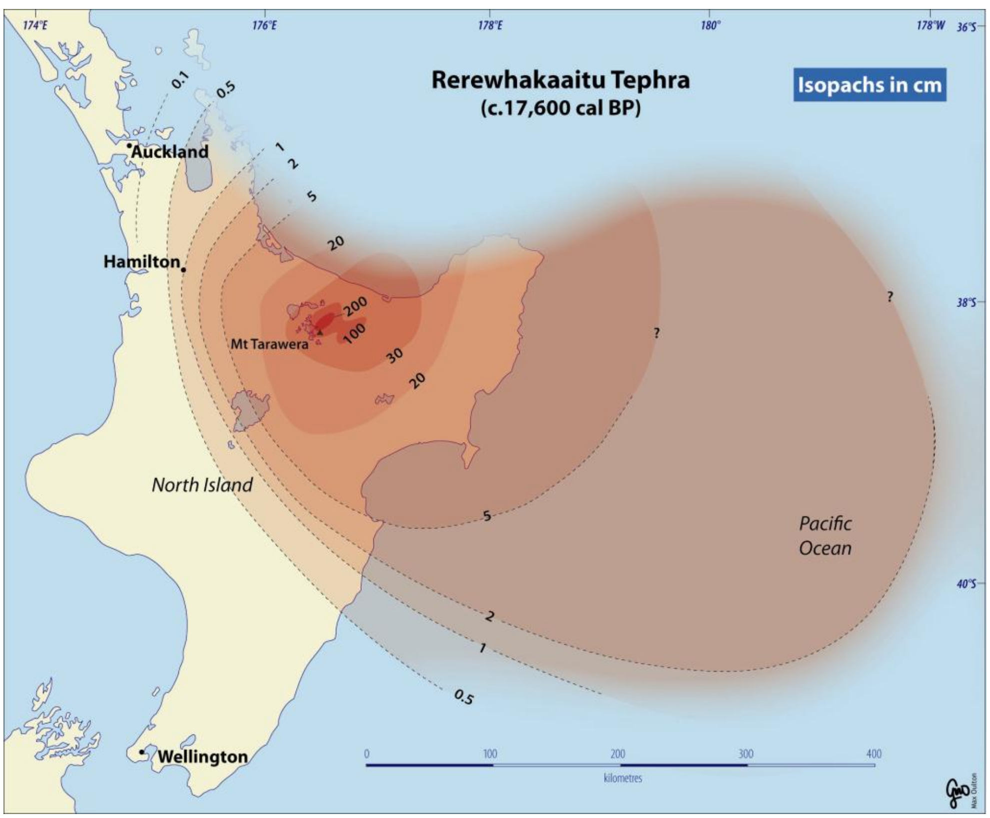

Figure 2.11 Isopach map in centimetres showing distribution of the Rerewhakaaitu Tephra (after Newnham *et al.*, 2003).

2.6.2 Lithology

The maximum thickness of Rk recorded within the field area is ~25 cm (Highlands Rd and Oturoa Rd). At a number of sites close to source (Highlands Rd, Oturoa Rd and Hamurana Rd), Rk has two distinct units: an upper unit with low chroma (pale) colours and a lower unit with higher chroma colours and white pebble-sized pumice clasts. At Oturoa Rd (Figure 2.12) the upper unit is dull yellow brown (10 YR 6/3) and coarse sand-sized. The lower unit is bright yellowish brown (10 YR 6/8) and coarse sand-sized with rare white pebble-sized pumice clasts. The heavy mineral assemblage of Rk is dominated by hypersthene, hornblende and Fe-Ti oxides at Dansey Rd and biotite at Maniatutu Rd (Table 2.2).

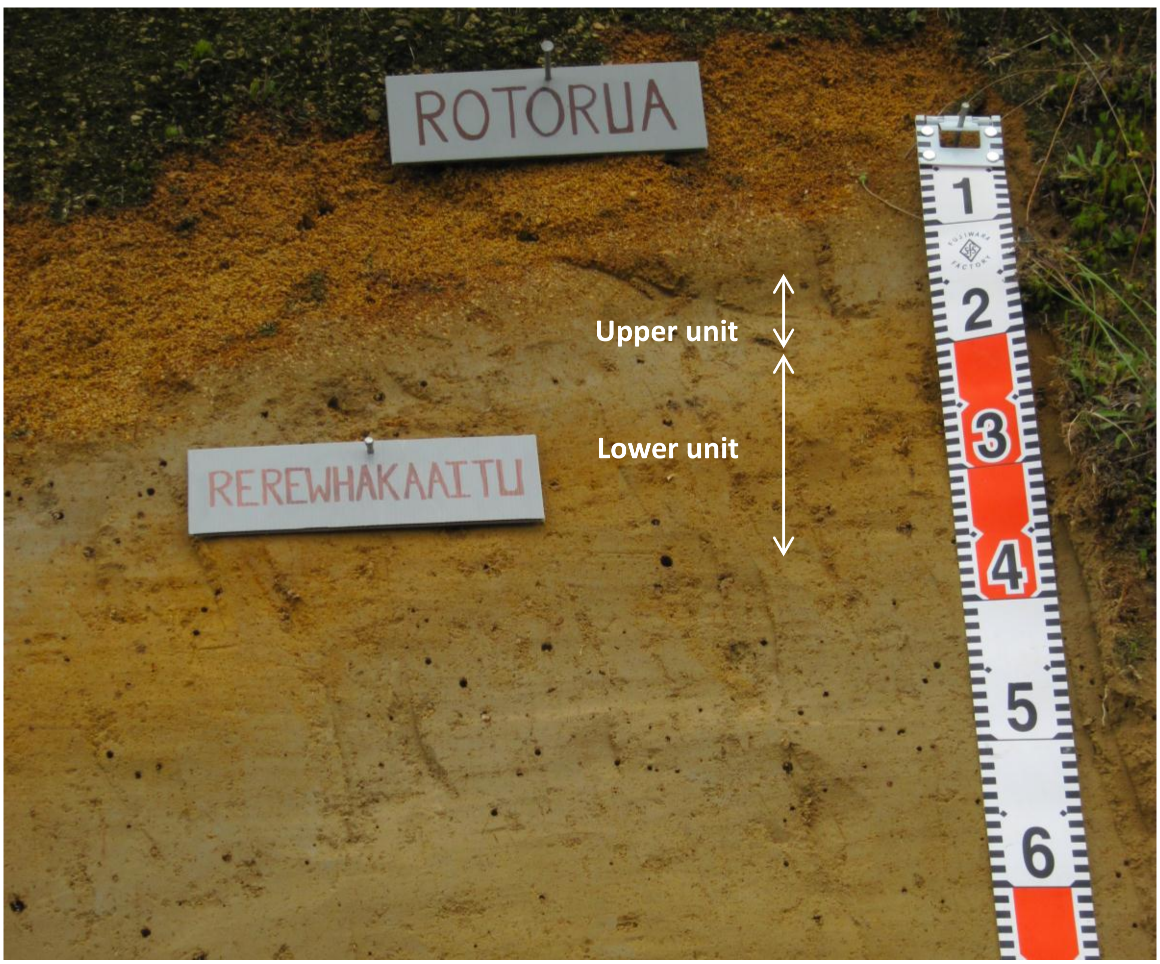

Figure 2.12 Rerewhakaaitu Tephra at Oturoa Road. Upper unit with low chroma (pale) colours and a lower unit with higher chroma colours. Note measuring tape numbers are decimetres; black/white ticks are centimetres.

2.7 Rotorua Tephra

2.7.1 Age, source and distribution

The partly biotite-bearing Rotorua Tephra (Rr) was produced during a rhyolitic plinian eruption which was part of a two phase eruptive episode (Nairn, 1980; Kilgour & Smith, 2008) from the Okareka basin region of the OVC (Smith *et al.*, 2004) at c. 15,556 cal yrs BP. Figure 2.13 shows the distribution of Rr. In this study, Rr was recorded at 12 of the 13 field sites (the exception being Leslie Rd).

2.7.2 Lithology

Rr forms a distinctive, coarse, pumice-rich unit within the field area (Figure 2.14). It is generally very coarse sand—pebble-sized, sometimes up to cobble-sized, and is often a massive unit; however, some sites do show bedding (Highlands Rd, Dalbeth Rd and Maniatutu Rd). Dark lithics are sometimes present (up to 12 mm in diameter at Highlands Road). The unit is often bright yellowish brown (10 YR 6/8). The heavy mineral assemblage of Rr is dominated by hypersthene and hornblende at Dansey Rd and biotite and hornblende at Maniatutu Rd (Table 2.2).

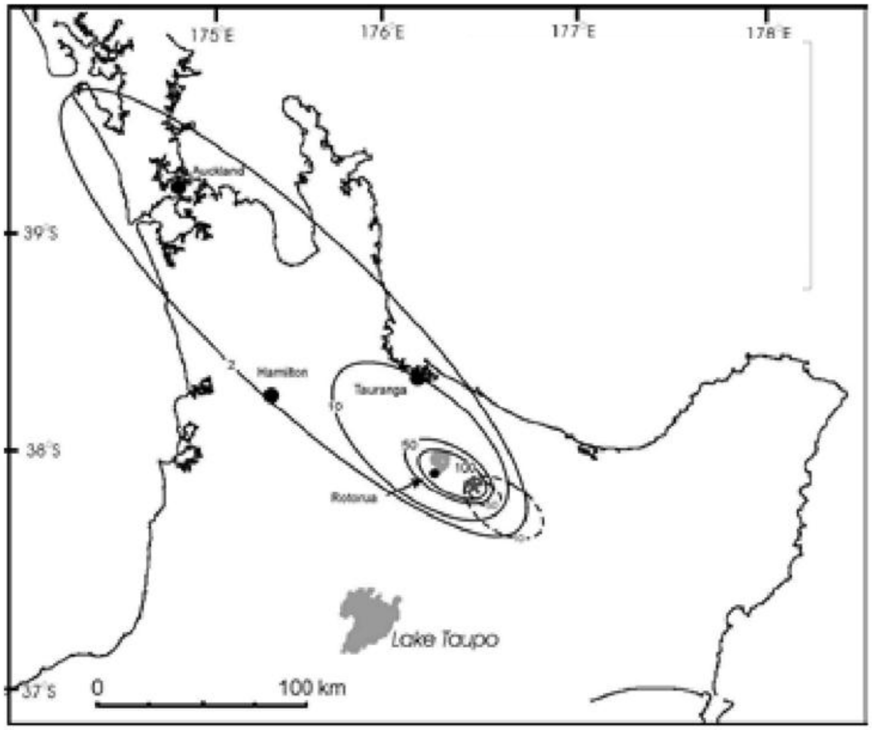

Figure 2.13 Isopach map in centimetres showing distribution of Rotorua Tephra. (Solid Isopach lines: phase 1 deposit; dashed Isopach line: phase 2 deposit) (adapted from Kilgour & Smith, 2008).

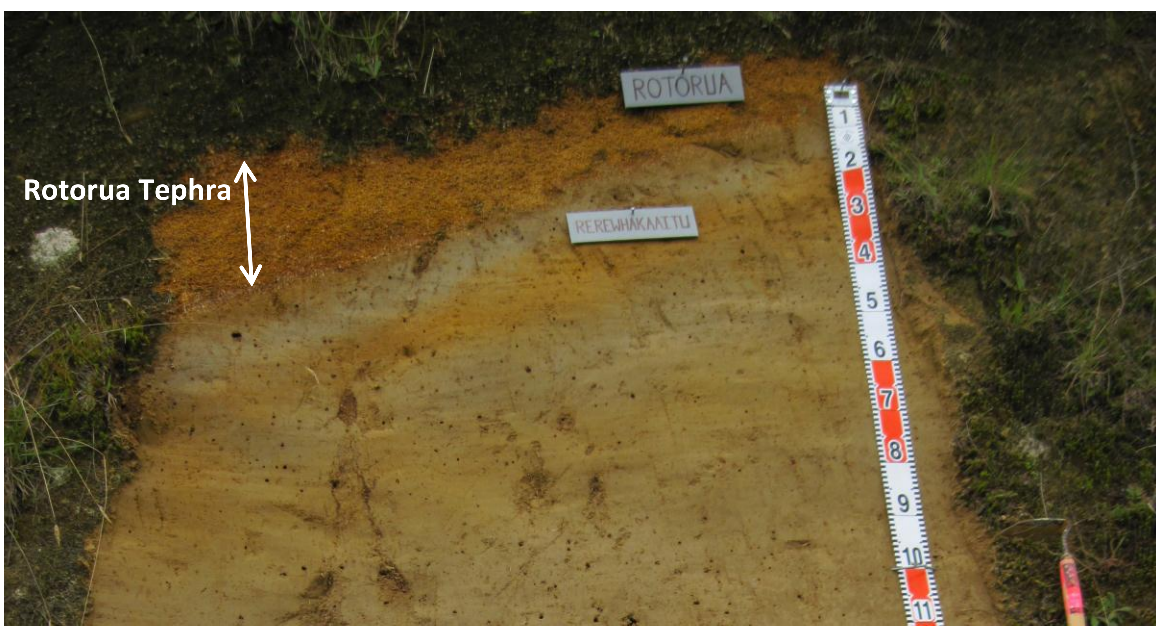

Figure 2.14 Distinctive pumice-rich Rotorua Tephra at Oturoa Rd. The upper boundary of Rotorua Tephra is not visible in this photo. Note measuring tape numbers are decimetres; black/white ticks are centimetres.

2.8 Waiohau Tephra and Rotoma Tephra

Waiohau Tephra (Wh) was erupted from the Tarawera linear vent zone of the OVC c. 13,635 cal yrs BP (Lowe *et al.*, 2008b). Rotoma Tephra (Rm) was erupted from the Haroharo linear vent zone of the OVC c. 9,498 cal yrs BP (Lowe *et al.*, 2008b). Wh and Rm were present at Dansey Rd, however detailed field investigation of these two tephras were not carried out as they are younger than the time interval of interest of this study.

2.9 Tephric loess

Tephric loess deposits in the Rotorua region located stratigraphically between Mangaone Subgroup Tephras and the Rk have been recognised (Benny *et al.*, 1988; Kennedy, 1994) and more recently between the Rerewhakaaitu Tephra and Rotorua Tephra (although thin) (Newnham *et al.*, 2003). This study has recognised tephric loess deposits located stratigraphically between Unit L and the Rotoma Tephra. The massive, light coloured, and fine grained nature of these deposits (Kennedy, 1994) are characteristic of loess deposits (Pecsi, 1995). The identification of these deposits as loess deposits occurred because associated tephra deposits showed apparent inconsistent variation in thickness with distance from tephra source (Vucetich & Pullar, 1969; Read, 1974). Re-worked tephric and volcanic material are assumed to be the dominant source material of these loess deposits (Benny *et al.*, 1988; Kennedy, 1994). At Tapapa Rd the loess is composed mainly of volcanic glass and may include charcoal and fresh water diatoms (Lowe & Briggs, 1994), possibly indicating a lack of ferromagnetic minerals (likely derived from volcanic eruptions) throughout many of these loess deposits. A study by Benny *et al*. (1988) in the Rotorua area showed that loess deposits immediately above Ok were predominantly derived from the Ok deposit, however, with time, other material (e.g. eroded ignimbrite) also became an important component of the loess.

The degree to which loess deposits are influenced by post-depositional alteration can be viewed as competition between loess accumulation and “top-down” pedogenesis governed by prevailing climatic and other conditions under which the loess was deposited (Verosub *et al.*, 1993; Almond & Tonkin, 1999; Lowe & Tonkin, 2010). In this thesis I recognise that the entire loess column has been altered to some degree by top-down pedogenesis because the rates of loess accumulation (described in Chapter 3) have been sufficiently slow to allow alteration of the loess by soil-forming processes as it accumulated (Lowe & Tonkin, 2010). However, as the loess accumulation rate decreased, top-down pedogenesis became more effective and hence more strongly altered soil features were developed in the loess columns, which were referred to as “paleosols” in Figure **2.1**.

In this chapter, for ease of discussion, the loess has been divided into six packets based on stratigraphic position. The upper and lower boundaries of each packet are defined by tephra marker beds. Packet 1 being the oldest and packet 6 being the youngest. The inferred age, distribution and lithology of each of the deposits are described.

2.10 Loess packet 1

2.10.1 Age and distribution

Loess packet 1 is stratigraphically located above Unit L and below Kk and thus has an age range of c. 32,700—25,384 cal yrs BP. Loess packet 1 is present throughout the field area, with the exceptions of Penny Rd (where the pre-Kk stratigraphy appears to be affected by fluvial reworking), Hamurana Rd (where Kk mostly sits unconformably on Rotoiti Ignimbrite lithic lag breccias), Dalbeth Rd (profile not deep enough) and Highlands Rd (stratigraphy uncertain).

2.10.2 Lithology

Although the lithology of loess packet 1 varies throughout the field area, it appears to typically consist of a paleosol horizon developed on Unit L, overlain by loess (Figure 2.1). Paleosol development was recognised based on visual field evidence (i.e. darker richer soil colours, usually with relatively lower colour values). However, at some sites (Oturoa Rd, Maniatutu Rd, Belk Rd and possibly Glue Pot Rd) a tephra (probably Okaia or Poihipi) appears to bisect the paleosol horizon. At sites where this unknown tephra appears to be absent there may be hidden unconformities in the stratigraphic record or the tephra may be present as a crypto-tephra. The maximum observed thickness of loess packet 1 was ~90 cm, observed at Oturoa Rd (Figure 2.15).

The paleosol horizon within loess packet 1 is on average clay/silt-sized and ranges from dull yellowish brown (10 YR 5/4) to yellowish brown (10 YR 5/6) to brown (10 YR 4/6). Loess within packet 1 is on average clay/silt-sized and tends to be dull yellow orange (10 YR 6/3). At Belk Road a paleosol, located directly beneath the Kk, is stratigraphically higher than at other sites. Apparent stratigraphic disturbance higher in the loess column and the presence of multiple possible fault scarps in the near vicinity suggests that this site may be affected by stratigraphic limitations.

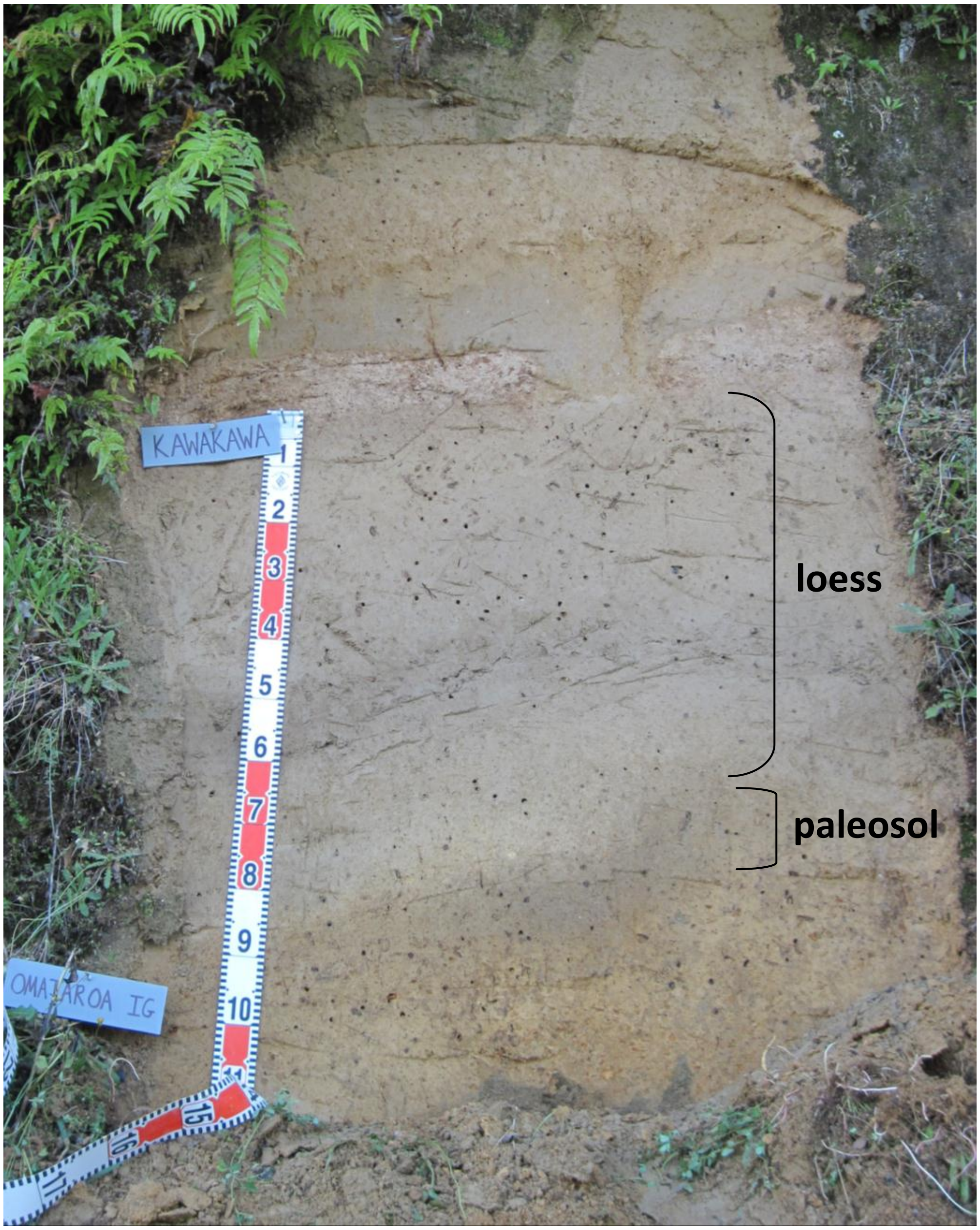

Figure 2.15 Loess packet 1 at Oturoa Road including a possible paleosol horizon (buried soil horizon with more strongly developed pedogenic features). Unit L is labelled 'Omataroa IG' in this photo. Note measuring tape numbers are decimetres; black/white ticks are centimetres.

2.11 Loess packet 2

2.11.1 Age and distribution

Loess packet 2 is stratigraphically located above Kk and below Ok and thus has an age range of c. 25,384—21,850 cal yrs BP. At some field sites Te bisects loess packet 2. Loess packet 2 is widespread throughout the field area.

2.11.2 Lithology

Loess packet 2 varies in lithology throughout the field, typically having a paleosol horizon directly above Kk overlain by a massive loess horizon which in turn is overlain by Ok (Figure 2.1& Figure 2.16). However, evidence at two field sites (Oturoa Rd and Maniatutu Rd) suggests the presence of 1 or 2 additional paleosol horizons within loess packet 2. The paleosol within loess packet 2 is typically clay/silt-sized and yellowish brown in colour. The overlying loess horizon is typically clay/silt-sized and dull yellow orange in colour. The maximum observed thickness of loess packet 2 was ~175 cm, observed at Dansey Rd.

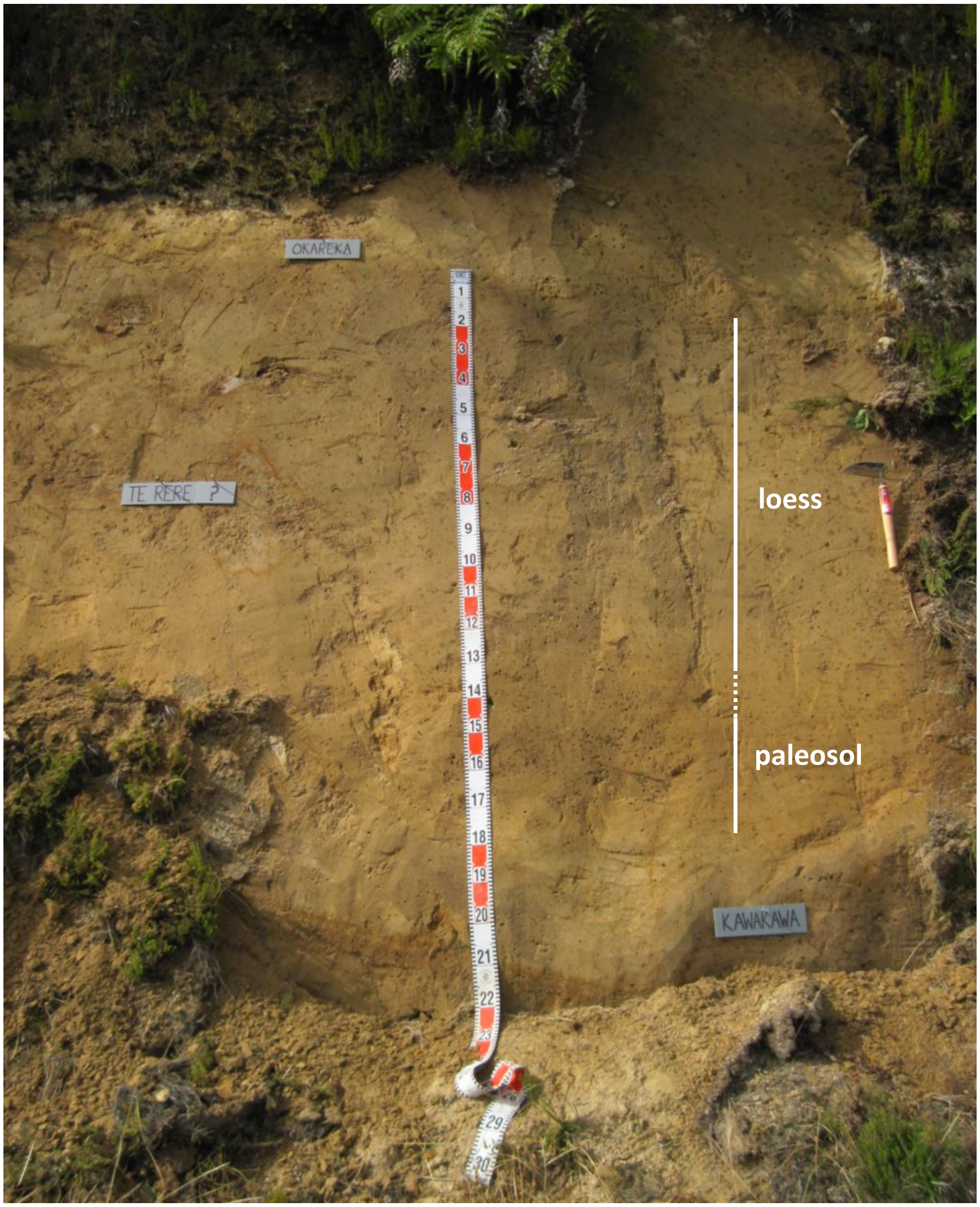

Figure 2.16 Loess packet 2 at Dansey Road including a paleosol horizon. Note measuring tape numbers are decimetres; black/white ticks are centimetres.

2.12 Loess packet 3

2.12.1 Age and distribution

Loess packet 3 is stratigraphically located above Ok and below Rk and thus has an age range of c. 21, 850—17,461 cal yrs BP. Benny *et al.* (1988) suggested that the material from which loess packet 3 is derived is mostly Ok; however, as the age gap between the time of Ok deposition and loess formation increased, material eroded from the Mamaku Ignimbrite also became an important component of the loess. Loess packet 3 is widely distributed across the field area, and identified at all but three field sites (Kaharoa Rd, Penny Rd and Leslie Rd). At Kaharoa Rd and Penny Rd, Rk, which marks the boundary between loess packet 3 and loess packet 4, is missing making it difficult to distinguish which loess packet/s is/are present or absent here. At Leslie Rd neither Rk or Rr were located; hence the material above the Ok was not stratigraphically age constrained.

2.12.2 Lithology

Loess packet 3 has a maximum thickness of approximately 3.3 m. Although some field sites show loess packet 3 to be a massive unit, there are at least four sites (Dalbeth Rd, Dansey Rd, Hamurana Rd and Oturoa Rd) which appear to show at least one "paleosol" horizon (Figure **2.1**). At Oturoa Rd (Figure **2.17**) this paleosol is clay/silt-sized and is yellowish brown (10 YR 5/6). Evidence at some sites (Dalbeth Rd, Dansey Rd and Oturoa Rd) also suggests a second (stratigraphically higher) paleosol horizon (Figure **2.17**). The loess material between the paleosol horizon/s is generally clay/silt-sized and variable in colour.

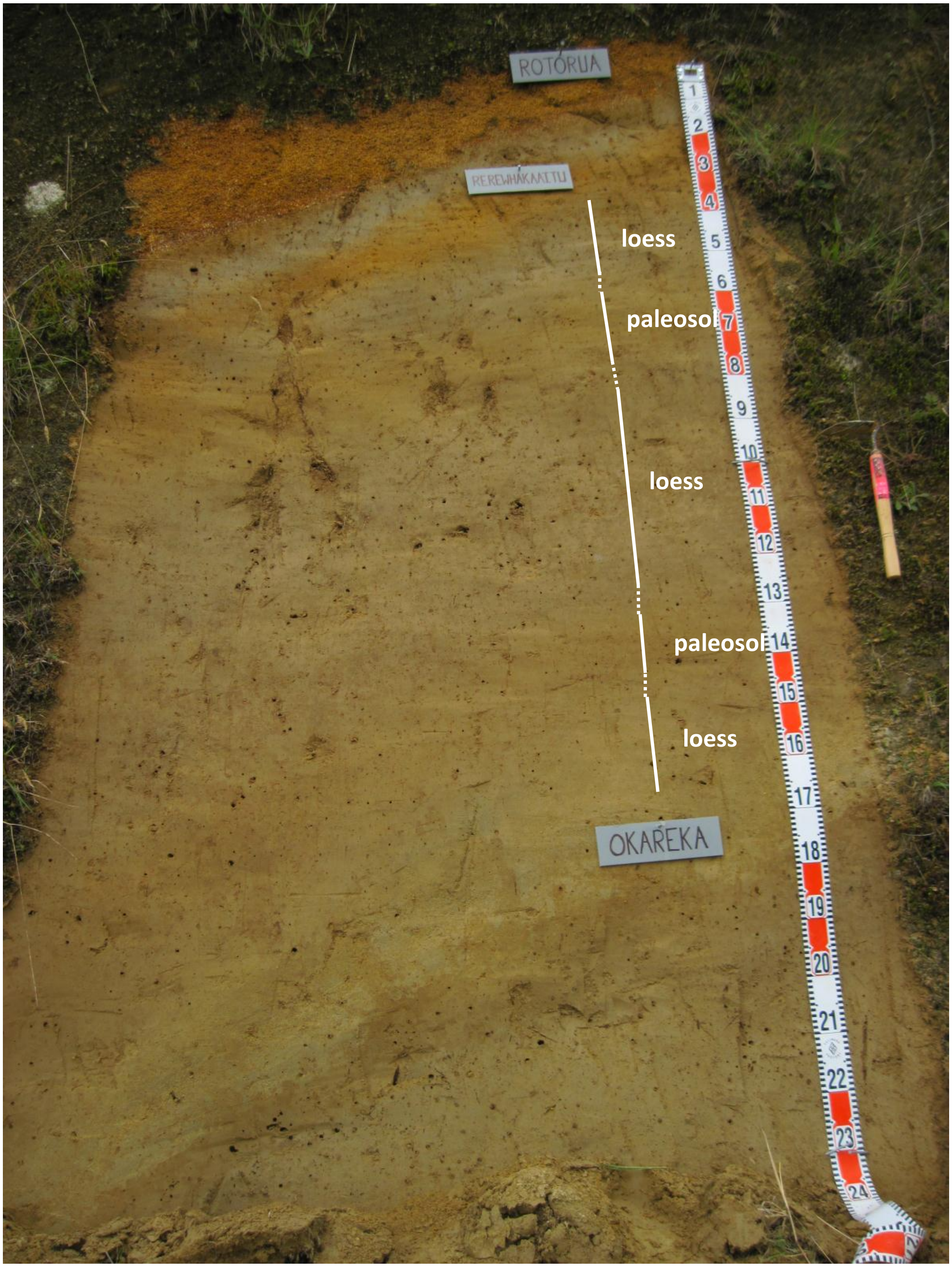

Figure 2.17 Loess packet 3 at Oturoa Rd including two possible paleosol horizons. Note measuring tape numbers are decimetres; black/white ticks are centimetres.

Deposits at two field sites (Dalbeth Rd (Figure 2.18) and Highlands Rd) contain a dune unit (Figure 2.1) within loess packet 3. The dunes are approximately 2.5—3 m thick and generally composed of clay/silt-sized material. At Highlands Rd the dune generally has a colour hue of 10 YR or 2.5 Y and has skeins of sand-sized material. These coarser beds may represent phases when a coarser sediment source was available and there were higher peak winds. The importance of these dunes will be discussed in a later chapter.

Figure 2.18 Dune within loess packet 3 at Dalbeth Road (A. & B.). Dune is approximately 2.7 m thick and appears to include up to 3 possible paleosol horizons. The dune is probably directly underlain by loess. Okareka Tephra occurs lower in the profile (C.). Note measuring tape numbers are decimetres; black/white ticks are centimetres.

2.13 Loess packet 4

2.13.1 Age and distribution

Loess packet 4 is stratigraphically located above Rk and below Rr and thus has an age range of c. 17,461—15,588 cal yrs BP. Loess packet 4 is not widely distributed throughout the field area; however, it was noted as present at at least four of the thirteen field sites: Highlands Rd, Hamurana Rd, Oturoa Rd (thin), and Dansey Rd (thin). Loess packet 4 material may have been present at Belk Rd, Taumata Rd and Tapapa Rd, though identification was difficult at these distal sites because of the discontinuous nature of Rk.

2.13.2 Lithology

Loess packet 4 appears to be a massive unit with a maximum thickness of approximately 60 cm (Highlands Rd). At Highlands Rd (Figure 2.19) loess packet 4 is yellowish brown (10 YR 5/8) and is clay/silt-sized with few pumice clasts; probably derived from tephra horizons above and below the unit, and has an indistinct smooth lower boundary.

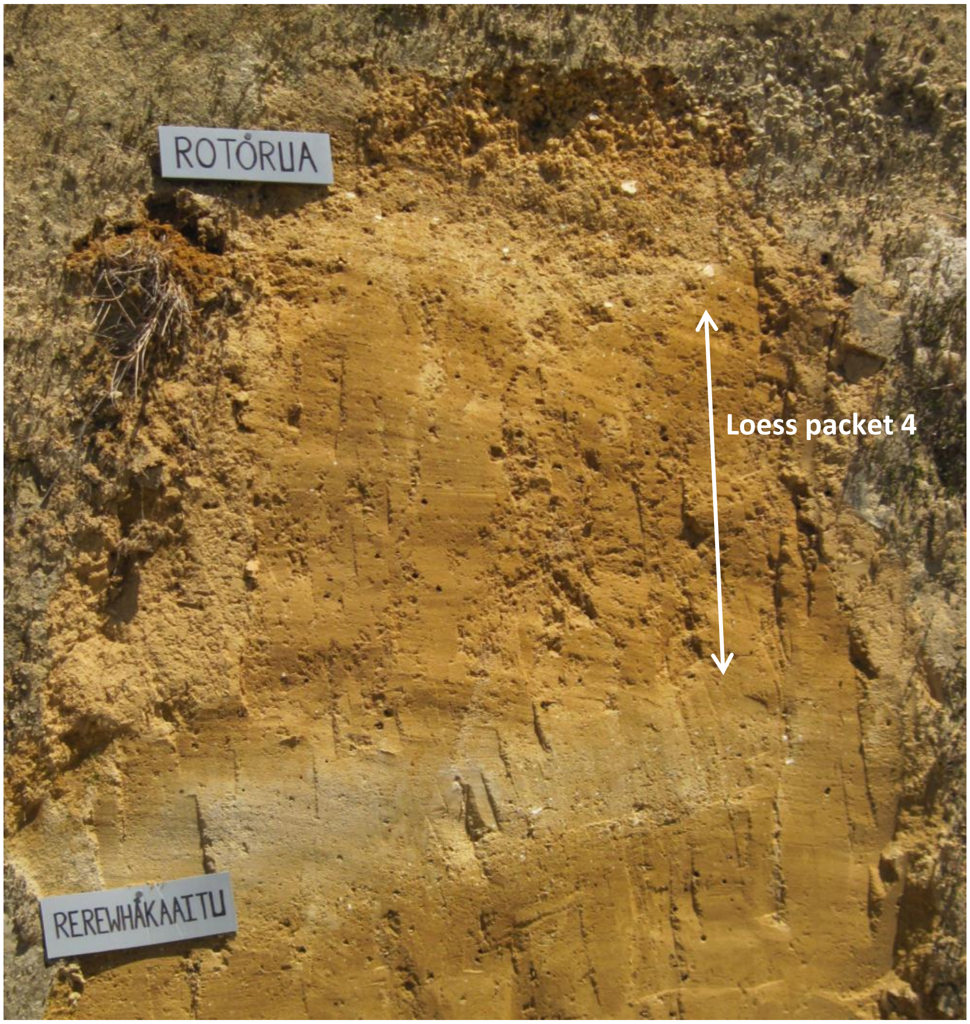

Figure 2.19 Loess packet 4 at Highlands Rd.

2.14 Loess packet 5

Loess packet 5 (Figure 2.20) is located stratigraphically above Rr and below Wh and thus has an age range of c. 15,588—13,635 cal yrs BP. Loess packet 5 was only examined in detail at Dansey Rd (although was also noted at Cameron's Quarry) and hence the distribution of this unit throughout the field area is unclear. At Dansey Rd loess packet 5 is up to 65 cm thick, contains many pumice clasts in the lower portion and shows some evidence of paleosol development beneath Wh.

2.15 Loess packet 6

Loess packet 6 (Figure 2.20) is located stratigraphically above Wh and below Rm and thus has an age range of c. 13,635—9,498 cal yrs BP. Loess packet 6 was only examined at Dansey Rd and hence the distribution of this unit elsewhere in the field area is unclear. At Dansey Rd loess packet 6 is up to 35 cm thick and shows evidence of podzolization at the upper boundary (Rm).

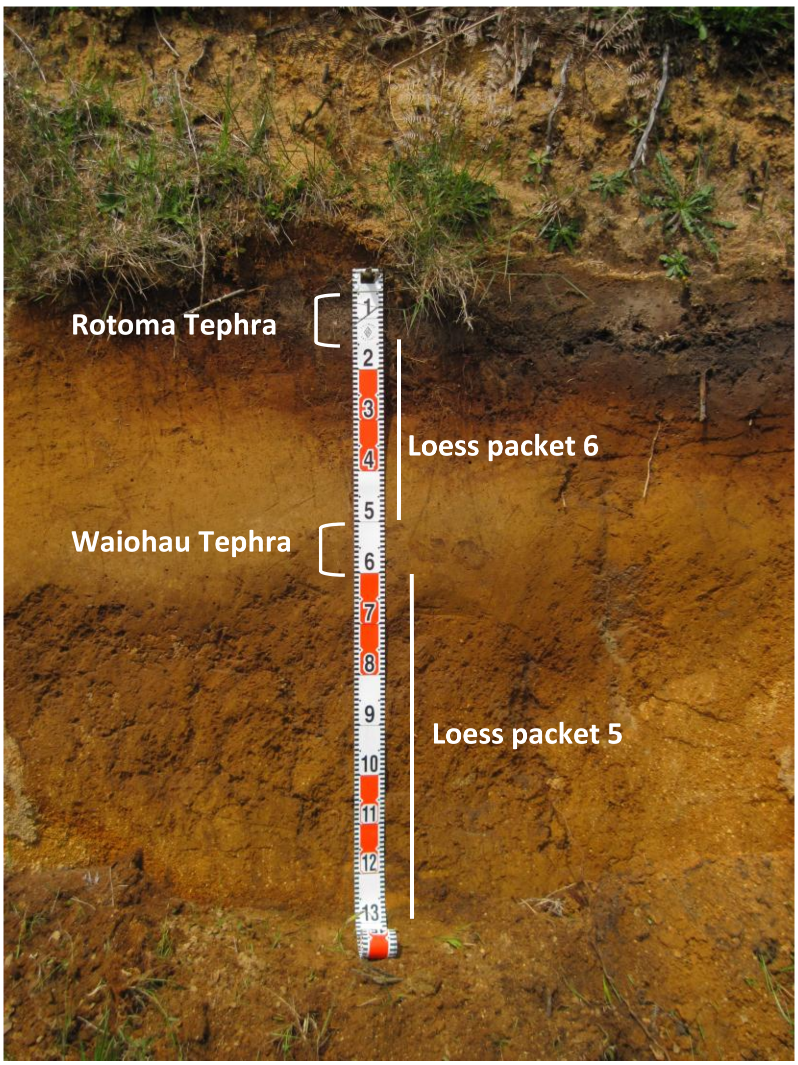

Figure 2.20 Loess packets 5 and 6 at Dansey Rd. Note evidence of podzolization at upper boundary of loess packet 6. Note also measuring tape numbers are decimetres; black/white ticks are centimetres.

2.16 Summary of tephric loess general properties and characteristics from this study

In this study, tephric loess was noted stratigraphically between Unit L and up to Rotoma Tephra. In contrast to previous studies (Vucetich & Pullar, 1969; Newnham *et al.*, 2003), these findings suggest that loess deposition continued, at least at some sites, in the Rotorua region until at least c. 9.5 cal ka. Loess was noted between Rotorua Tephra and Waiohau Tephra at Dansey Rd and Cameron's Quarry and loess between Waiohau Tephra and Rotoma Tephra was noted at Dansey Rd. In general, loess deposits throughout the field area were dominantly massive, largely silt/clay—very fine sand (defined here as <0.125 mm) and often yellowish brown, dull yellowish brown or dull yellow orange in colour (Munsell colour codes 10YR 5/4, 5/6, 5/8 or 6/4). The thickest (tephra-free) loess sequence occurs at Dansey Rd where a total of 4.3 m of loess was recorded between Unit L and Rotoma Tephra.

2.17 Age-derivation of loess deposits

Ages were assigned throughout each loess packet by assuming a constant rate of loess deposition between the bounding tephra layers of each loess packet. The tephra ages shown in Table 2.1 along with depth measurements from selected field sites were used to derive average loess accumulation rates for each loess packet. Average accumulation rates (at 5 cm resolution) were then used to assign ages throughout the loess packets.

2.18 Stratigraphic limitations

Although the stratigraphy at most of field sites is relatively well constrained by multiple tephra deposits, which provide valuable tie points and act as time planes, there are limitations to this field work. Some stratigraphic limitations are outlined below which may affect the reliability of a number of different properties, discussed in later chapters, to be used as paleoclimatic proxies.

- It is possible that hidden unconformities may exist and where not identified at field sites in this study.
- Disturbance of stratigraphy (e.g. as a result of earthquakes, mass movement, chemical weathering and/or bioturbation) may have occurred at sites.
- Some tephra layers were thin and discontinuous, particularly with increased distance from source. This meant that some tephra markers beds were not able to be definitively identified.
- Some mixing of tephras (e.g. bioturbation) into under or overlying loess deposits may have influenced the properties of the loess measured for potential paleoclimatic proxies.

Chapter 3 Physical & biological Paleoclimatic proxies

3.1 Introduction

This chapter outlines the loess physical and biological properties analysed through stratigraphic columns as potential paleoclimatic proxies, which are grain-size, accumulation rate, phytolith analysis and magnetic susceptibility. Each property is discussed in turn with a brief background summarising the basis of the property as a potential paleoclimatic proxy, an outline of the analytical methods, followed by the presentation and discussion of the results.

3.2 Grain-size

3.2.1 Introduction and background

Loess grain-size has been used as a proxy of wind speed (An *et al.*, 1991) and wind strength (Xiao *et al.*, 1995). Xiao (1995) assumed that high median and maximum quartz (from loess) grain-size values correlate with stronger winter monsoonal winds and that variation in median grain-size values indicate changes in average wind strength. In New Zealand, at c. 21 cal ka during the Last Glacial Maximum (LGM), in general there was an enhanced southerly/south-westerly wind regime (Lorrey *et al.*, in press), climatic conditions were generally drier and vegetation cover was reduced (Eden & Hammond, 2003; Lorrey *et al.*, in press). It follows that, in New Zealand, increases in the grain-size of loess would likely reflect phases of stronger wind strength which may have been associated with cooler drier climatic conditions during, at least part, of the LGM (Lorrey *et al.*, in press).

Several factors other than wind strength, dryness, and vegetation cover, may also influence loess grain-size. One such factor is post-depositional weathering (pedogenesis) which results in an increase in the proportion of clay sized grains in the soil (Xiao *et al.*, 1995) (i.e. particles with a modal grain-size of about 0.37 μm; Sun *et al*., 2011). Another factor influencing loess grain-size is the grain-size of the parent material from which the loess originates (Benny *et al.*, 1988; Eden & Hammond, 2003). Eden & Hammond (2003) noted a number of loess deposits around New Zealand which differ in grain-size according to the parent material from which they were derived. Benny *et al*. (1988) carried out a study on tephric loess in the Rotorua region and found that the grain-size of the associated tephra layer was the most important control in determining the grain-size of the associated loess deposit.

3.2.2 Method

Samples were taken at 5 cm intervals throughout the loess sequence from Unit L to Rotorua Tephra at Dansey Rd and from Unit L to Rerewhakaaitu Tephra at Maniatutu Rd. These sites are ~25 km apart and on different sides of the Rotorua caldera. Loess samples (excluding tephra layers) were prepared by digesting the organic matter out of samples using H_2O_2 and heat. Samples were sonified and a deflocculant (calgon) added before being analysed with a Malvern Mastersizer 2000 lasersizer. Modal grain-size through the loess sequence at each site was graphed (excluding apparent outliers near tephra layers). The modal grain-size parameter was used as a measure of loess grain-size as it is less likely to be influenced by outlier values than some other parameters (e.g. mean).

3.2.3 Results

In general the grain-size at Maniatutu Rd is coarser than that at Dansey Rd (Figure 3.1). However, the general pattern of changes at each site between c. 32 cal ka and c. 18 cal ka appears to be remarkably similar.

Dansey Road

The modal grain-size at Dansey Rd varies through time. There appears to be an overall increase in modal grain-size (from about 55 µm to 60 µm) between the time of Unit L and Kk deposition. However, during this time there appears to be a peak in modal grain-size of about 61 µm at c. 31 cal ka and a trough in modal grain-size of about 50 µm at c. 29.5 cal ka. Following the deposition of Kk, in general, modal grain-size begins to decrease reaching about 55 µm between c. 24.4—23.4 cal ka. There is a sharp peak in modal grain-size at c. 25.3 cal ka which may relate to the presence of Te or mixing of Kk into the loess sequence. Modal grain-size increases again between c. 23.4 cal ka and c. 19.4 cal ka, reaching a peak of about 65 µm. Following this, modal grain-size decreases between c. 19.4—18 cal ka, reaching a trough of about 45 µm. A sharp increase in modal grain-size between c. 17.8—15.5 cal ka may relate to mixing of Rk and Rr into the loess sequence.

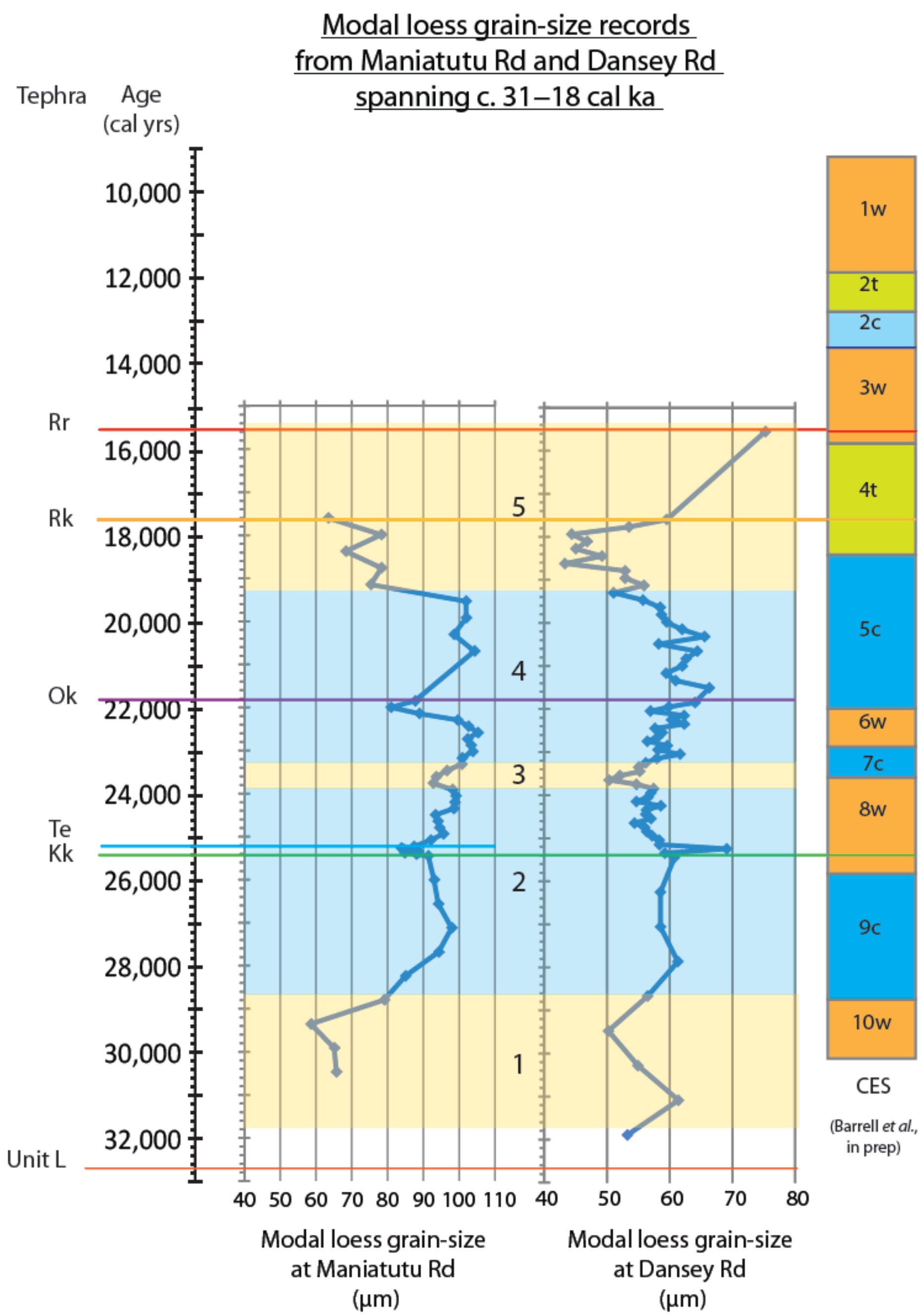

Figure 3.1 Modal loess grain-size at Maniatutu Rd and Dansey Rd. Coloured zones numbered 1-5 indicate inferred climatic phases from this study (yellow: less windy and possibly warmer, blue: windier and possibly cooler; see text for further explanation). The New Zealand climate event stratigraphy (CES) is shown for comparison.

Maniatutu Road

Modal grain-size varies through time at Maniatutu Rd. Between c. 30.6—29.2 cal ka modal grain-size is low, about 60 µm. Following c. 29.2 cal ka there is a relatively sharp increase in modal grain-size to about 95 µm. Modal grain-size is sustained around 95 µm (with fluctuations, in particular a decrease in modal grain-size between c. 25.4—25 cal ka which may be related to mixing of Kk and/or Te into the loess sequence at this time) until c. 23.8 cal ka. Between c. 23.8—23.4 cal ka there is a slight decrease in modal grain-size to about 93 µm. Between c. 23.4—19.4 cal ka modal grain-size is dominantly relatively large, around 102 µm, although there is a decrease in modal grain-size to about 80 µm just prior to the time of deposition of Ok. Modal grain-size decreases significantly, from about 102µm to about 63 µm, between c. 19.4—17.6 cal ka.

3.2.4 Discussion

In general, the grain-size at Maniatutu Rd is coarser than that at Dansey Rd. This difference is likely due to the slightly closer proximity of Maniatutu Rd to the source location of the tephras (i.e. Okataina Volcanic Centre) which has likely resulted in a courser-grained parent material from which the loess has been derived. As noted earlier, the general pattern of changes in grain-size are similar at each site, suggesting that regional climatic processes, rather than local parent material effects, are controlling grain-size variation stratigraphically. It is likely that an increase in loess grain-size generally reflects phases of stronger wind strength (Xiao *et al.*, 1995) which may have been associated with cooler drier (more glacial) climatic conditions during at least part the LGM (Lorrey *et al.*, in press). It is likely that a decrease in loess grain-size reflects phases of enhanced pedogenic alteration forming finer-grained secondary minerals (Xiao *et al.*, 1995) under relatively warmer wetter climatic conditions and possibly a decrease in wind strength.

The trends in loess grain-size at Dansey Rd and Maniatutu Rd have been summarised into five climatic phases (Figure 3.1) and are compared to the New Zealand Climate Event Stratigraphy (CES) (Barrell *et al.*, in prep.) as outlined below.

Phase 1 (c. 32—28.8 cal ka) warm, possibly decreased wind strength

Phase 1 spans c. 32—28.8 cal ka and in general at both sites is characterised by some of the finest loess grain-sizes throughout the records. These fine loess grain-sizes suggest enhanced pedogenic alteration indicating warmer climatic conditions and possibly weaker wind strengths during this phase. However, at Dansey Rd at c. 31.2 cal ka there is an increase in loess grain-size. This increase in grain-size may indicate a temporary change to more glacial climatic conditions or it may be a result of mixing of Unit L into the loess resulting in variations in loess grain-size around this time. The Maniatutu Rd loess grain-size record does not span this time frame. Phase 1 may relate to warm event 10w of the CES.

Phase 2 (c. 28.8—24 cal ka) increased wind strength

Phase 2 spans c. 28.8—24 cal ka and is generally characterised by coarser loess grain-sizes possibly indicating stronger wind strengths. At Dansey Rd, shortly after Kk deposition there is a peak in loess grain-size. Because this peak is supported by only one sample at Dansey Rd this sample may be an anomaly. It is possible, given the timing of this peak occurring at c. 25.2 cal ka, that it is related to Te, which was not observed as a distinct layer at Dansey Rd, although it may be present as a cryptotephra. At Maniatutu Rd, the decrease in loess grass size between the time of Kk and Te deposition may be due to a parent material effect, rather than a climatic influence, due to the short space of time between these two eruptions. Phase 2 may relate to cool event 9c (and possibly 7c) of the CES.

Phase 3 (c. 24—23.4 cal ka) warmer, possibly decreased wind strength

Phase 3 spans c. 24—23.4 cal ka and is generally characterised by a decrease in loess grain-size indicating weaker wind strengths and enhanced pedogenic alteration and hence less glacial climatic conditions during this phase. Phase 3 may relate to warmer event 8w and/or 6w of the CES.

Phase 4 (c. 23.4—19.4 cal ka) increased wind strength

Phase 4 spans c. 23.4—19.4 cal ka and is generally characterised by coarser loess grain-sizes possibly indicating stronger wind strengths. At Dansey Rd loess grain-size values appear to show increased variability during this time, possibly a reflection of the mobility of a larger size range of particles during increased windiness. At Maniatutu Rd loess grain-size decreases significantly around the time of Ok deposition, although it is possible that this decrease in grain-size may be a result of mixing of fine-grained Ok into the loess. Phase 4 may relate to cooler event 5c (and possibly 7c) of the CES.

Phase 5 (c. 19.4—15.5 cal ka) warm, possibly decreased wind strength

Phase 5 spans c. 19.4—15.5 cal ka and is generally characterised by finer loess grain-sizes indicating weaker wind strengths and enhanced pedogenic alteration and hence less glacial climatic conditions during this phase. At Dansey Rd there is a significant increase in loess grain-size around the time of deposition of Rk and again around the time of deposition of Rr. It is likely that these increases are due to mixing of these tephras into the loess, especially as Rr has a relatively coarse grain-size. Phase 5 may relate to event 4t (transitional event) and/or 3w (warmer event) of the CES.

3.3 Loess accumulation rate

3.3.1 Introduction & background

Loess accumulation has commonly been linked to processes associated with glacial climatic conditions (Alloway *et al.*, 1992; Palmer & Pillans, 1996; Alloway *et al.*, 2007) such as glacial grinding, freeze-thaw processes, reduced vegetation cover, widespread erosion (Eden & Hammond, 2003). However, studies show that 'non-classical' type loess can also accumulate under different climatic and environmental conditions in non-glacial environments (Iriondo & Krohling, 2007). A study by Alloway *et al*., (1992) showed that quartz accumulation rate in the Taranaki region increased during MOIS 2. Loess deposits in the central North Island, derived from re-worked tephra and volcanic material (Benny *et al.*, 1988; Eden & Hammond, 2003) and referred to as tephric loess, were formed during the extended Last Glacial Maximum (eLGM) and Last Glacial-Interglacial Transition (LGIT). During this time, conditions such as low temperatures (Lorrey *et al.*, in press), a drier climate (Litchfield & Berryman, 2005; Lorrey *et al.*, in press), strong south-westerly/southerly winds (Lorrey *et al.*, in press), a dramatically reduced forest vegetation cover (Barrell *et al.*, 2005), increased erosion (Eden & Hammond, 2003; Litchfield & Berryman, 2005) and aggrading river systems (Litchfield & Berryman, 2005), were favourable for loess formation (Iriondo & Krohling, 2007; Lowe *et al.*, 2008a).

The accumulation of loess requires four processes to occur (see summary in Lorrey *et al*., in press): 1) silt production; 2) silt entrainment by wind; 3) silt transport by wind; and 4) silt sedimentation. Production of silt can occur through a number of different processes such as glacial grinding, frost weathering, eolian abrasion, salt weathering, insolation weathering, explosive volcanism, even eluviation during pedogenesis (Iriondo & Krohling, 2007). In New Zealand, a main process responsible for the production of silt as a loess source is river abrasion (Lowe *et al.*, 2008a). Silt is susceptible to entrainment by wind when humidity is low and irregularities (such as those caused by course-grained saltating particles) exist in the silt surface. Silt transport may occur by winds such as trade-winds, monsoonal, continental anticyclones, meso-scale regional winds. Silt sedimentation can occur through a variety of mechanisms such as gravitational settling, advection, wash out by rain etc (Lorrey *et al.*, in press). Vegetation (Iriondo & Krohling, 2007) and certain topographic settings can act to trap dust (Lorrey *et al.*, in press).

3.3.2 Methods

At each field site a profile was prepared and the thickness of loess between each known tephra layer (loess packet) was measured (not including the tephra thickness). The wavy shape and/or gradational nature of the boundaries of some tephra layers made this difficult. Where boundaries between loess and tephra layers were gradational the boundary was decided based on a significant change in texture and/or colour. Loess thicknesses were rounded to the nearest 5 cm. The accumulation rate of loess between each known tephra layer was calculated using the tephra ages given in Chapter 2 and assuming a constant rate of deposition between eruptions. Only loess packets at sites where the bounding tephra layers were able to be identified and were not discontinuous were combined to obtain an average accumulation rate for each loess packet across the field area. Accumulation rate measurements for loess packets 6 and 7 were only made at one site and hence these two values are not averages. Also, loess packets where dunes were present were not included in the average. It is likely that some/all sites may be affected by stratigraphic limitations as discussed in Chapter 2. The average loess accumulation rates were graphed against age.

3.3.3 Results

There appears to be variability in loess accumulation rate through time within the field area (Figure 3.2). Between the time of Unit L and Kk deposition, the lowest rate of loess accumulation occurred, an average of ~0.5 cm/100 years. Between the time of Kk and Te deposition the highest rate of loess accumulation occurred, average ~6 cm/100 years. Following the deposition of Te, loess accumulation rate decreased to an average of ~2 cm/100 years between the time of Te and Ok deposition. This was followed by a slight increase in loess accumulation rate to ~2.5 cm/100 years on average between Ok and Rk deposition. Between the time of deposition of Rk and Rr, loess accumulation rate decreased to an average of ~1 cm/100 years. Between the time of deposition of Rr and

Wh, loess accumulation rate increased to ~3 cm/100 years on average. This was then followed by a decrease in loess accumulation to ~1 cm/100 years on average between the time of deposition of Wh and Rm.

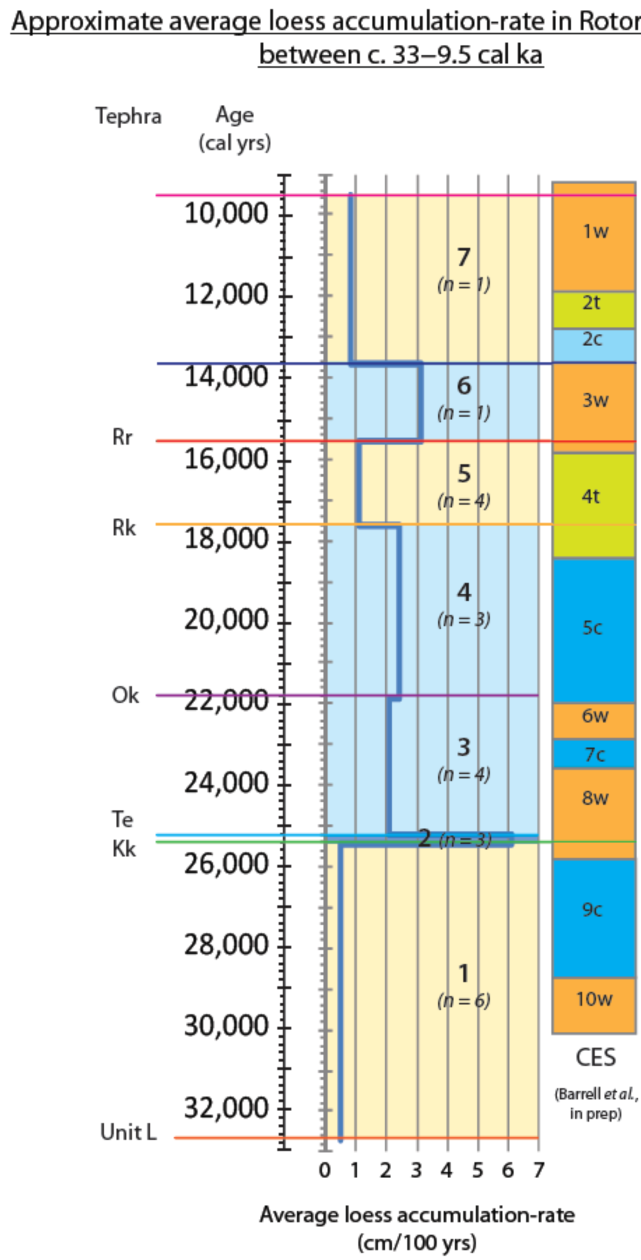

Figure 3.2 Graph of average loess accumulation rate (cm/100 yrs) throughout the field area (n = number of sites measured for each loess packet) Coloured zones numbered 1-7 indicate inferred climatic phases from this study. The New Zealand climate event stratigraphy (CES) is shown for comparison.

3.3.4 Discussion

Environmental conditions between c. 33—15 cal ka in the study field area were favourable for loess accumulation (i.e. the four processes required for loess accumulation outlined previously) to occur. For example, the proximity of the field area to the Okataina Volcanic Centre (OVC) and Taupo Volcanic Centre (TVC) and the multiple eruptions from these centres would have provided a significant source of sediment; climatic conditions were dry (Newnham *et al.*, 1999) encouraging sediment entrainment by wind; relatively course-grained tephra particles capable of saltating may have contributed to silt entrainment and further silt production; and the area was dominated by grassland vegetation (Newnham *et al.*, 1999) which likely acted as a sediment trap encouraging silt sedimentation. Because loess accumulation may result from a number of different, possibly interrelated processes it is difficult to develop a paleoclimatic interpretation based on loess accumulation rate alone (Lorrey *et al.*, in press). However, I make the assumption in this study that higher loess accumulation rates reflect drier and possibly windier and cooler climatic conditions (Lorrey *et al.*, in press) whereas lower loess accumulation rates likely reflect wetter and possibly less windy and warmer climatic conditions.

Based on the results of the loess accumulation rates throughout the field area, I have inferred five climatic phases within the field area between c. 33—9.5 cal ka (Figure 3.2). Possible links with the New Zealand Climate Event Stratigraphy (CES) (Barrell *et al.*, in prep.) have also been made, as outlined below.

Phase 1 (Unit L—Kk)

The lowest loess accumulation rate in the field area within the time frame of interest of this study appears to have occurred between the time of Unit L and Kk deposition (phase 1). This low accumulation rate suggests that climatic conditions during phase 1 were likely relatively moist and possibly warmer and less windy. Phase 1 may relate to the dominantly warm event 10w of the CES.

Phase 2 (Kk—Te)

Between the time of deposition of Kk and Te (phase 2), the highest rates of loess accumulation were recorded suggesting climatic conditions may have been relatively dry and possibly cooler and windier during this phase. It is possible that the apparent high loess accumulation rate between Kk and Te is, at least in part, due to the large volume of potential loess source material which would have been available following the widespread Kk eruption. Phase 2 may relate to the cool event 9c of the CES.

Phase 3 (Te—Ok)

Between the time of deposition of Te and Ok deposition (phase 3) a significant decrease in loess accumulation rate is recorded, compared to phase 2, however rates remain comparatively high. This suggests that climatic conditions became somewhat moister and possibly warmer and less windy. Phase 3 may correlate with warmer events 8w and/or 6w of the CES.

Phase 4 (Ok—Rk)

Loess accumulation rate increased slightly between the time of deposition of Ok and Rk tephras (phase 4), suggesting climatic conditions may have become a little drier and possibly a little cooler and windier again compared to phase 3. This slight deterioration in climatic conditions may also be supported by the phytolith results from this study (see section 3.4), where grass phytoliths show a slight increase around this time. Phase 4 may relate to the cooler event 5c of the CES.

Phase 5 (Rk—Rr)

Between the time of deposition of Rr and Rk tephras (phase 5) loess accumulation rate decreased, suggesting climatic conditions became relatively more moist, and possibly warmer, and less windy than the preceding two phases. Phase 5 may relate to transitional event 4t and/or warmer event 3w of the CES.

Phase 6 (Rr—Wh)

Between the time of deposition of Rr and Wh tephras loess accumulation rate increased suggesting climatic conditions may have again become drier and possibly cooler and windier, similar to climatic conditions during phases 3 and 4. Phase 6 may relate to cooler event 2c of the CES.

Phase 7 (Wh—Rm)

Loess accumulation rate decreased between the time of deposition of Wh and Rm (phase 7), suggesting climatic conditions improved, becoming more moist, and possibly warmer and less windy during this time, similar to conditions during phase 5. Phase 7 may relate to transitional event 2t and/or warm event 1w of the CES.

These loess accumulation rates are only capable of providing average climatic conditions throughout the time between tephra eruptions and are unable to show smaller-scale variations in loess accumulation rates and hence climatic conditions. Pedogenic development within loess deposits reflect a break or slowing in loess accumulation (Lowe & Tonkin, 2010). In this study, evidence, in the form of relatively more strongly developed soil features, within some loess packets (Figure 2.1) suggests that loess accumulation rates were not uniform and that smaller-scale climatic variations did occur throughout the time between tephra eruptions.

The occurrence of dune deposits at two sites (Highlands Rd and Dalbeth Rd) between the time of Ok and Rk deposition appear to be localised features, possibly reflecting these sites' proximities to gullies/water courses, providing a local sediment source and resulting in unique localised wind patterns.

3.4 Phytoliths

3.4.1 Introduction and background

Phytoliths, other wise known as opal phytoliths, plant opal or opaline silica (Piperno, 2006), are "amorphous hydrated silica" grains that are produced within many plants (Kondo *et al.*, 1994) following the uptake of soluble silica (Piperno, 2006). When the plant dies these inorganic silica grains are released into the soil where they are reasonably resistant to decay – in fact they have been called the "most durable terrestrial plant fossils known to science" (Piperno, 2006). In New Zealand, it has been found that phytoliths are more common in the silt-sized fraction, rather than the sand-sized fraction, of the soil (Claridge & Weatherhead, 1978, as cited in Kondo *et al.*, 1994). Most phytoliths range in size between about 2-200 µm in diameter (Almond *et al.*, 2001). Phytoliths vary widely in morphology depending on the plant type from which they originate (Kondo *et al.*, 1994). In some cases, unique morphologies can be used to identify phytoliths back to the plant species level (Piperno, 1988, as cited in Carter & Lian, 2000). More generally, however, morphology may be used to link phytoliths to a grass, tree & shrub or fern origin and in this way phytoliths may be used to reconstruct paleovegetation histories (Kondo *et al.*, 1994; Carter & Lian, 2000).

Phytolith studies in New Zealand

Raeside (1964, as cited in Kondo *et al*., 1994) was the first to report phytoliths in New Zealand soils (within loess deposits in the South Island). Weatherhead (1988 as cited in Kondo *et al*., 1994) produced a report on the widespread occurrence and variety of morphologies of phytoliths in soils in New Zealand, although no link to the source plants were made (Kondo *et al.*, 1994).

Kondo (1994) attempted to make links between some native New Zealand plants and phytolith morphologies and also produced three phytolith-based paleovegetation records: Wanganui/Taranaki area (past ~500,000 yrs); Rotorua area (spanning Te Rere Tephra to

Rotomahana Mud) and Taupo area (spanning Kawakawa Tephra to Taupo Tephra) The paleovegetation record from Wanagnui/Taranaki area (Rangitatau East Rd), composed of loess and tephra layers, showed that grass phytoliths were dominant around the time of the Kawakawa Tephra and in the upper section of the last glacial–aged loess deposit (Kondo *et al.*, 1994). The paleovegetation record from Rotorua area (Te Ngae Rd, see Figure 3.3) showed that grass phytoliths were dominant throughout the last glacial phase, suggesting dry cold climatic conditions. These findings were supported by clay mineralogical data shown in Lowe and Percival (1993) and Churchman and Lowe (2012) . Both tree and grass phytoliths were present above the Waiohau Tephra suggesting a change to warmer and wetter climatic conditions and following this tree phytoliths became most dominant up until about 700 yrs B.P (Kondo *et al.*, 1994; Churchman & Lowe, 2012).

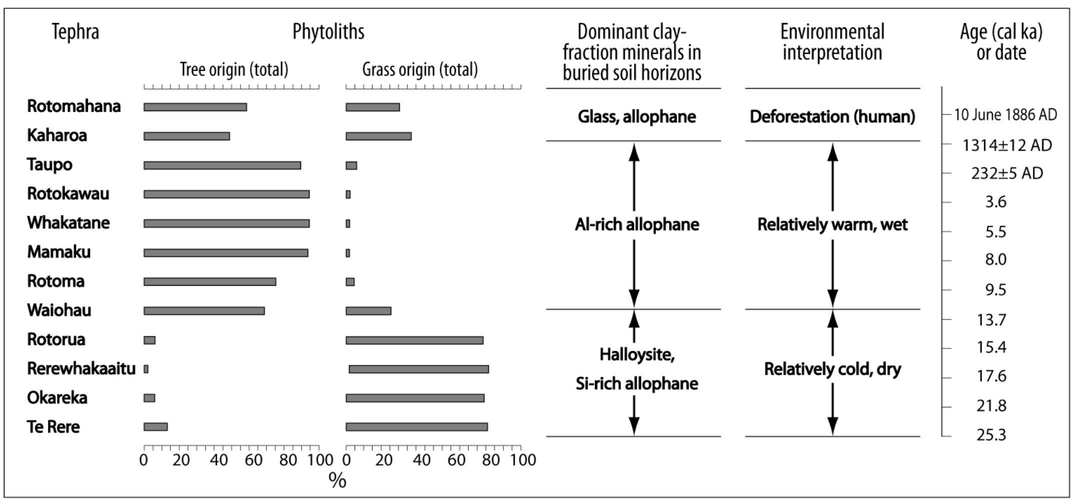

Figure 3.3 Phytolith analysis, clay mineralogy and environmental interpretation from Te Ngae Rd, Rotorua, from c. 25.3 cal ka to about 1886 AD (Churchman & Lowe, 2012).

Other phytolith based paleovegetation reconstructions have since been carried out in New Zealand (Carter & Lian, 2000; Carter, 2002). Carter & Lian (2000) presented a phytolith based vegetation record from southeastern North Island, spanning approximately the last Interglacial to present, showing changes in vegetation which closely match the SPECMAP oxygen isotope record during this time. Carter (2002) produced a phytolith-based vegetation record from a lake core from Lake Poukawa in the Hawke's Bay, spanning approximately the Last Interglacial to present. This record showed that during phases of warmer climate (i.e. present Interglacial) when a lake occupied the basin, grasses dominated in the area, where as, during phases of cooler and drier climatic conditions when the lake dried out, the area was dominated by woody vegetation. The record also demonstrated grass colonisation and vegetation succession following deposition of tephras.

Considerations in phytolith studies

Consideration of a number of factors, outlined below, is needed when using phytolith analysis to reconstruct vegetation histories.

- Although phytoliths are produced by many plants, some plants do not produce phytoliths (Kondo *et al.*, 1994; Piperno, 2006; Carter, 2007b).
- Some species produce more than one type of phytolith (Piperno, 2006).
- In general, phytolith preservation/durability is good (Carter, 2000; Piperno, 2006), but phytoliths can be susceptible to decay (i.e. dissolution) with age and under certain environmental conditions (e.g. pH above 9, Piperno, 2006). Phytolith types with larger surface areas may be more prone to dissolution (Piperno, 2006) and this may result in an under representation of these types of phytoliths as well as small-sized phytoliths in samples of increasing age (Almond *et al.*, 2001).
- Horizontal transport of phytoliths (sometimes more than 2,000 km), before deposition and preservation, can result in the preservation of non-local phytolith assemblages at some sites (i.e. phytoliths may not be preserved in-situ) (Piperno, 2006). A number of factors may be responsible for enhanced phytolith movement including strong winds, dry climatic conditions and a sparsely vegetated landscape. Phytolith movement may also occur via river transport, during fire, via herbivores. However, under other conditions (e.g. closed forest conditions where large herbivores are absent) phytolith movement may be much reduced (possibly no more than 20 m, Piperno, 2006) and hence provide a relatively reliable

indication of the vegetation growing in the area (Thorn, 2006). In general, significant vertical transport of phytoliths within soils is not considered to occur (Piperno, 2006).

3.4.2 Methods

A selection of 15 loess samples were chosen (based mainly on the fluctuations seen in the field magnetic susceptibility record) for phytolith analysis from the Dansey Rd site. Phytoliths were extracted from the samples, identified and counted using the methods outlined in appendix 3. Due to limited time and resources sample numbers for phytolith analysis were limited.

Eight general phytolith types (based on morphology) were recognised in this study: bilobate, trapeziform, conical, saddle, elongate, cuniform, polyhedral and spherical. These types were grouped into either the grass or tree/shrub category and the total percentage of grass phytoliths in each sample (compared to percentage of tree/shrub phytoliths) were graphed.

3.4.3 Results

The eight general phytolith types recognised in this study were classified as having either a *grass* origin: bilobate, trapeziform, conical, saddle, elongate, cuniform; or *tree/shrub* origin: polyhedral and spherical. Diatoms and sponge spicule were also noted in some samples. Scanning electron microscope (SEM) images were obtained of some of these phytolith types, and of a diatom, from within a sample from Dansey Rd (Figure 3.4).

The results of phytolith analysis of selected loess samples at Dansey Rd show that the percentages of bilobate, trapeziform, cuniform and polyhedral type phytoliths within the selected samples are very low, usually ≤ 10% of the total phytolith count (Figure **3.5**). The percentages of conical, elongate and saddle type phytoliths, although variable, are more common and spherical type phytoliths are, in general, the most common phytolith type (constituting about 90% of the total phytolith count at some points).

At c. 31 cal ka the phytolith assemblage was dominated by saddle (about 55% of total count), conical (about 30%) and, to a lesser extent, spherical (about 10%) and elongate (about 5%) types. A dramatic shift in phytolith assemblage occurs between c. 31 cal ka and c. 26 cal ka, where spherical types increase considerably (to about 80% of total count), and saddle (about 10%), conical (about 5%) and elongate (about 3 %) types all decrease. From c. 26 cal ka to c. 24 cal ka, there is a general increase in saddle (to about 40% of total count), conical (about 30%) and elongate (about 10%), types and a decrease in spherical types (about 10%). Bilobate (about 5%) and trapeziform (about 5%) phytoliths also begin to increase during this time. Between c. 24-23 cal ka, there is variability in the phytolith assemblage. Conical types decrease, saddle types decrease and then increase again at c. 23 cal ka, elongate types reach a peak c. 23.5 cal ka and then decrease, spherical types increase then decrease slightly at c. 23 cal ka, bilobate and trapeziform types remain relatively low. From c. 23-22 cal ka spherical types increase significantly (to about 90 % of total count) whereas saddle, conical, elongate, bilobate and trapeziform types all decrease. Between c. 22-20 cal ka there is a slight decrease in spherical types (to about 80% of total count) and a corresponding slight increase in saddle, conical and elongate types. From c. 20-18 cal ka, spherical types increase again (to about 90% of total count).

I have attempted to link each of these phytolith types to their likely plant type origin: either grass or tree/shrub, based mainly on Carter (2000), Carter & Lian (2000), Almond *et al*. (2001), and Carter (2002) (Table 3.1). I infer bilobate, trapeziform, conical, saddle, elongate and cuniform type phytoliths to have a grass origin, and polyhedral and spherical type phytoliths to have a tree or shrub origin.

The total percentage of phytoliths with an inferred grass origin, compared to the total percentage of phytoliths with an inferred tree/shrub origin, has also been graphed (Figure

3.5) and shows variability through time. This variability mirrors the trends of the spherical phytoliths through time, as outlined above, suggesting that the presence or absence of sphericals is the main driver of this variability.

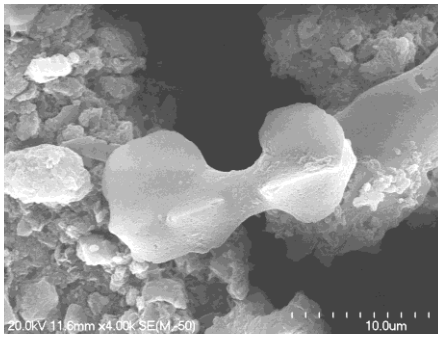

Bilobate

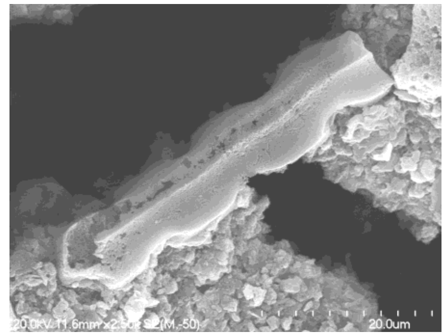

Trapeziform

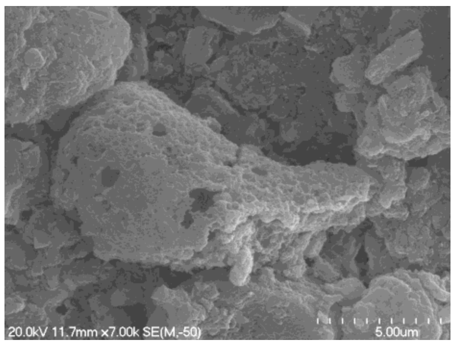

Cuniform

Elongate

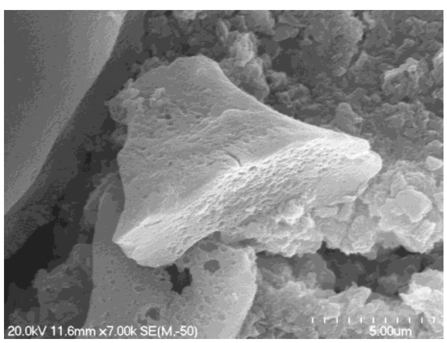

Conical

Saddle?

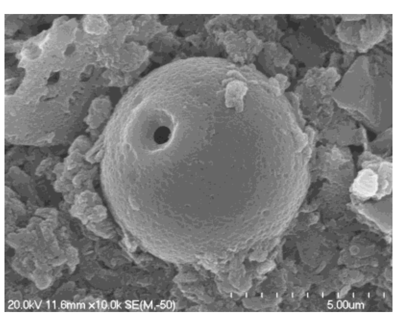

Spherical?

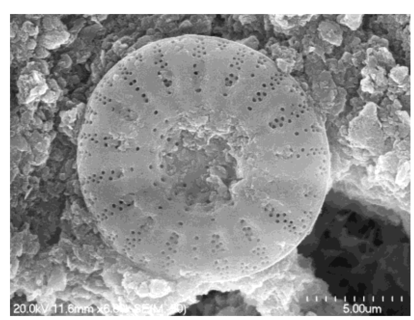

Diatom

Figure 3.4 Selected SEM images of phytoliths (+ diatom) within loess at Dansey Rd

Table 3.1 Summary table showing the eight phytolith types recognised in this study and their inferred plant type origin.

Name	Picture [a]	Origin [b]
Bilobate	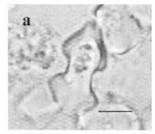 Bilobate short cell (grass origin)	Grass (warm climate)
Trapeziform	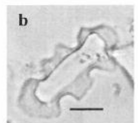 Trapeziform polylobate (grass origin)	Grass
Conical	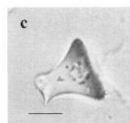 Conical short cell (grass origin)	Grass (e.g. *Chionochloa*)
Saddle	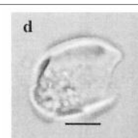 Saddle short cell (grass origin)	Grass (e.g. tussock grasses)
Elongate	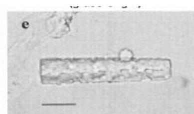 Elongate long cell (grass origin)	Grass (e.g. *Poa, Festuca*)
Cuniform	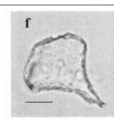 Cuniform bulliform (grass origin)	Grass (e.g. *Microlaena avenacea*)
Polyhedral	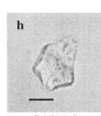 Polyhedral (tree/shrub origin)	tree/shrub
Spherical	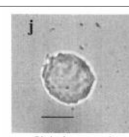 Globular granular (tree/shrub origin)	tree/shrub

a = Images from Carter (2007a)
b = from Carter (2000), Carter & Lian (2000), Almond *et al*. (2001), and Carter (2002)

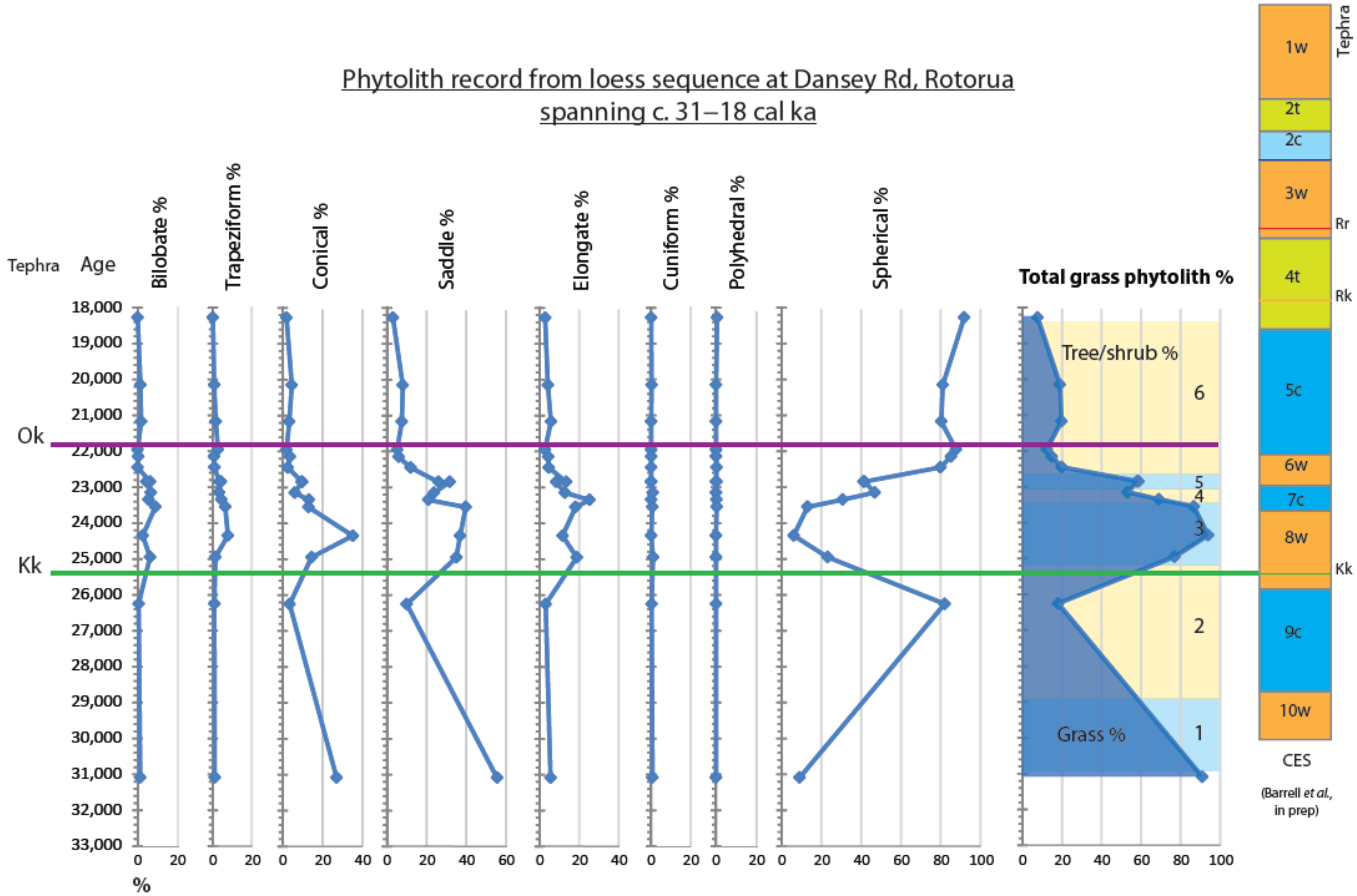

Figure 3.5 Phytolith diagram showing the percentage of each phytolith type recognised in selected loess samples at Dansey Rd. The final graph (far right) shows a summary of the total percentage of phytoliths with an inferred grass origin, compared to total percentage of phytoliths with an inferred tree/shrub origin. The coloured zones number 1-6 on the final graph indicate inferred climatic phases (yellow: warmer and wetter, blue: cooler and drier). The New Zealand climate event stratigraphy (CES) is shown for comparison.

3.4.4 Discussion

As noted earlier, phytolith morphology may be used to link phytoliths to a grass, tree and shrub or fern origin and in this way phytoliths can be used to reconstruct paleovegetation histories (Kondo *et al.*, 1994; Carter & Lian, 2000). In general, vegetation dominated by grass is assumed to represent colder, drier climatic conditions, whereas, an environment dominated mainly by trees is assumed to represent warmer, wetter climatic conditions (Kondo *et al.*, 1994; Carter & Lian, 2000)). However, in a study by Carter (2002), this pattern is reversed. Lake and fen development in a basin in Hawke's Bay were associated with warm wet conditions when grasses dominated, where as cooler, drier climatic conditions were associated with lake drainage and dry land conditions and consequently woody vegetation dominated.

For this present study, Dansey Rd site has most likely been a terrestrial site throughout the c. 33—18 cal ka time frame of interest, and hence the general assumption, where a dominance of grass correlates with cooler, drier climatic conditions and a dominance of trees correlates with warmer, wetter conditions, is accepted here. However, within this assumption there are also exceptions to the rule, for example bilobate type phytoliths have a 'warm' grass origin (Carter & Lian, 2000), contrary to the general link between grass and cold climatic conditions. Also, within this study I have not distinguished between phytoliths from tree versus shrub origins, which may therefore represent a combination of both cool and warm climatic conditions.

Another consideration in this study is the possible horizontal transport (reworking) of phytoliths which may have occurred before their deposition and preservation. Climatic conditions favourable to the horizontal movement of phytoliths (e.g. strong winds, dry climatic conditions and a sparsely vegetated landscape (Piperno, 2006)) were likely prevalent at this site throughout much, if not all, of the time frame of interest (Eden & Hammond, 2003; Barrell *et al.*, 2005; Shulmeister & McGlone, 2008; Williams *et al.*, 2010; Lorrey *et al.*, in press). Winds were dominantly westerly during the eLGM (Shulmeister &

McGlone, 2008) and it follows that any phytolith movement was probably dominantly in a westerly direction also. If this was the case, then it is expected that areas to the west of the field area (i.e. similar latitude) and hence experiencing similar climatic conditions, would likely have had a similar vegetation pattern to that present in the field area and therefore have likely produced a similar phytolith assemblage to that of the field area. For this reason, possibly horizontal phytolith movement is not considered to have produced phytoliths assemblages significantly non-representative of the vegetation pattern in the field area during the timeframe of interest.

The results of phytolith analysis in this study have been divided into 6 main climatic phases based on the total percentage of grass phytoliths compared to tree/shrub phytoliths (Figure **3.5**). I have attempted to link these phases with the events of the New Zealand Climate Event Stratigraphy (CES) (Barrell *et al.*, in prep.). Because of the coarse sampling resolution through parts of this record it is likely that some fluctuations which may have occurred in the vegetation assemblage throughout this time have not been noted.

Phase 1 (c. 31—29 cal ka) warm?

Phase 1 spans c. 31—29 cal ka and is dominated by grass phytoliths (mainly saddle type). This suggests that during phase 1 climatic conditions were cool. However, phase 1 occurs not long after the deposition of Unit L and the dominance of grass phytoliths at this time may potentially represent grass colonisation following this event rather than a response to climatic conditions. The limited number of samples between c. 31—25.2 cal ka makes it difficult to make inferences about likely climatic conditions throughout this time.

Phase 2 (c. 29—25.2 cal ka) warm

Phase 2 spans c. 29—25.2 cal ka and is dominated by tree/shrub phytoliths. It is possible that this increase in tree/shrub phytoliths during phase 2 may in part represent continued vegetation succession (under warm and wet climatic conditions) in response to the deposition of Unit L. Phase 2 may also correlate with warm event 10w of the CES.

Phase 3 (c. 25.2—23.4 cal ka) cold

Phase 3 spans c. 25.2—23.4 cal ka and is dominated strongly by grass phytoliths suggesting that climatic conditions during this time were likely cold and dry. The Kawakawa eruption and widespread tephra deposition occurred shortly before the beginning of phase 2 and consequently the dominance of grass phytoliths within this phase may in part be due to grass colonisation following this event. However, grass phytoliths continue to increase for a time after the deposition of the Kawakawa Tephra, until c. 24.4 cal ka, which seems to suggest that this increase may also have been influenced by climatic conditions. Pollen evidence from elsewhere during this time also generally indicates grassland or shrubland dominated the central North Island region (Newnham *et al.*, 1999). Phase 3 may correlate with cool event 9c of the CES.

Phase 4 (c. 23.4—23 cal ka) warmer

Phase 4 spans the short time between c.23.4—23 cal ka and is characterised by a decrease in grass phytoliths and increase in tree/shrub phytoliths which indicates slightly warmer and wetter conditions. Phase 4 may correlate with warmer event 8w of the CES.

Phase 5 (c. 23—22.6 cal ka) colder

Phase 5 spans the short time between c. 23—22.6 cal ka and is characterised by a short increase in grass phytoliths suggesting slight deterioration in climatic conditions. Phase 5 may correlate with cooler event 7c of the CES.

Phase 6 (c. 22.6—18 cal ka) warm

Phase 6 spans c. 22.6—18 cal ka and, in general, is dominated by tree/shrub phytoliths indicating warm climatic conditions. There is a slight increase in grass phytoliths following the Ok deposition which may in part be due to grass colonisation after this event.

However, the persistence of the slight increase in grass phytoliths (until c. 20.2 cal ka) suggests that this increase may also be a response to climatic conditions. Following c. 20.2 cal ka grass phytoliths decrease again and tree/shrub phytoliths increase. The early part of phase 6 (c. 22.6—21.9 cal ka) before Ok deposition may correlate with warm event 6w of the CES; the slightly cooler middle part of phase 6 (c. 21.9—19.4 cal ka) may relate to cooler event 5c of the CES; the late part of phase 6 (c. 19.4—18 cal ka) may correlate to transitional event 4t of the CES.

3.5 Magnetic susceptibility and pedogenesis

3.5.1 Introduction & background

Magnetic susceptibility (MS) is "a measure of the degree to which a substance can be magnetised. Its value is roughly proportional to the concentration of ferromagnetic and paramagnetic minerals within the sample" (Gonzalez *et al.*, 1999, p. 125). Numerous studies show that there is a relationship between paleoclimate and MS in Quaternary loess-paleosol sequences which correlates well with the MOI record (Zhou *et al.*, 1990; Maher & Thompson, 1991; Heller & Evans, 1995; Tang *et al.*, 2003; Dodonov, 2007). This relationship appears to be site specific and may depend on factors such as loess source material (Heller & Evans, 1995; Maher, 1998) and/or effective precipitation (Liu *et al.*, 2001). For example, in China, the Czech Republic, and Tajikistan, high MS values are associated with weathered paleosols (i.e. buried soil horizons with relatively more strongly developed pedogenic features imprinted on loess deposited under warmer and wetter climates) and low MS values are associated with less weathered loess material (deposited under cooler climates). However, in Alaska, Siberia, and Argentina, relatively high MS values are typically associated with loess and relatively low MS values are associated with paleosols (Maher, 1998). In Alaskan and Siberian loess at least, this opposite association (i.e. where low MS values correlate with paleosol) may be a result of the destruction of ferromagnetic minerals under water logged conditions caused by high effective precipitation which is enhanced during pedogenic conditions (Liu *et al.*, 2001).

Loess-paleosol sequences in the North Island generally appear to follow the Chinese model of higher MS values associated with paleosols than less-pedogenically altered loess, once the parent material effect has been removed (Palmer & Pillans, 1996). In a study by Palmer & Pillans (1996) of the MS of a loess-paleosol sequence in the Wanganui area the authors suggested that, in general, the loess-paleosol sequence followed the Chinese model of higher MS values associated with paleosols and lower values associated with loess, but that the effects of distal andesitic and rhyolitic tephra layers were also evident. Their MS record showed that increased MS values were associated with (titanomagnetite-rich) andesitic tephra layers and a sand dune unit and that low MS values were associated with two rhyolitic tephra layers (Rangitawa Tephra and Kawakawa Tephra). The authors noted that by disregarding the anomalies caused by the tephras there appeared to be a good match with the MOI record.

The means by which soils develop MS enhancement is not fully understood (Liu *et al.*, 2007), although a variety of mechanisms have been suggested (Singer *et al.*, 1996; Tang *et al.*, 2003). One well recognised mechanism of MS enhancement of soils (which eventually become buried paleosols) is the pedogenic hypothesis which suggests that MS enhancement of soils results from the in situ inorganic production of ultrafine magnetite grains during pedogenesis (Zhou *et al.*, 1990; Maher & Thompson, 1991; Heller & Evans, 1995; Tang *et al.*, 2003). It has been shown, involving the use of the citrate-bicarbonate-dithionite (CBD) extraction method, that fine grained (≤ 0.3 μm) magnetic particles (inferred to be of pedogenic origin) do contribute significantly to the MS value of paleosols (Xie *et al.*, 2009). The CBD extraction method can be used to remove ultrafine-grained magnetic particles of pedogenic origin (as well as some coarser magnetic grains) from bulk loess/soil samples (Xie *et al.*, 2009). MS data (Table 3.2) (D.J. Lowe, pers. comm., 2011) from an earlier study at the Tapapa Rd site using the CBD extraction method, suggest that this loess/paleosol/tephra sequence contains ultrafine-grained magnetic particles and that these particles probably contribute most significantly to the MS value of loess above the Okareka Tephra (Ok).

Table 3.2 Table showing the MS (measured using Bartington laboratory method) of loess, paleosols (i.e. stronger developed pedogenic layers) and tephra samples from Tapapa Rd site, Waikato, before and after CBD treatment (CBD treatment used to remove pedogenic magnetic minerals) and hence the contribution of pedogenic magnetic minerals to the MS of the units (data from D.J. Lowe, pers. comm., 2011).

Unit	Lab MS value (before CBD treatment) (SI units)	Lab MS value (after CBD treatment) (SI units)	Contribution of ultrafine-grained (pedogenic) magnetic minerals to MS
loess	238.69	141.56	97.13
Ok?	161.56	86.38	75.18
loess	140.56	66.25	74.31
Kk	120.25	54.69	65.56
Kk	112.06	54.13	57.93
loess	464.38	425.31	39.07
paleosol	696.63	657.75	38.88
Mangone/paleosol	517.06	513.13	3.93

Other suggested paleosol MS enhancement mechanisms include: (i) the removal of carbonate via leaching from paleosols and hence relative enrichment of ferromagnetic minerals in paleosols (though not considered in this study as loess in the study area is non-calcareous: Eden & Hammond, 2003); (ii) production of ultrafine magnetic minerals during vegetation decay; (iii) the differing loess and paleosol sediment sources; and (iv) fire where the addition of combusted vegetation may alter sediment MS values and/or where temperatures reach 200^{O}C and conversion of non-ferromagnetic minerals to ferromagnetic ones may occur (Tang *et al.*, 2003). In this study I adopt the well-recognised pedogenic hypothesis, acknowledging however that this hypothesis seems insufficient to fully explain MS enhancement in paleosols and recognising that further work is needed in this area to fully understand the mechanism of paleosol MS enhancement (Tang *et al.*, 2003).

The loess-paleosol sequences in the field area of this study are not classical Chinese loess-paleosol sequences (of quartzo-feldspathic origin), but rather have a tephric origin and a somewhat different mineralogy (McCraw, 1975). Hence it is reasonable to suspect that variations in the MS of sediments may potentially reflect a parent material effect, considering that some Okataina derived tephras contain notable amounts of primary Fe-Ti oxides (Lowe, 2011). Distal and very thin andesitic tephras from central North Island volcanoes (such as the 1995 Mt Ruapehu eruption fallout, Prince *et al*., 2008) may also constitute fine grained Fe-rich minerals to the land surface. In this study, in light of the potential parent material effect, we have analysed the MS of loess and tephra layers at multiple sites, both proximal and more distal sites to help identify any influence of parent material on the MS of sediments. We have also analysed a range of different paleoclimatic proxies to help "see past" this possible parent material effect.

Another consideration in this study is the interaction between loess accumulation rate, pedogenesis and tephra fall deposition. It is recognised that pedogenesis continues to occur at the same time that loess is being deposited, in most locations, resulting in a loess column in which each part has at one point in time been a soil A horizon (Almond & Tonkin, 1999; Lowe & Tonkin, 2010). Such pedogenesis can occur because in many locations in New Zealand the rates of loess accumulation are usually very slow, around 3—10 mm per century on average (Lowe *et al.*, 2008a). The degree to which pedogenesis influences loess can be thought of as 'competition' between the rate of loess accumulation and pedogenesis governed by prevailing climatic conditions and other features (Verosub *et al.*, 1993). During times of cold climate when loess accumulation rates are relatively high, the pedogenic imprint on the loess will be minimal, but still evident, as the rising surface of the loess is not exposed long enough to pedogenic processes for strong soil horizon development to occur before being buried by further loess accumulation. During times of warmer and wetter climate when loess accumulation rates are minimal or stop altogether, the imprint of pedogenesis on the loess column will be stronger as the loess surface is exposed to pedogenic processes for longer and climatic conditions are more favourable for soil formation (Lowe & Tonkin, 2010). Additions of thin tephras to the loess column act in a similar way to loess deposition in that pedogenesis can continue to act on the loess column. However, thick tephra fallout (about 20-30 cm or greater – see Lowe & Tonkin, 2010) may terminate the accumulation of loess, shutting the loess-soil below the tephra layer off from the reach of most pedogenic processes, and causing the loess to begin accumulating afresh above the tephra layer (Lowe & Tonkin, 2010).

Advantages of MS of sediment as a paleoclimatic proxy

- MS is able to be measured relatively inexpensively and easily in the field.
- MS may aid in delineating phases of weak pedogenesis which may not be visible, as more strongly developed evidence of pedogenesis stratigraphically.

Limitations of MS of sediment as a paleoclimatic proxy

- Within tephric loess-paleosol sequences, climate-related MS signals derived from pedogenesis may be masked by a parent material effect (as discussed earlier) (Palmer & Pillans, 1996).
- Stratigraphic limitations (discussed in Chapter 2), such as hidden unconformities, stratigraphic disturbances, thickness of tephra layers and tephra mixing, may result in variations in MS records that cannot be easily related to climatic and/or other parameters.

3.5.2 Methods

MS measurements were made at sections uncovered at each of the thirteen field sites and using a 'magROCK' magnetic susceptibility meter. Each site was cleared of vegetative matter and scraped down to give a somewhat flat profile surface. Tephra layers were identified in each section. Usually 5 measurements of MS were taken at approximately 5 cm intervals, generally from top to base of the section. The measurements at each 5 cm interval were averaged and graphed for each site, excluding the tephra layers (i.e. as tephra-free loess-soil sequences). All MS values noted here are x10^5 (dimensionless units).

3.5.3 Results

MS records spanning the time frame from c. 33 to 15.5 cal ka were recorded at Tapapa Rd, Dansey R, Oturoa Rd, Taumata Rd and Belk Rd (Figure 3.6). MS records spanning part of the timeframe between c. 33—15.5 were recorded at the other eight field sites (Figure 3.6). The longest MS record was recorded at Dansey Rd (spanning c. 33—9.5 cal ka). Relatively high resolution records were recorded at Dansey Rd, Oturoa Rd and Maniatutu Rd and were relatively well constrained chronologically by the presence of multiple marker tephras. Some other sites, such as Dalbeth Rd, also produced relatively high resolution MS records although only partial sequences were obtained.

At most sites, including Dansey Rd, Oturoa Rd and Maniatutu Rd (i.e. sites with high resolution records), there appears to be a general decrease in MS values, from around 400 units (at some sites about 600 units) to around 150 units, between Unit L and Kk tephra. There are peaks (high values) in MS values during this time at Oturoa Rd, Maniatutu Rd and Belk Rd (and marginally at Tapapa Rd). At Oturoa Rd, Maniatutu Rd, Glue Pot Rd and Taumata Rd, high MS values appear to correlate with field evidence for paleosol development (i.e. darker richer soil colours, usually with relatively lower soil colour value) soon after the time of Unit L. At Belk Rd a peak in MS values (around 750 units) correlates with a paleosol near the time of Kk tephra.

At most sites MS values are lowest following the Kk tephra (about 150 units). Following this minimum, there appears to be a general increase in MS values, with some sites reaching a modest but distinct peak (around 250 units) between c. 23—24 cal ka, followed by a decrease to low MS values (around 200 units) which continue until c. 21.5 cal ka. At Oturoa Rd and Hamurana Rd, these low MS values appear to occur a little later than at the other sites. Between c. 21.5—20.5 cal ka, a number of sites show a peak in MS values (around 350 units). This peak is eventually followed by a decrease in MS values again, to around 200 units, until c. 18 cal ka. MS values are variable between c. 18—15.5 cal ka. Some sites show a slight increase whereas others show a slight decrease during this time.

After c. 15.5 cal ka, MS values were recorded only at Dansey Rd. Between c. 15.5—13.5 cal ka there is a peak in MS values (around 300 units) followed by a decrease between c. 13.5—13 cal ka (to about 200 units). MS values increase and then decrease slightly between c. 13—9.5 cal ka.

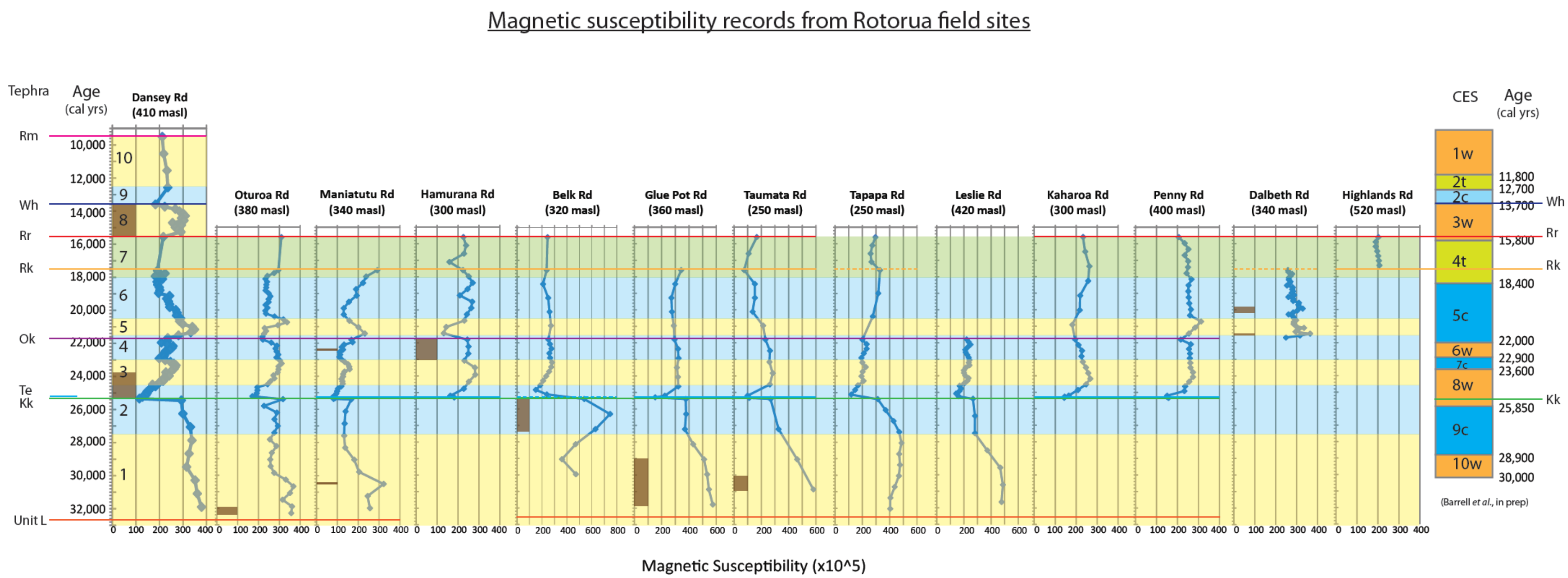

Figure 3.6 Magnetic susceptibility through loess sequences at field sites. Brown bars represent paleosol development at corresponding sites based on visual field observation (see text). The coloured zones numbered 1-10 indicate generalised climatic phases inferred from all the MS records from this study (yellow: warmer and wetter; blue: cooler and drier; green: transitional climatic conditions; see text for further explanation). The New Zealand climate event stratigraphy (CES) is shown for comparison.

.

3.5.4 Discussion

As noted earlier, loess-paleosol sequences in the North Island appear to generally follow the Chinese MS model (Maher, 1998) of relatively higher MS values associated with more strongly developed soil features ("paleosol") formed under warmer and wetter climates and relatively lower MS values associated with more weakly developed loess formed during cooler climates and with a weaker pedogenic imprint. Because the visible tephra layers have been removed from the MS records in Figure 3.6 it is then assumed that variations within the loess, not immediately adjacent to known tephra layers, represent climatic signals. It is possible, however, that the loess sequences contain thin hidden 'cryptic' tephras. The general trends in the MS records have been summarised into seven climatic phases as outlined below and possible links between these phases and the New Zealand Climate Event Stratigraphy (CES) (Barrell *et al.*, in prep.) are noted.

Phase 1 (c. 32.7—27.5 cal ka) warm

Phase 1 spans c. 32.7 cal ka (Unit L) to c. 27.5 cal ka. Phase 1 is generally characterised by high MS values representing warm conditions, although a decrease in MS values at some sites at c. 29 cal ka suggests that climate began to cool at this time consistent with the CES as well as Vandergoes *et al.* (2005) and Newnham *et al*. (2007a) who both record the start of the extended Last Glacial Maximum (eLGM) at c. 29 cal ka. At Maniatutu Rd, Oturoa Rd, Glue Pot Rd and Taumata Rd, high MS values generally correlate with field evidence of paleosol development (stronger soil features) which adds support to warm climatic conditions prevailing during at least part of this phase. It is likely that phase 1 correlates with event 10w of the CES.

Phase 2 (c. 27.5—24.5 cal ka) cooling & cold

Phase 2 spans c. 27.5—24.5 cal ka and is characterised by generally decreasing MS values at most sites, representing cooling climatic conditions. However, at Belk Rd alone there is a significant peak in MS values during this time which correlates with field evidence for paleosol development. However, it may be that hidden unconformities or stratigraphic disturbances have affected the MS record at Belk Rd as other stratigraphic evidence seems to suggest (see Chapter 2). Also, it is unlikely that the paleosol development and enhanced MS values relate to a local climatic imprint at the Belk Rd site during this time because near-by sites (i.e. Glue Pot Rd & Taumata Rd) do not record a similar trend; rather they support a climatic cooling trend during this time.

At most sites, the lowest MS values throughout the loess column occur at c. 25 cal ka just after the deposition of the Kk. It is unclear whether these low values are a result of a parent material effect from Kk or a climatic effect, or both. It is likely that the deposition of the thick Kk (typically greater than 20 cm, except at some distal sites) caused retardant upbuilding, shutting-off the antecedent soil from most surface soil forming processes and causing developmental upbuilding and topdown pedogenic processes to begin again at the new land surface. It is likely that phase 2 correlates with event 9c of the CES, the beginning of and the first stadial of the eLGM (extended Last Glacial Maximum)/LGCP (Last Glacial Coldest Period).

Phase 3 (c. 24.5—23 cal ka) warm

Phase 3 spans c. 24.5—23 cal ka and is generally characterised by a peak in MS values representing warmer climatic conditions. This peak is most evident at Dansey Rd, Maniatutu Rd, Hamurana Rd and Kaharoa Rd. At Oturoa Rd and Penny Rd this peak is sustained until c. 22 cal ka.

Not all sites show a distinctive peak in MS values during this time. At some distal north and northwest sites, such as Belk Rd, Glue Pot Rd, Taumata Rd, Tapapa Rd and Leslie Rd, MS values appear to remain relatively constant and do not show much variation in MS during this time. This constancy could be a result of the more northerly location of these sites resulting in a more stable and warmer climate. Another possible explanation for the trend seen in MS values at these sites could relate to the possible inability of the MS method used here to detect fine-scale variations in climate due to low loess accumulation rates (i.e. as a consequence of tephra thicknesses being reduced because of increasing distance from the main source at Okataina and Taupo) combined with the use of a too coarser sampling resolution. It is likely that phase 3 correlates with event 8w of the CES (first eLGM interstadial).

Phase 4 (c. 23—21.5 cal ka) cool & variable

Phase 4 spans c. 23—21.5 cal ka (including the time of the Ok deposition) and is generally characterised by low MS values indicating cool variable climatic conditions. At Oturoa Rd and Penny Rd MS values suggest that cool conditions there began later, c. 22 cal ka rather than c. 23 cal ka. At Hamurana Rd MS values suggest that cool conditions persisted up until c. 21 cal ka. It is unclear whether these apparent variations in the time of phase 4 relate to local climate anomalies or stratigraphic or measurement limitations. Some distal north and northwest sites do not appear to show significant cooling trends during this time, possibly due to reasons discussed for the previous "phase 3" section. It is likely that phase 4 correlates with event 7c (second stadial of the eLGM) of the CES.

Phase 5 (c. 21.5—20.5 cal ka) warm

Phase 5 spans c. 21.5—20.5 cal ka (just after Ok deposition) and is generally characterised by a peak in MS values possibly indicating warm climatic conditions. This peak is most evident at Dansey Rd, Oturoa Rd, Maniatutu Rd and Penny Rd, although the timing of this peak appears to vary slightly. There is no strong field evidence of paleosol development during this time at most sites, except at Dalbeth Rd where field evidence suggests paleosol development around the end of phase 4 and start of phase 5. It is possible that peak MS values during phase 5 may be a result of an unknown tephra deposition and hence not climate related. Some distal north and northwest sites do not appear to show peak MS values during this time, possibly because of reasons discussed in the phase 3 section. It is likely that phase 5 correlates with event 6w (second interstadial of the eLGM) of the CES.

Phase 6 (c. 20.5—18 cal ka) cool

Phase 6 spans c. 20.5—18 cal ka and is generally characterised by low MS values indicating cool climatic conditions. Low MS values during phase 6 are most evident at Dansey Rd, Oturoa Rd and Maniatutu Rd. Hamurana Rd shows variable MS values during this phase. Some distal north and northwest sites do not appear to show a significant change to lower MS values during this time, possibly because of reasons discussed in the phase 3 section. It is likely that phase 6 correlates with event 5c (third stadial of the eLGM) of the CES.

Phase 7 (c. 18—15.5 cal ka) variable

Phase 7 spans c. 18—15.5 cal ka (including the times of Rk (c. 17.5 cal ka) and Rr (c. 15.6 cal ka) deposition) and trends in MS values are variable from site to site. Some sites show a general but subtle increase in MS values, whereas others show a slight decrease or variability in MS values during this phase. At a number of sites only a few MS measurements were obtained for this phase as a result of a lack of loess thickness which indicates low loess accumulation rates and hence probably warmer climatic conditions and an increase in landscape stability (i.e. as discussed in Newnham *et al.* 2003). Phase 7 possibly correlates with event 4t (Post-Termination 1 transition) of the CES.

Phase 8 (c. 15.5—13.8 cal ka) warm

Phase 8 spans c. 15.5—13.8 cal ka and has high MS values correlating in part to field evidence of paleosol development and indicating warm climatic conditions. It is likely that phase 8 corresponds with event 3w of the CES.

Phase 9 (c. 13.8—12.8 cal ka) cool

Phase 9 spans c. 13.8—12.8 cal ka (including the time of the Wh deposition, c. 13.6 cal ka) and has lower MS values than the previous phase 8 indicating cooler climatic conditions. It is possible that phase 9 correlates with the cool Late Glacial Reversal (LGR) phase identified at Kaipo bog (Hajdas *et al.*, 2006) and elsewhere (Alloway *et al.*, 2007) and also with the Antarctic Cold Reversal (ACR) (although offset) (EPICA Community Members, 2006) identified in the EPICA ice core record. Phase 9 may relate to event 2c of the CES.

Phase 10 (c. 12.8—9.5 cal ka) variable

Phase 10 spans c. 12.8—9.5 cal ka (ending at the time of the Rm deposition, c. 9.5 cal ka) and shows little variability in MS values, apart from a slight increase followed by a slight decrease in MS values. Phase 10 may correlate with event 2t and/or event 1w of the CES.

Chapter 4 Chemical paleoclimatic proxies

4.1 Introduction

This chapter outlines the chemical properties of the loess sequence analysed through the stratigraphic column at the Dansey Rd master site as potential paleoclimatic proxies, including total carbon content, carbon isotopes and potassium and phosphorus content. Each property is discussed in turn with a brief background summarising the basis of the property as a potential paleoclimatic proxy, an outline of the analytical methods used, followed by a presentation and discussion of the results.

4.2 Total carbon content of loess

4.2.1 Introduction and background

Inputs of carbon into soil may occur by the addition of organic matter (i.e. plant and animal residues). Outputs of carbon may occur by microbial decomposition of organic matter and subsequent loss of CO_2 to the atmosphere and/or leaching, and through harvesting (e.g. cropping) in farming or forestry activities. Internal cycling and transformation of carbon may also occur, in particular, organic matter may be transformed into humus, a more resistant form of organic matter (McLaren & Cameron, 2008). Outlined below are a number of factors which may affect the amount of carbon present in a soil (McLaren & Cameron, 2008).

- **Temperature** can affect the rate of microbial decomposition and plant productivity. In general, cold temperatures act to increase soil carbon content as a result of decreased rates of microbial decomposition.
- **Rainfall** can affect plant productivity. In general, increased rainfall results in an increase in organic matter input into the soil which may then result in an increase in the soil carbon content. Rainfall also influences the extent of leaching which

occurs in a soil and hence the type of clay formation. Clay type may in turn influence the carbon content of a soil (see *soil texture* below).

- **Soil pH** conditions can affect microbial activity. Highly acidic soils are not favourable to the functioning of microbial decomposers and hence soil carbon is usually increased in acidic soils.
- **Soil drainage** can affect microbial activity. Water logging may create anaerobic conditions in the soil which are unfavourable to the function of most microbial decomposers and consequently result in a build up of carbon in these soils.
- **The availability of nitrogen** can affect microbial decomposition. Decomposers need sufficient nitrogen to function and consequently in conditions where nitrogen is limited it is likely that not all organic matter will be decomposed resulting in an increase in soil carbon content.
- **Soil texture** may indirectly affect microbial activity by influencing the susceptibility of the soil to water logging and anaerobic conditions (e.g. fine textured soils may experience anaerobic conditions unfavourable to organic matter decomposition relatively more often/longer than coarser textured soils and hence have a greater carbon content). Soil texture, as a measure of clay content, may also affect the amount of carbon present in a soil. Organic matter may become 'locked away' within clay complexes, particularly allophane (Churchman & Lowe, 2012), from microbial decomposition.

Soil carbon content may give an indication of prevailing climatic conditions at the time of soil development. As mentioned previously, soil carbon contents are likely to increase during cool temperatures and moist climatic conditions. Also, increased carbon contents in fine grained soils, indicating protection of organic matter by the formation of clay complexes, may indicate the dominant presence of allophane clay. Soils dominated by allophane indicate strong leaching has occurred, and therefore indicate wetter climatic conditions, whereas soils dominated by halloysite indicate less leaching and hence relatively drier climatic conditions (Lowe, 1995). A study by Childs & Searle (1975) showed some correlation between paleosols and relatively increased soil carbon contents in two loess sequences in New Zealand.

4.2.2 Methods

Loess samples were collected each 5 cm through the loess sequence between Unit L and Rr Tephra at Dansey Rd and were analysed for total carbon and nitrogen contents (excluding tephra layers). Measurements were carried out on oven-dried, ground samples. Approximately 0.25 g of each sample was weighed into individual tin capsules. Samples were then analysed for total carbon and nitrogen contents, using a LECO TruSpec Carbon/Nitrogen Determinator at The Waikato Stable Isotope Unit (WSIU), University of Waikato, Hamilton. Total carbon content results and C:N ratio values [(total carbon %/total nitrogen %)/(14/12)] were graphed against age, using tephra layers as age markers (apparent outliner points were removed).

4.2.3 Results

Carbon content

The carbon content of loess at Dansey Road in most cases is very low; however, there are variations in carbon content throughout the loess sequence (Figure 4.1). Between the time of Unit L and Kk deposition there is a general decrease in carbon content from about 0.22 % to 0.20 %. Between c. 25.4 cal ka (time of Kk deposition) and c. 23.8 cal ka, carbon content is variable with two peaks occurring at c. 25 cal ka (0.30 %) (possibly a result of impact of Kk) and c. 24.1 cal ka (0.25 %). Carbon content is low (0.16—0.20 %) between c. 23.8—21 cal ka with a slight increase between c. 22.6—23 cal ka and a peak (about 0.25 %) at c. 21.8 cal ka (possibly a result of impact of Ok). Between c. 21—18.2 cal ka, carbon content increases significantly from about 0.20—0.70 % with a slight peak occurring c. 19.8 cal ka and the maximum peak occurring c. 18.2 cal ka. Between c. 18.2—15.5 cal ka carbon content decreases to about 0.35 %.

C:N ratio

The C:N ratio values vary between about 2—7 through the loess sequence at Dansey Rd (Figure 4.1). Between c. 32—24 cal ka the C:N ratio values are variable between about 3—4. Between c. 24—20.5 cal ka the C:N ratio values decrease to about 2.5—2. There is a general increase in C:N ratio values to about 6.5 between c. 20.5—18 cal ka. C:N ratio values generally decrease again, to about 4, between c. 18—15.5 cal ka.

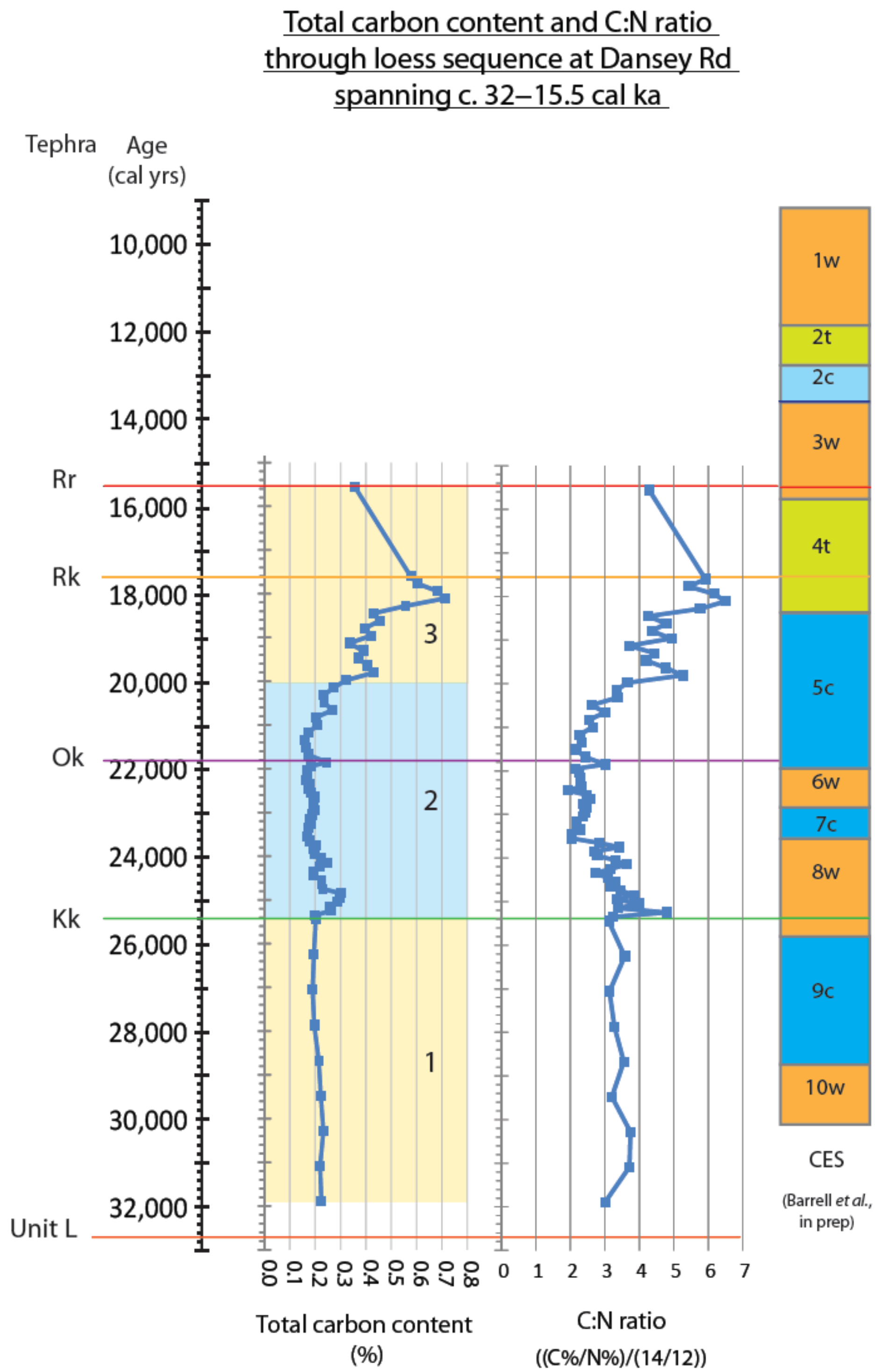

Figure 4.1 Total soil carbon content and C:N ratio values through loess sequence at Dansey Rd. Coloured zones numbered 1—3 on total carbon graph indicate inferred climatic phases (see text for explanation). The New Zealand climate event stratigraphy (CES) is shown for comparison.

4.2.4 Discussion

There is variation in carbon content through the loess sequence at Dansey Rd, the most obvious being the general increase in carbon values beginning c. 20 cal ka and reaching a peak c. 18 cal ka. The carbon content record does not appear to record finer scale variations as seen in some other proxy records in this study. This may be a result of very low soil carbon contents during this time. As outlined earlier, variation in soil carbon content can be due to the influence of a number of different factors. At Dansey Rd low soil pH is not likely to have been the cause of the main increase in soil carbon content as there is no visual evidence (e.g. podzolisation) indicating strongly acidic soil conditions during this time. Similarly, water logged conditions are not likely to have caused the increased soil carbon contents as the lack of low chroma colours and redox segregations throughout the sequence indicates the soil has been generally well drained. It appears limited nitrogen availability has not been the likely cause of the increase in soil carbon content as the low C:N ratio values (between about 2—6, Figure 4.1) indicate that nitrogen was not limiting the microbial decomposition process (C:N ratio values above about 25 suggest nitrogen may be limiting microbial decomposition, McLaren & Cameron, 2008). It is, however, likely that the variation in carbon contents seen at Dansey Rd may be due to the influence of rainfall and/or temperature as discussed below.

Based on other results from this study (e.g. soil $\delta^{13}C$ values) it appears that rainfall/water availability varied through time at Dansey Rd and, in general, it appears that between c. 32—25.4 cal ka (phase 1) and c. 20—15.5 cal ka (phase 3) climate was relatively wetter than it was between c. 25.4—20 cal ka (phase 2). During these times of wetter climate (phases 1 and 3) it is possible that plant productivity increased, resulting in higher inputs of organic matter and hence possibly higher soil carbon contents. Although results show that soil carbon content increased during phase 3, results do not show a similar increase in soil carbon content during phase 1. A possible explanation for this apparent anomaly may be that climatic conditions were not quite as moist and hence plant productivity and organic matter input may not have been as high during phase 1 compared to phase 3.

Some clay mineralogy results from a loess and tephra sequence spanning this timeframe from the Tapapa sequence (D.J. Lowe, pers. comm., 2011), near Rotorua, show that halloysite (a clay type indicative of relatively drier climatic conditions, Lowe, 1995) was more dominant during phases 1 and 2 than it was during phase 3. The clay mineralogy results also show that allophane (a clay type indicative of relatively wetter climatic conditions, Lowe, 1995) was more dominant during phase 3 than it was during phases 1 and 2. The allophane itself, where present, may also have acted to protect organic matter from microbial decomposition and hence increase the soil carbon content (Churchman & Lowe, 2012).

It is recognised, based on other New Zealand paleoclimatic proxy records (Barrell *et al.*, in prep.), that temperature also varied throughout the time represented by the loess sequence at Dansey Rd and, in particular, that a change from dominantly cool and variable climatic conditions (dominant since c. 29 cal ka) to dominantly warmer and variable conditions occurred around the time of deposition of Rk (i.e. c. 17.5 cal ka) (Newnham *et al.*, 2003). Climatic conditions between c. 30—29 cal ka (Barrell *et al.*, 2005) and possibly up to c. 25.4 cal ka (as suggested by other proxy records from this study) were also likely dominantly warm. In general, increased temperature results in increased rates of microbial decomposition and hence decreases soil carbon content. At Dansey Rd, the decrease in soil carbon content which begins c. 18 cal ka and the low soil carbon values between c. 32—25.4 cal ka may be a result of increasing temperatures, resulting in increased rates of decomposition of available organic matter and hence causing an overall decrease in soil carbon content.

In summary, the soil carbon content at Dansey Rd seems to confirm that between c. 32—20 cal ka climatic conditions were dry or somewhat moist whereas between c. 20—15.5 cal ka climatic conditions were moist and from c. 18 cal ka temperatures began to increase.

4.3 Carbon isotopes

4.3.1 Introduction and background

Sheldon & Tabor (2009) suggested that the $\delta^{13}C$ value of a soil will reflect the $\delta^{13}C$ value of the vegetative material from which the carbon was derived; hence, variations in the $\delta^{13}C$ value of the vegetative material will likely be reflected in the $\delta^{13}C$ value of the associated soil. The $\delta^{13}C$ value of vegetative material may be influenced by a number of different factors including the type of photosynthetic pathway used by the plant (e.g. C_3 or C_4 type plants) and water availability (Swap *et al.*, 2004). Plants which use a C_3 type photosynthetic pathway, and the resulting soil organic matter produced, typically have $\delta^{13}C$ values between about -32 ‰ to -22 ‰, whereas C_4 type plants, and the resulting soil organic matter produced, typically have $\delta^{13}C$ values between about -16 ‰ to -9 ‰ (Rogers, 2010). Water availability/mean annual rainfall has also been shown to influence the $\delta^{13}C$ value of plant vegetative material (Swap *et al.*, 2004), particularly that of C_3 type plants (Murphy & Bowman, 2009). As water availability decreases, plant water-use efficiency increases and this results in an increase in the $\delta^{13}C$ value of the vegetative material (Swap *et al.*, 2004; Murphy & Bowman, 2009). Also, plants that are adapted to drier conditions typically have higher water-use efficiencies and therefore higher (less negative) $\delta^{13}C$ values (Murphy & Bowman, 2009). Sheldon & Tabor (2009) suggested that this pattern of higher $\delta^{13}C$ values associated with low water availability in plants may also be recorded in paleosols. Also, higher soil $\delta^{13}C$ values in low productivity soils may be caused by diffusion of more atmospheric-derived CO_2 into the soil, relative to plant-derived carbon, as a result of incomplete respiration occurring in these soils (Sheldon & Tabor, 2009).

4.3.2 Methods

Loess samples from Dansey Rd were collected every 5 cm through the loess sequence between Unit L and Rr Tephra and were then analyzed for $\delta^{13}C$ and $\delta^{15}N$ contents.

However, $\delta^{15}N$ results are not presented here as their paleoclimatic significance was not clear. The $\delta^{15}N$ results are shown in appendix 4. Measurements were carried out on oven-dried, ground samples. Approximately 55 mg of each sample was weighed into individual tin capsules. Samples were then analysed for $\delta^{13}C$ content, using a LECO TruSpec Carbon/Nitrogen Determinator at the Waikato Stable Isotope Unit (WSIU) at The University of Waikato in Hamilton. Results (excluding apparent outliers) were then graphed against age (the derivation of the loess timescale was described in Chapter 2).

4.3.3 Results

Repeats of selected samples were analysed to assess the variation in $\delta^{13}C$ contents within samples and hence obtain a measure of error (Table 4.1). Results show a maximum variation in $\delta^{13}C$ contents of about ± 0.13 ‰ within samples. The amounts of carbon in most samples, particularly those earlier than c. 19.8 cal ka, were well below the optimum required for $\delta^{13}C$ analysis (similarly, nitrogen contents were also well below the optimum required for $\delta^{15}N$ analysis) (see Appendix 4) and this may have resulted in some further (non-quantified) error in the measurement of the $\delta^{13}C$ values. One sample directly prior to the deposition of the Ok tephra appeared to be an outlier and was subsequently removed from the record.

All samples at Dansey Rd have negative $\delta^{13}C$ values (Figure 4.2). Between c. 32-25.4 cal ka, the $\delta^{13}C$ values are around -24.5 ‰. Around the time of the Kk Tephra, the $\delta^{13}C$ values increase (become less negative) significantly to about -22.7 ‰. Between c. 25.4-24 cal ka, there is a general decrease in the $\delta^{13}C$ values, reaching a trough of about -24 ‰. The $\delta^{13}C$ values increase again to about -23.3 ‰ between c. 24-22.6 cal ka. Between c. 22.6-21.8 cal ka, the $\delta^{13}C$ values become more negative again, reaching a trough of about -24.3 ‰ at c. 22.2 cal ka. Another increase in the $\delta^{13}C$ values occurs between c. 21.8-20.4 cal ka, reaching a peak of about -22.8 ‰, although it is interrupted by a decrease at c. 21.2 cal ka. Between c. 20.4-15.6 cal ka, there is a general decrease in the $\delta^{13}C$ values from about -23.7 to -25.7 ‰.

Table 4.1 Repeat $\delta^{13}C$ analysis on selected samples to assess potential variation within samples.

Sample Number	$\delta^{13}C$ (‰)	Maximum $\delta^{13}C$ variation between repeat samples
D7	-24.73	
D7	-24.76	
D7	-24.68	0.09
D49	-23.35	
D49	-23.23	0.12
D50	-23.35	
D50	-23.23	0.12
D51	-23.46	
D51	-23.33	
D51	-23.40	
D51	-23.20	0.26
D64	-23.34	
D64	-23.46	0.12
D65	-23.12	
D65	-22.96	0.16

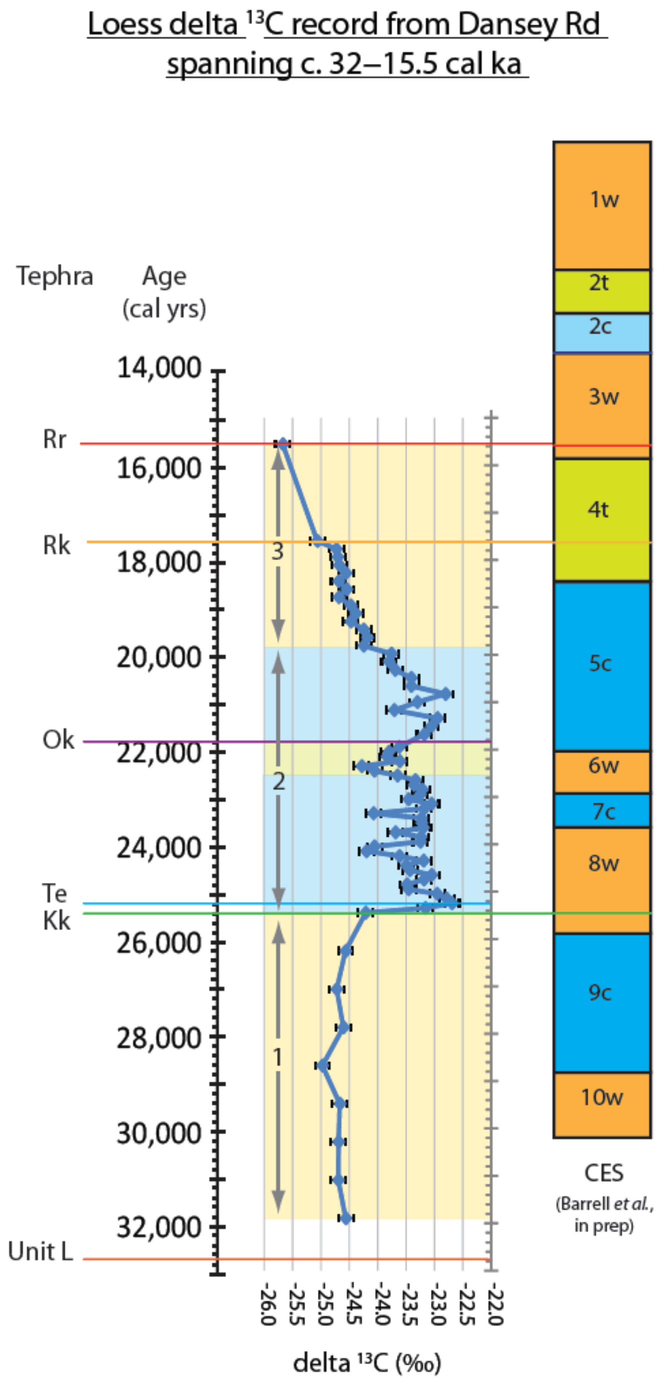

Figure 4.2 Soil $\delta^{13}C$ record through loess column at Dansey Rd. The coloured zones numbered 1-3 indicate inferred climatic phases from this study (yellow: wetter; blue: drier) (see text for explanation). The New Zealand climate event stratigraphy (CES) is shown for comparison.

4.3.4 Discussion

In this study, where virtually all plants and hence vegetative material, growing at the time of loess deposition/soil development were C_3 type plants (C. Hendy pers. comm., 2011), I assume that variations in soil $\delta^{13}C$ values reflect variability in water availability through time rather than the influence of differing amounts of C_3 vs C_4 type vegetative material. Lorrey et al. (in press) suggested that at c. 21 cal ka (i.e. during in the LGM) in New Zealand climatic conditions were generally both drier and cooler, however, some regional variations in climate due to the effects of different climate regimes on different parts of the country were also likely recognised (Lorrey *et al.*, in press). Variability in the diffusion of atmospheric-derived CO_2 into the soil may also have affected soil $\delta^{13}C$ values (Sheldon & Tabor, 2009), although this variable was not analysed in this study.

I have identified three main phases in the $\delta^{13}C$ record (Figure 4.2) and have linked these to times of relatively drier or wetter environmental conditions. I have also attempted to draw some comparisons between results of the $\delta^{13}C$ record and the New Zealand Climate Event Stratigraphy (CES) of Barrell *et al.* (in prep.).

Phase 1 (c. 32—25.4 cal ka) wetter

Phase 1 spans c. 32 to 25.4 cal ka and is characterised by low $\delta^{13}C$ values indicating relatively wetter conditions. It is likely that that phase 1 relates to warm event 10w of the CES.

Phase 2 (c. 25.4—19.8 cal ka) drier

Phase 2 spans c. 25.4 to 19.8 cal ka and is generally characterised by higher (and more variable) $\delta^{13}C$ values indicating drier climatic conditions, which may also correlate at times with cooler conditions (Lorrey *et al.*, in press). The lower boundary of this phase (c. 25.4 cal ka) coincides with the deposition of the Kk Tephra. It is possible that the deposition of this widespread tephra may have influenced soil $\delta^{13}C$ values at this time through the associated disturbance of landscapes and ecosystems (e.g. Manville & Wilson, 2004).

Within phase 2 there is a zone, between c. 22.5 to 21.8 cal ka, where $\delta^{13}C$ values, in general, appear to decrease slightly possibly indicating slightly wetter and possibly warmer climatic conditions. The Ok Tephra deposition occurred at c. 21.9 cal ka and may also have influenced $\delta^{13}C$ values, but because the general decrease in $\delta^{13}C$ values appears to begin somewhat earlier than the deposition of Ok (i.e. c. 22.2 cal ka), at a time when some other proxies in this study do not suggest a parent material effect on the generation of loess, it is possible that $\delta^{13}C$ values are responding to a climatic influence. It is thus suggested here that phase 2 relates mainly to cold events 9c, 7c and 5c of the CES and the wetter zone within phase 2 may relate to either 8w or 6w of the CES.

Phase 3 (c. 19.8—15.5 cal ka) wetter

Phase 3 spans c. 19.8 to 15.5 cal ka and is characterised by significantly decreasing $\delta^{13}C$ values indicating increasingly wetter conditions. It appears that the wettest part of the record occurred at the end of this phase. Rk and Rr were also deposited during this time (c. 17.5 and 15.6 cal ka respectively). It is likely that phase 3 correlates to transitional event 4t and warm event 3w of the CES.

4.4 Potassium and phosphorus weathering

4.4.1 Introduction and background

In general, an increase in temperature and water availability causes an increase in the rate of weathering of soils (McLaren & Cameron, 2008). Weathering can result in soil mineralogical transformations, such as the release of ions from minerals by the process of hydrolysis, and subsequent synthesis to form clay minerals, or loss from the profile via leaching (McLaren & Cameron, 2008). One such element which may undergo transformation during the weathering processes is potassium (K). During weathering, K is released out of primary minerals such as micas and potassium-feldspars and may then be integrated into secondary clay minerals or freed into soil solution, where it is available for plant use or leaching (Palmer & Pillans, 1996). This may result in a unique K content pattern through a weathered soil profile, where the A horizon (although experiencing loss of K via leaching also experiences K input via plant and animal waste and decay) and C horizon (containing unweathered primary minerals) have relatively higher K contents than the leached B horizon (Palmer & Pillans, 1996). Phosphorus is another mineral which may undergo transformation during the weathering process and can then be lost from soils via leaching (McLaren & Cameron, 2008). However, P is less susceptible to leaching compared to K (Palmer & Pillans, 1996).

In loess soils especially, where each part of the soil profile has at one point been an A horizon and hence susceptible to weathering and leaching of K, the degree to which K losses have occurred will depend on the intensity of weathering and the duration of weathering which has occurred (Palmer & Pillans, 1996). Increased weathering occurs under warmer climatic conditions (which also coincides with nil or low loess accumulation rates (Lowe & Tonkin, 2010), and increased leaching occurs with increased water availability (McLaren & Cameron, 2008). A study carried out in New Zealand by Hay *et al*. (1976) concluded that the K content of loessial-soils decreased as the rate of loess accumulation decreased and rainfall increased.

A study by Palmer & Pillans (1996) showed that changes in K content through a loess sequence can be a useful paleoclimatic proxy (when interpreted along with stratigraphic evidence). Palmer & Pillans (1996) analysed K contents through a tephra-containing loess column from the Wanganui region. They assume that the lowest K values correlate with the strongest phases of weathering and enhanced soil development (i.e. “paleosols”) occurring during interglacials, and that the highest K values correlate with the weakest phases of weathering occurring during glacials. The authors also noted that some variation in K values may be a result of tephra-derived mineral input during tephra deposition (e.g. Kawakawa Tephra shows high values relative to the loess at this study site). Another New Zealand study by Childs & Searle (1975) also supports the use of variations of K values through loess deposits as a means of delineating phases of stronger soil weathering/development.

4.4.2 Methods

Samples from Dansey Road were collected every 5 cm through the loess sequence between Unit L Tephra and Rotorua Tephra. Loess samples only (i.e. excluding tephra layers) were oven-dried, ground and formed into pressed pellets and measured for a variety of major (in oxide form) and trace element contents using X-ray fluorescence (XRF) spectrometry. The results for potassium (the main element of interest in this study) were graphed against age (the derivation of the loess timescale was described in Chapter 2). The results of detectable major elements are given in appendix 5.

4.4.3 Results

The XRF results for K (as K20) at Dansey Rd show variability through the loess column (Figure 4.3). In general the results show: (1) low K values between c. 32—24 cal ka; (2) higher and variable K values between c. 24—18.4 cal ka; (3) lower (decreasing) K values between c. 18.4—15.5 cal ka.

(1) K values increase from about 1.8% at c. 32 cal ka to about 2.4% by c. 29.4 cal ka. K values remain around 2.4—2.5% through to c. 26.4 cal ka when they begin to decrease, reaching about 2.3% at c. 25.4 cal ka (the time of deposition of the Kawakawa Tephra). Following this, K values begin to increase relatively steadily until about c. 23.4 cal ka.

(2) By c. 23.4 cal ka, K values reach about 2.9% and between c. 23.4—18.4 cal ka K values are variable around 2.9%. A small decrease in K values, to about 2.8% occurs c. 22.8 cal ka. Between c. 22.6—21.2 cal ka K values vary around 2.9—3%, except for a decrease to about 2.7% after c. 21.7 cal ka (i.e. around the time of the Ok Tephra deposition and possibly an effect of this event). K values decrease again slightly between c. 21.2—20.6 cal ka, increase slightly between c. 20.6—20 cal ka,

decrease slightly between c. 20—19.4 cal ka and increase again between c. 19.4—18.4 cal ka.

(3) Between c. 18.4—15.5 cal ka, K values generally decrease from about 2.7% to 2.3%.

The XRF results for P values through the loess column at Dansey Rd, although they appear to show variability, involve a large error, suggesting that the apparent variability in P may not be significant. Therefore P has not been used in this study as a paleoclimatic proxy.
10

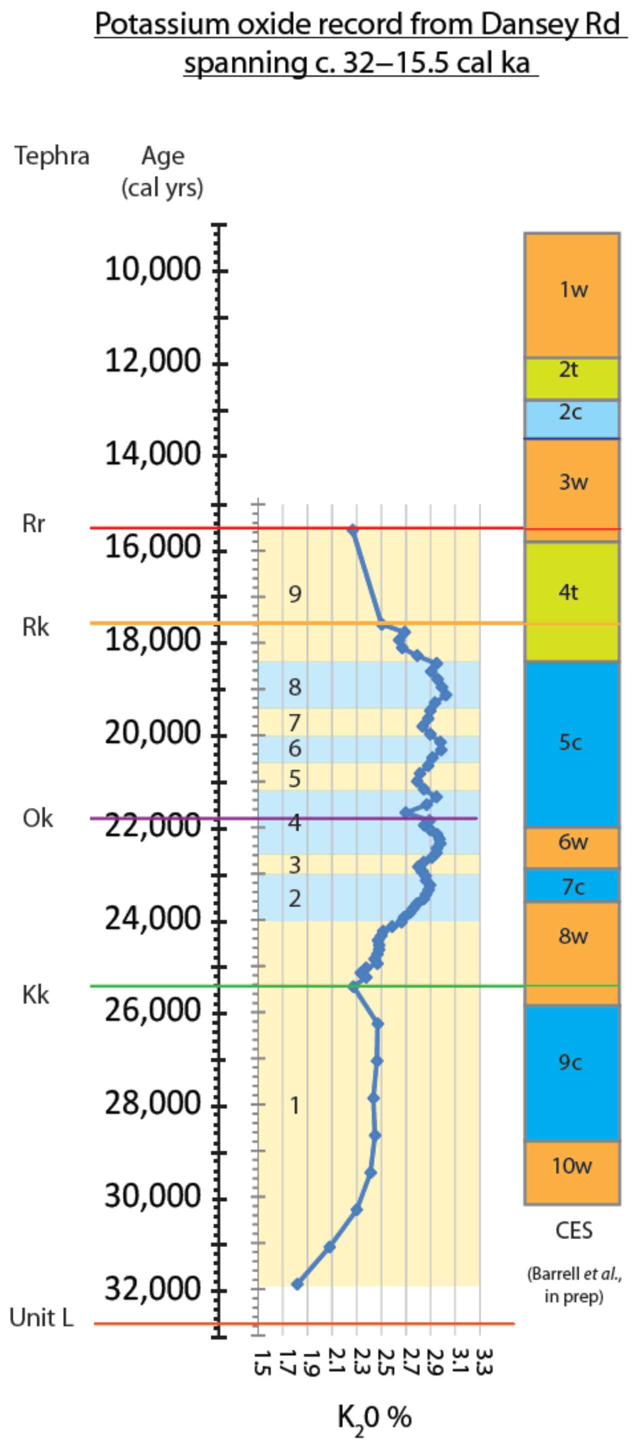

Figure 4.3 Potassium oxide content through loess at Dansey Rd (tephra layers excluded). Coloured zones numbered 1-9 indicate inferred climatic phases from this study (yellow: warmer and wetter; blue: cooler and drier). The New Zealand climate event stratigraphy (CES) is shown for comparison.

4.4.4 Discussion

In this study, based on the studies of Palmer & Pillans (1996) and Childs & Searle (1975), I assume that lower K values reflect phases of warmer and wetter climatic conditions (i.e. soil has been more intensely weathered) relative to higher K values which reflect cooler and drier climatic conditions (i.e. soil has been less weathered).

Childs & Searle (1975) showed that minimum K values tend to be associated with the upper part of B horizons and the lower part of the A horizons, as opposed to the A horizon alone. Hence minimum K values do not likely correlate with the soil developed during times of most intense weathering/warmest climatic conditions but rather correlate with the soil material formed during pre-warm climatic conditions. It is likely that soil developed during the warmest climatic conditions actually correlates with slightly higher than minimum K values.

Based on the variations in the K values throughout the loess column at Dansey Rd, I have inferred the presence of 9 climatic phases (Figure 4.3). The boundaries of these climatic phases have been drawn at about the mid-point between neighbouring peaks and troughs in K values. This depiction adds confidence that 'warm' climatic phases will include the slightly higher than minimum K values assumed to represent the actual warmest climatic conditions. I have also attempted to link these climatic phases to the New Zealand CES (Barrell *et al.*, in prep.), as described below.

Phase 1 (c. 32—24 cal ka) warm & wet

Phase 1 spans c. 32—24 cal ka and is characterised by some of the lowest K values within the loess column, especially between c. 32—30 cal ka, suggesting significant weathering and hence likely warmer and wetter climatic conditions relative to other parts of the record. K values either side of the Kk deposition decrease slightly and this change could be due to a parent material effect of the tephra on the loess. Phase 1 may relate to warm event 10w of the CES.

Phase 2 (c. 24—23 cal ka) cool & dry

Phase 2 spanning c. 24—23 cal ka, is characterised by high K values reflecting nil or only weak weathering during this time and hence likely indicates cooler and drier climatic conditions. Phase 2 may relate in part to cool event 9c of the CES.

Phase 3 (c. 23—22.6 cal ka) warmer & wetter

Phase 3 spans c. 23—22.6 cal ka and is delineated by slightly lower K values than that of the surrounding loess possibly suggesting some weathering occurred during this time and hence indicating slightly warmer and wetter climatic conditions. However, phase 3 does not appear to correlate with a warmer phase in the CES. Two possible explanations for this lack of correlation could be: (1) phase 3 may not be a response to climatic conditions, but rather due to the input of primary minerals (e.g. as a result of a tephra deposition, possibly Te); or (2) phase 3 may be a response to local climatic conditions which are not recorded in the CES, which is of national extent.

Phase 4 (c. 22.6—21.2 cal ka) cool & dry

Phase 4 spans c. 22.6—21.2 cal ka and is characterised by high K values reflecting nil or only weak weathering and hence suggests cooler and drier climatic conditions during this time. Following the Ok deposition, at c. 21.9 cal ka, there is a sharp drop in K values; however, because this drop only involves one data point it is possible that it is a result of a parent material effect on the loess from the deposition of Ok tephra. Phase 4 may also relate to cool event 9c of the CES.

Phase 5 (c. 21.2—20.6 cal ka) warmer & wetter

Phase 5 spans c. 21.2—20.6 cal ka and is characterised by slightly lower K values suggesting some weathering may have occurred during this time and hence indicating slightly warmer and wetter climatic conditions. Phase 5 may relate to warmer event 8w of the CES.

Phase 6 (c. 20.6—20 cal ka) cool & dry

Phase 6, spanning c. 20.6—20 cal ka, is characterised by slightly higher K values reflecting nil or only weak weathering hence suggesting cooler and drier climatic conditions during this time. Phase 6 may relate to cool event 7c of the CES.

Phase 7 (c. 20—19.4 cal ka) warmer & wetter

Phase 7 spans c. 20—19.4 cal ka and is defined by slightly lower K values suggesting some weathering occurred during this time and hence probably reflects slightly warmer and wetter climatic conditions. Phase 7 may relate to event 6w of the CES.

Phase 8 (c. 19.4—18.4 cal ka) cool & dry

Phase 8 spans c. 19.4—18.4 cal ka and is characterised by higher K values reflecting nil or only weak weathering, hence indicating cooler drier climatic conditions during this time. Phase 8 may relate to cool event 5c of the CES.

Phase 9 (c. 18.4—15.5 cal ka) warming & warm & wet

Phase 9, spanning c. 19.4—15.5 cal ka, is characterised by significantly decreasing K values, indicating relatively more intense weathering than preceding warm phases 7, 5 and 3 and hence relatively warmer and wetter climatic conditions, similar to those of phase 1. The Rk deposition occurred during this phase at c. 17.5 cal ka and the Rr deposition occurred just after the end of this phase, at c. 15.6 cal ka. Phase 9 may correlate with transitional event 4t and/or warm event 3w of the CES.

Chapter 5 Synthesis and evaluation of paleoclimate proxies

5.1 Introduction

This chapter brings together the results of the physical, biological and chemical proxy records described in the previous two chapters and attempts to develop a general summary of the inferred climatic conditions between c. 32.7—9.5 cal ka in the Rotorua region. This summary of inferred climatic conditions, dated using tephrochronology, is then compared with other New Zealand climatic records from this time frame.

5.2 Synthesis of paleoclimatic proxy records

The combined results from the physical, biological and chemical proxy records described in the previous two chapters are shown in Figure 5.1, along with the climatic conditions which they are assumed to indicate. Based on these results, I have attempted to develop a general summary of climatic conditions in the study field area (Rotorua climate event stratigraphy, RCES) for the time interval from c. 32.7—9.5 cal ka (Figure 5.1). In general, three broad climate periods were recognised: 1) warm interstadial (c. 32.7—25.4 cal ka); 2) cold stadial/extended last glacial maximum (c. 25.4—18.4 cal ka) with interstadials; and 3) warming/transitional to interglacial (c. 18.4—9.5 cal ka) including a late glacial reversal (c. 13.8—12.8 cal ka). Within these periods, nine climate phases were recognised and are described below.

In summarising the records shown in Figure 5.1, I note that some are of lower resolution than others (e.g. phytolith record and loess accumulation rate record). Consequently there are limitations in recording finer-scale climatic changes. Because the RCES is a merging of various records from this study into a single climate record, not all the climatic changes observed in every record are expected to be represented in the RCES. Instead, it is intended that the RCES may show a *general summary* of climatic conditions in the Rotorua area throughout the time frame of interest.

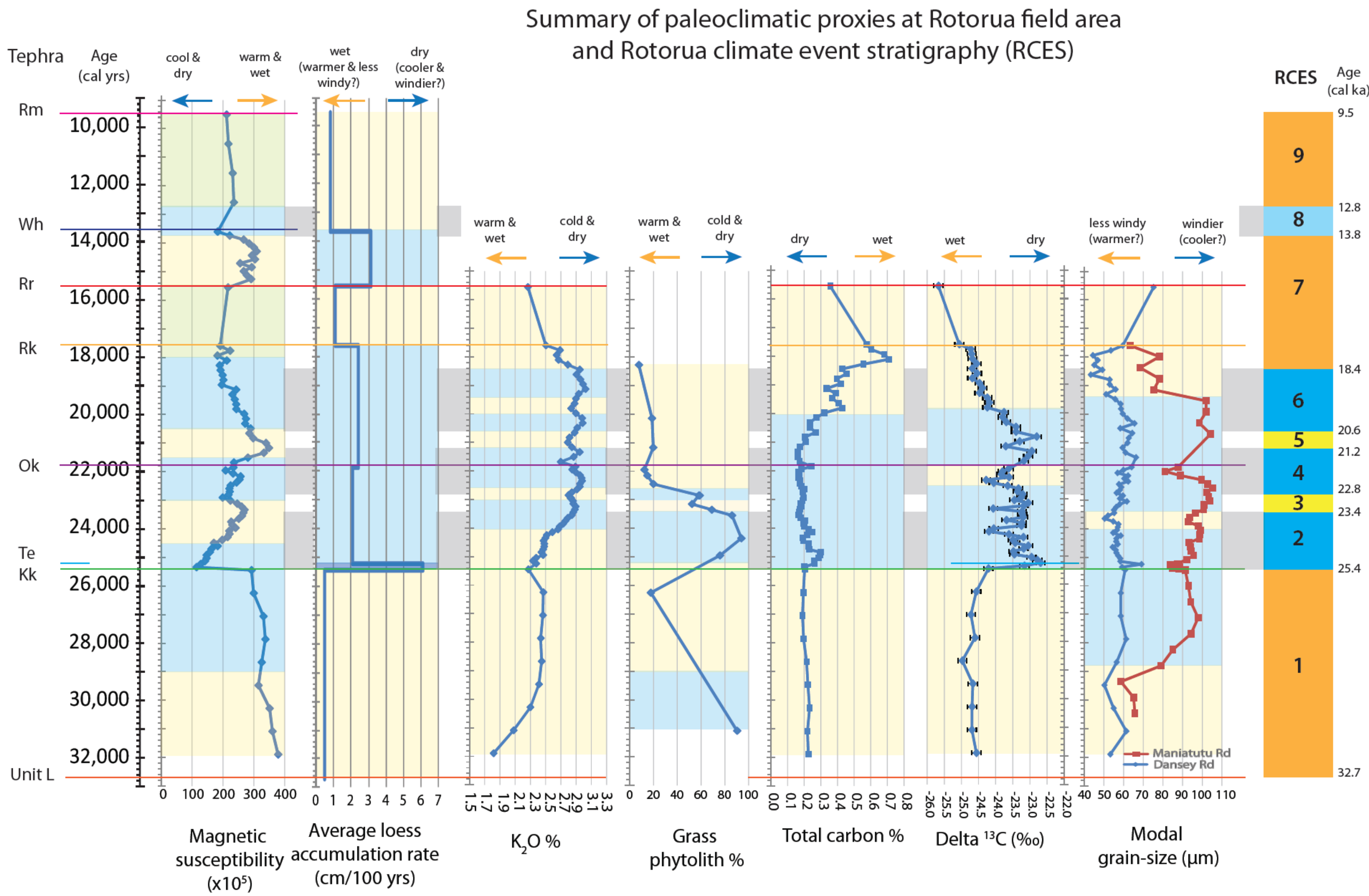

Figure 5.1 Summary graphs of all chemical, physical and biological proxy records from this study, including the climatic phases inferred from each individual proxy (light coloured zones on graphs – see chapters 3 and 4 for explanation). The Rotorua climate event stratigraphy (RCES) on the far right, a synthesis of the proxy records, presents a summary of climatic conditions in the Rotorua region between c. 33—9.5 cal ka.

5.2.1 Phase 1 (c. 32.7—25.4 cal ka) relatively warm and wet interstadial

Phase 1 spans c. 32.7—25.4 cal ka and in general is characterised by relatively warm, wet, and in part less windy climatic conditions than the following phase as supported by the K, $\delta^{13}C$, loess accumulation rate and phytolith records (and possibly the total carbon record – see discussion in Chapter 4) and in part by the MS and grain-size records. In the phytolith record, a peak in grass phytoliths during the early part of phase 1 appears to suggest cooler and drier conditions. However, it is possible that this grass peak may be related to colonisation following Unit L deposition (similarly, Newnham *et al.* (2007b) recorded an increase in herb pollen in a proxy climatic record from the Auckland area following volcanic activity). Also, other proxy records from this study do not generally support cooler and drier conditions as suggested by the phytolith record during this time. Some proxy records (e.g. MS and grain-size records) suggest that climatic conditions may have begun to deteriorate to cooler, drier and windier conditions during phase 1, between c. 28.8—27.5 cal ka. The grain-size record suggests that climatic conditions became windier at c. 28.8 cal ka and continued to be windy into phase 2. It may be that climatic conditions did begin to deteriorate early (i.e. during phase 1) as recorded by the MS and grain-size records, though possibly only slightly. It is also possible that grain-size, at least, may have a relatively faster response to changing climatic conditions, compared to some other proxy records. In general, phase 1 shows warm, wet and in part less windy climatic conditions.

5.2.2 Phase 2 (c. 25.4—23.4 cal ka) cold, dry and generally windy stadial

Phase 2 spans c. 25.4—23.4 cal ka and in general is characterised by dry, cold and generally windy climatic conditions as supported by the phytolith, $\delta^{13}C$, total carbon, loess accumulation rate records and in part by the grain-size and MS records. Possibly the most significant exception within phase 2 is the K record which suggests that warm, wet conditions continued up until c. 24 cal ka. The reason for this apparent lag is unclear. The grain-size record suggests less windy conditions during the latter part of phase 2 and may indicate the faster response time of grain-size to changes in climatic conditions and may correlate with phase 3 observed in some of the other records.

5.2.3 Phase 3 (c. 23.4—22.8 cal ka) warmer and wetter interstadial

Phase 3 spans c. 23.4—22.8 cal ka and in general is delineated by a return to warmer and wetter climatic conditions as supported by the MS and phytolith records and to a lesser extent by the K record. However, the timing of this climatic event seems somewhat variable from record to record. As noted earlier, the grain-size record may record this event as occurring during the latter part of phase 2. The $\delta^{13}C$ record does not appear to record a wetter climatic event during this phase. A possible explanation for this is that the magnitude or length of the climatic change was not enough to cause a significant change in the water-use efficiency of plant types growing over the time frame of phase 3 and hence was not registered as a significant change in the $\delta^{13}C$ record.

5.2.4 Phase 4 (c. 22.8—21.2 cal ka) cold, dry and windy stadial

Phase 4 spans c. 22.8—21.2 cal ka and in general climatic conditions were cold, dry and windy as shown broadly by the MS, loess accumulation rate, K, total carbon and grain-size records. However, in the phytolith record a significant decrease to lower values of grass phytoliths throughout much of phase 4 appears to suggest warmer and wetter climatic conditions. A possible explanation for this anomaly is that the decrease in grass phytoliths may represent an increase in shrub-type vegetation, rather than trees, in response to a subtle change in climate or some other factor. It is possible that shrub-type vegetation was representative of continued relatively cold and dry climatic conditions rather than warmer and wetter conditions. The $\delta^{13}C$ record shows a subtle change to slightly wetter conditions for a time (c. 22.4—21.8 cal ka) during phase 4, also possibly reflecting a change in vegetation type.

5.2.5 Phase 5 (c. 21.2—20.6 cal ka) warmer and wetter interstadial

Phase 5 spans c. 21.2—20.6 cal ka and, although not apparent in all records, is characterised by warmer and wetter climatic conditions in the MS and K records than those of the preceding phase 4. The total carbon, $\delta^{13}C$ and grain-size records do not appear to indicate a warmer and wetter event during this time for reasons unknown. As alluded to previously, it not completely clear whether the low percentage of grass phytoliths in the phytolith record represents an increase in shrub-type vegetation or in trees. Hence it is unclear whether the phytolith record supports warmer and wetter climatic conditions during phase 5 or not.

5.2.6 Phase 6 (c. 20.6—18.4 cal ka) cold, dry and partly windy stadial

Phase 6 spans c. 20.6—18.4 cal ka and in general is characterised by cold, dry, and partly windy conditions, supported by the MS and loess accumulation rate records and in part by the K, total carbon, $\delta^{13}C$, and grain-size records. The K record suggests a short phase of warmer and wetter conditions within the middle of phase 6 though there is no strong support for this in other records. The total carbon, $\delta^{13}C$ and grain-size records suggest an early start (within the latter part of phase 6) to warmer, wetter and less windy conditions indicative of phase 7. It could be that conditions became *wetter* (i.e. recorded by total carbon and $\delta^{13}C$ records) and *less windy* (i.e. recorded in the grain-size record) before *temperatures* began to increase, possibly indicated by the later start in the MS and K records to phase 7. The apparent early start of phase 7 suggested by the grain-size record could also in part be due to a faster response time of this proxy. It is unclear whether the phytolith record supports cold and dry climatic conditions during phase 6 – see phase 5 discussion.

5.2.7 Phase 7 (c. 18.4—13.8 cal ka) warm, wet and less windy transition to interglacial

Phase 7 spans c. 18.4—13.8 cal ka and is characterised by warmer, moister and less windy climatic conditions than the processing phase 6 as shown generally by all records which span all or part of this time frame. The increase in loess accumulation rate during the later part of phase 7 may be associated with the cooler and drier conditions of the following phase 8, but may have been offset due to low resolution of measurements.

5.2.8 Phase 8 (c. 13.8—12.8 cal ka) cool and dry late glacial reversal

The MS and loess accumulation rate records (together with stratigraphy) are the only records that span the time frame of phase 8 (c. 13.8—12.8 cal ka). The MS record indicates this phase was characterised by colder and drier climatic conditions. As noted previously, the increase in the loess accumulation rate record which occurs mostly during the later part of phase 7 may have been offset and hence may also be related to cooler and drier conditions of phase 8.

5.2.9 Phase 9 (c. 12.8—9.5 cal ka) warmer and wetter transition to interglacial

The MS and loess accumulation rate records (together with stratigraphy) are the only records that span the time frame of phase 9 (c. 12.8—9.5 cal ka). These records indicate that this phase was characterised by either transitional or warmer and wetter climatic conditions.

5.3 Comparison between RCES and other New Zealand climate records

The RCES is compared with other climate records from New Zealand, including the New Zealand Climate Event Stratigraphy (CES) (Barrell *et al.*, in prep.), to test its validity. It is recognised that particular climate regimes can result in different climatic conditions in different parts of the country (climate districts) at the same time and hence it is not surprising that climate records from different parts of the country may show some contemporaneous differences in climatic conditions (Lorrey *et al.*, in press). For this reason I have chosen to compare the RCES with records mainly from the same climate district or districts near-by (Table 5.1 and Figure 5.2). Variations between climate records from different parts of the country may also have resulted from differences in elevation of sites or differences in the degree of sensitivity of some sites to changes in climate possibly resulting in more or less intense climate signals.

Table 5.1 Selected climate records from the North Island spanning at least part of the time frame between c. 33—9.5 cal ka.

Name	**Location**	**Type of record**	**Proxy record**	**Reference/s**	**Notes**
Onepoto maar	Auckland	Sediment core	$\delta^{13}C$ LPG[a]	Alloway *et al.* (2007), Augustinus *et al.* (2011)	
Pukaki maar	Auckland	Sediment core	LPG[a]	Alloway *et al.* (2007)	
Kohuora maar	Auckland	Sediment core	% herb pollen	Newnham *et al.* (2007b)	

Mt Richmond maar	Auckland	Sediment core	% dryland herbs	Newnham *et al.* (2007b), Sandiford *et al.* (2002)	
Lake Maratoto	Waikato	Lake core	Mean annual temperature reconstruction	Wilmshurst *et al.* (2007)	
Kaipo bog	East central North Island	Peat sequence	LPG[a]	Hajdas *et al.* (2006)	Not in same climate district as field area
Taranaki quartz	Taranaki	Tephra-soil sequence	Quartz accumulation rate	Newnham *et al.* (2007b), Alloway *et al.* (1992)	Not in same climate district as field area

a = LPG: lowland-montane podocarp pollen to upland grass pollen ratio (semi-quantitative temperature measurement: high values = warmer; low values = cooler) (Newnham & Lowe, 2000)

The Onepoto maar records and the Pukaki maar record are the most complete records spanning the time between c. 30—9.5 cal ka. The Kohuora maar, Mt Richmond maar and Taranaki quartz records span the earlier part of this time frame, whereas the Lake Maratoto and Kaipo bog records span the later part. Comparisons between the RCES and the selected climatic records are outlined. Comparisons are assisted by the use of tephra layers common to both the RCES and the other records.

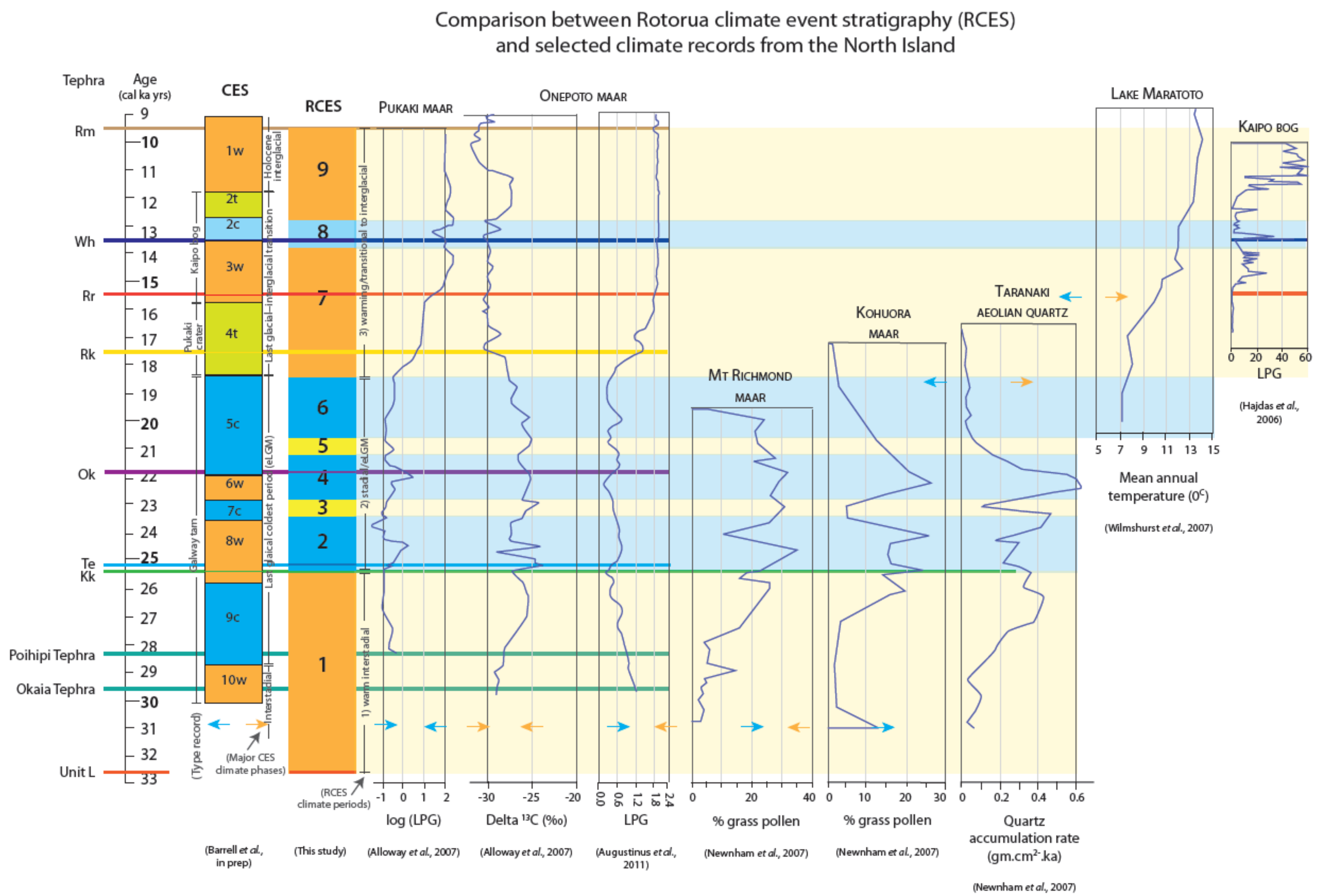

Figure 5.2 Comparison between the Rotorua climate event stratigraphy (RCES) (this study) and selected climate records from the North Island spanning at least part of the time frame between c. 33—9.5 cal ka, and the New Zealand climate event stratigraphy (CES).

5.3.1 Onepoto maar records

The Onepoto maar site is near present sea level; approximately 300 m lower than most of the Rotorua field sites in this study. Warm phase 1 of the RCES appears to be recorded in the Onepoto records (represented as relatively lower $\delta^{13}C$ values and a relatively high LPG ratio), although the timing of the end of phase 1 appears to be earlier in the Onepoto records (c. 28 cal ka) than that for the RCES. The following cool phases of the RCES (phases 2, 4 and 6) may be present in the Onepoto records because the $\delta^{13}C$ and LPG records generally suggest cooler climatic conditions between c. 28—17.5 cal ka. The warmer interstadial phases (phases 3 and 5) of the RCES do not appear strongly in the Onepoto records, although there is evidence of possible short interstadials just prior to the timing of phases 3 and 5 (e.g. between c. 24.6—23.6 cal ka and between c. 21.8—21 cal ka). The beginning of warmer phase 7 of the RCES appears to correlate in general with the start of warming shown in the Onepoto records. Cooler phase 8 (late glacial reversal) of the RCES, although offset, may correlate with a relative increase in $\delta^{13}C$ values between c. 12.5—11 cal ka. Onepoto LPG record does not show evidence of correlation with phase 8. Both Onepoto $\delta^{13}C$ and LPG records suggest warmer conditions during phase 9 of the RCES.

5.3.2 Pukaki maar record

The Pukaki record does not appear to record an early warm phase that might correlate with warm phase 1 of the RCES. Instead, the Pukaki record appears to generally show cool conditions from at least the time of the Poihipi Tephra (c. 28.2 cal ka) until c. 17.5 cal ka, correlating in part with cool phases 2, 4 and 6 of the RCES. Warmer phase 3 of the RCES does not appear to correlate with warmer conditions in the Pukaki record. Phase 5 of the RCES appears to correlate with short-lived slightly warmer conditions in the Pukaki record. The beginning of warmer phase 7 of the RCES appears to correlate with the start of warming shown in the Pukaki record. Also, phase 8 of the RCES (late glacial reversal) appears to correlate with the onset of relatively cooler conditions in the Pukaki record, although conditions in the Pukaki record appear to be shorter-lived. Warm phase 9 of the RCES also correlates with warm conditions in the Pukaki record.

5.3.3 Mt Richmond maar record

The grass pollen record from Mt Richmond supports warm conditions during at least the first part of phase 1 of the RCES. From c. 27.5—19.8 cal ka, the Mt Richmond record supports cool conditions generally matching cool phases 2, 4 and, in part, phase 6 of the RCES. Although the Mt Richmond record does not strongly support warmer phase 3 of the RCES there is some evidence for warmer climatic conditions around the time of phase 5.

5.3.4 Kohuora maar record

In general, the Kohuroa maar herb pollen record supports warm conditions during the time of warm phase 1 of the RCES. An increase in herb pollen between c. 32—30.2 cal ka in the Kohuora record was attributed to vegetation succession following volcanic activity rather than a climatic response (Newnham *et al.*, 2007b). The transition to cooler conditions at the end of phase 1 appears to begin earlier in the Kohuora record than in the RCES. Cool phases 2 and 4 of the RCES are supported by cool conditions in the Kohuora record and evidence of warmer conditions c. 23.2 cal ka in the Kohuora record closely matches warmer phase 3 of the RCES. However, the following warmer phase 5 and cooler phase 6 of the RCES do not appear to be supported in the Kohuora record. Significant warming in the Kohuora record begins c. 20 cal ka, earlier than the beginning of warm phase 7 of the RCES.

5.3.5 Taranaki quartz record

Although the timing of variations in the Taranaki quartz accumulation rate record is not well constrained (only one tephra tie-point, Kawakawa Tephra (c. 25.4 cal ka)), Newnham *et al.* (2007b) noted that there does appear to be some correlation with the Kohuora maar record and some other Auckland maar records. For this study, which includes the use of the Kawakawa Tephra, I have assumed the same chronology for the Taranaki quartz record as that of Newnham *et al*. (2007b). Based on this chronology it appears that the Taranaki quartz record supports an early warm phase correlating in part with warm phase 1 of the RCES, followed by a cooler and variable phase correlating in part with cool phase 2 of the RCES. A relatively short-lived warmer phase at c. 23 cal ka possibly relates to warm phase 3 of the RCES. This is followed by a cool phase possibly correlating with cool phase 4 of the RCES follows and finally a warm phase possibly correlating in part with warm phase 7 of the RCES is evident (i.e. phases 5 and 6 of the RCES may not be represented in the Taranaki quartz record). However, the imprecise timing of this record makes correlations with the RCES approximate.

5.3.6 Lake Maratoto record

The Lake Maratoto mean annual temperature record spans the latter part of the RCES (i.e. c. 20—9.5 cal ka) and supports a general warming in temperature beginning c. 19.5 cal ka (i.e. during cool phase 6 of the RCES) and continuing until c. 9.5 cal ka (i.e. warm phase 9 of the RCES). The Lake Maratoto record does not show significant evidence of cooling at the time of cool phase 8 (late glacial reversal).

5.3.7 Kaipo bog record

The climatically-sensitive location of the Kaipo bog site (montane-subalpine) means that subtle changes in climate have likely impacted the vegetation at this site and hence the Kaipo bog LPG record has been interpreted as providing a detailed record of climate change at this site (Newnham & Lowe, 2000; Hajdas *et al.*, 2006; Alloway *et al.*, 2007). The Kaipo bog LPG record spans the latter part of the RCES (c. 18—10 cal ka). In part, the Kaipo record supports warm phase 7 of the RCES, although the beginning of phase 7 appears to occur later in the Kaipo record (c. 15.5 cal ka). In particular, the Kaipo record supports cool phase 8 (late glacial reversal) and also warm phase 9 of the RCES, although the exact timing is offset slightly. The Kaipo bog LGP record is the designated stratigraphic type record for the late glacial cool episode (late glacial reversal) in the CES (Barrell *et al.*, in prep.).

5.3.8 Comparison between RCES and CES

The CES of Barrell *et al.* (in prep.) is a compilation of a number of continuous and fragmentary climatic records spanning c. 30—8 cal ka. Four major climate phases are recognised in the CES: preceding interglacial (ending at c. 28.9 cal ka); last glacial coldest period (c. 28.9—18.4 cal ka); last glacial – interglacial transition (c. 18.4—11.8); Holocene interglacial (c. 11.8—present) (Figure 5.2). In the absence of a single, continuous, high resolution climate record which is representative of the New Zealand region, the timing of climatic events of the CES (10w—1w) are based on a number of individual high-resolution records from different parts of the country: Galway tarn pollen record, western South Island (10w—5c); Pukaki maar pollen record, Auckland (4t); and Kaipo bog peat sequence, eastern North Island (3w-2t). By basing the CES on a number of type climatic records it is hoped that as much 'real' data as possible be preserved, especially regarding chronology, which may other wise be lost or blurred in a composite record. It is intended that the CES act as a 'work-in-progress' New Zealand baseline standard to which other climatic records can be compared. It is hoped that by comparison with other climatic records, the CES will be further refined, potentially including the detection of finer scale variations in climate and regional climate differences.

The RCES supports at least the first three major climatic phases of the CES (and probably the fourth), although there are differences in timing between the RCES and the phase and event boundaries of the CES. It is likely that event 10w of the CES (preceding interstadial) correlates with RCES phase 1. Events 9c, 7c and 5c of the CES (last glacial coldest period) likely correlate with RCES cool phases 2, 4 and 6. The two interstadials within the last glacial coldest period (events 8w and 6w) may relate to RCES interstadial phases 3 and 5. CES events 4t and 3w likely relate to RCES phase 7 and CES event 2c correlates well with RCES phase 8. It is unclear whether event 2t and 1w of the CES relate to RCES phase 8 and phase 9 respectively, or to only one of these two phases. The RCES appears to be better synchronised with the latter events of the CES (4t—1w) than with the earlier events (10w—5c). These differences in synchronicity may be due to the difference in location between the Galway tarn type record (type record for the earlier events of the CES) and the Rotorua field area compared to the locations of the other North Island type records (type records for the latter events) in relation to the field area.

5.4 Summary of comparisons between RCES and other New Zealand climate records

In summary, there is generally strong support from the selected climate records from the North Island for at least three major climate periods within the RCES, similar to the phases of the CES: 1) warm preceding interstadial; 2) cold stadial/extended last glacial maximum; and 3) warming/transitional to Holocene interglacial. However, the exact timing of these periods in the RCES (especially the transition from period 1 to period 2) are not perfectly synchronised with those in the other selected climatic records and the CES. Some of the selected North Island records show ‘blips’ in proxies corresponding to interstadial phase 5 of the RCES but are subdued. At least one and possibly two records support interstadial phase 3 of the RCES. There is relatively good support from the selected climatic records for late glacial reversal phase 8. Some possible reasons for the imperfect synchronisation between the RCES and some of the selected climatic records and climatic events in the CES may relate to differences in site locations (including elevation differences and differences in climatic-sensitivity of sites) and hence possibly slight differences in climatic conditions even within the same climate district; differences in sampling resolution; stratigraphic limitations and errors in chronology.

Chapter 6 Conclusions

This study is the first to analyse in detail tephric loess deposits from the Rotorua region using laboratory-based methods. Previously, the only published laboratory-based study was that of Benny *et al*. (1988), which focused on grain-size and mineralogical analysis of tephric loess associated with the Okareka Tephra mainly in the Mamaku Plateau region north-west of Rotorua.

The main aim of my study was to characterise tephric loess deposits aged c. 33—9.5 cal ka in the Rotorua region and to develop a tephrostratigraphic framework for these deposits in order to reconstruct past climates for this time interval (with an emphasis on the eLGM and the phases leading into and following it). To meet this aim, three main objectives were developed, namely:

1. To characterise tephric loess and develop a tephra and tephric loess stratigraphic framework (using a tephra-based chronology) spanning c. 33—9.5 cal ka for the Rotorua region.
2. To investigate tephric loess sequences spanning mainly c. 33—15 cal ka (in some instances up to c. 9.5 cal ka) for evidence of regional paleoclimatic signals using a variety of biological, physical and chemical proxies obtained from analyses of the loess deposits and from morphological features of the loess.
3. To compare any inferred paleoclimatic signals with other paleoclimatic records from New Zealand, including the CES of Barrell *et al*. (in prep.).

A tephra and tephric loess stratigraphic framework was developed for the Rotorua region spanning c. 33—9.5 cal ka. Thirteen sites were examined in the field and loess deposits and intervening tephra layers were identified and described based on their morphological features and stratigraphic positions which were informed by previous studies including those of (Nairn, 1992; Kennedy, 1994; Esler, 2010; Lowe *et al.*, 2010). Eight key marker tephras identified provided isochronous tie-points between field sites as well as ages based on Lowe *et al.* (2008b) and new age-modelling data (D.J. Lowe pers. comm., 2012) within the tephric loess sequences. Unlike most previous studies which suggest that loess deposition ceased around the time of deposition of the Rerewhakaaitu Tephra (Vucetich & Pullar, 1969) or soon after (around the time of the Rotorua Tephra: Newnham *et al.,* 2003), my study has identified continuing loess deposition at some sites as young as c. 9.5 cal ka (i.e. around the time of deposition of the Rotoma Tephra) in the Rotorua region. Such young loess was identified between the Rotorua and Waiohau tephras at two sites (Dansey Rd and Cameron's Quarry) and between Waiohau and Rotoma tephras at one site (Dansey Rd).

In general, the tephric loess deposits examined in this study were dominantly massive, largely silt/clay—very fine sand (defined here as <0.125 mm) and typically yellowish brown, dull yellowish brown or dull yellow orange in colour (Munsell colour codes 10YR 5/4, 5/6, 5/8 or 6/4). The thickest (tephra-free) loess sequence occurs at Dansey Rd where a total of 4.3 m of loess was recorded between Unit L and Rotoma Tephra. The thicknesses of loess packets between the dated tephra layers were recorded and hence loess accumulation rates were able to be compared through time. On average, loess accumulation rates were relatively slow, 2.3 cm/100 yrs on average throughout the field area, ranging from 0.5 cm/100 yrs on average (between the time of deposition of Unit L and Kawakawa Tephra) to 6.1 cm/100 yrs (between the time of deposition of Kawakawa Tephra and Te Rere Tephra, although the imprecise age of the latter tephra makes this accumulation rate only approximate). These slow rates of accumulation – only a few centimetres per century – as well as the presence of subtle changes in colour and other properties through the loess columns, indicate that these deposits were formed via developmental upbuilding with topdown pedogenic processes influencing soil formation simultaneously whilst the land surface was slowly rising (Almond & Tonkin, 1999; Lowe & Tonkin, 2010). Loess accumulation was interrupted intermittently by tephra deposition, which ranged in thickness from a few millimetres to greater than 1 metre. Where these tephra layers were of substantial thickness (i.e. at least c. 20-30 cm), the antecedent soil/loess column was shut-off from surface soil-forming processes, causing retardant upbuilding, and hence loess accumulation, developmental upbuilding and topdown pedogenic processes resumed at the new land surface.

It is inferred that past climates and related factors have broadly controlled the production, deposition and rate of accumulation of tephric loess across the relatively large Rotorua field area that extends about 45 km north to south and about 50 km west to east. This inference derives from the general similarity between many of the measured proxies from selected field sites, showing a broad, three-unit pattern of change (c. 33—24.5 cal ka, c. 25.4—18.4 cal ka, and c. 18.4—9.5 cal ka). Of the thirteen sites examined, Dansey Rd and Maniatutu Rd were selected as primary and secondary master sites, respectively, for detailed laboratory analysis of a number of properties which could be used as potential paleoclimatic proxies. These two sites were selected for the laboratory analysis because they contained a large number of tephra marker beds and relatively thick loess deposits, thus providing a potentially high-resolution record of climatic change. Properties analysed as climate proxies included loess grain-size, accumulation rate, phytoliths, magnetic susceptibility, total carbon content, carbon isotopes and potassium content.

The results from the proxies mentioned previously showed evidence of climatic variability and were summarised into a composite Rotorua climate event stratigraphy (RCES) spanning c. 33—9.5 cal ka. Three broad *climate periods* were recognised within the RCES: **1)** a warm interstadial period (c. 32.7—25.4 cal ka); **2)** a cold stadial/extended last glacial maximum period (c. 25.4—18.4 cal ka) with interstadials; and **3)** a warming/transitional period leading to an interglacial (c. 18.4—9.5 cal ka) but including a late glacial reversal (c. 13.8—12.8 cal ka). Within these three periods, nine shorter *climate phases* were recognised as follows: **Phase 1** – relatively warm and wet interstadial (c. 32.7—25.4 cal ka); **Phase 2** – cold, dry and generally windy stadial (c. 25.4—23.4 cal ka); **Phase 3** – warmer and wetter interstadial (c. 23.4—22.8 cal ka); **Phase 4** – cold, dry and windy stadial (c. 22.8—21.2 cal ka); **Phase 5** – warmer and wetter interstadial (c. 21.2—20.6 cal ka); **Phase 6** – cold, dry and partly windy stadial (20.6—18.4 cal ka); **Phase 7** – warm wet and less windy transition to interglacial (c. 18.4—13.8 cal ka); **Phase 8** – cold and dry late glacial reversal (c. 13.8—12.8 cal ka); **Phase 9** – warmer and wetter interglacial (c. 12.8—9.5 cal ka). Of the paleoclimatic properties measured, magnetic susceptibility, potassium content and grain-size seem to have resulted in the most detailed records (including support for one or more of the nine recognised shorter climate phases from this study) in which trends were comparable with one another. The loess accumulation rate record shows general agreement with the three broad climate periods recognised in the previously mentioned records as well as support in part for the late glacial reversal phase. However, the relatively low resolution of this record has prevented the detection of climatic variability at a finer scale. Phytoliths were analysed at a relatively low resolution in this study and the resulting phytolith record shows some agreement with the previously mentioned records. Further phytolith analysis at a higher resolution and an increased number of sites may potentially prove a more useful proxy of paleoclimate in the Rotorua region. The resulting record from carbon isotope analysis, although it supported the three broad climate periods recognised in this study, did not strongly support the occurrence and timing of the shorter-lived climate phases recognised in this study. Also, the loess total carbon content record did not show evidence of fine-scale climatic variation. This lack of support and finer-scale variation may have been a result of the very low carbon content of the loess.

The RCES was compared with other climate records (including both continuous and fragmentary records) from the North Island from the same or neighboring climate districts as the Rotorua field area. The RCES was also compared with the New Zealand CES of Barrell *et al*. (in prep.). In general, the three broad *climate periods* of the RCES were well supported by the occurrence of similar periods in the climate records from the North Island and the CES, although the timing of these periods were not always well synchronised. Warm interstadial period 1 of the RCES ended later than the associated warm interstadial of the CES by c. 3.5 kyrs. Cool stadial period 2 of the RCES was shorter in duration (c. 7 kyrs) compared to the associated eLGM period of the CES (c. 10.5 kyrs). Transitional period 3 of the RCES began around the same time as the associated transitional period of the CES (c. 18.4 cal ka). There was also some agreement between the nine relatively short-lived *climate phases* recognised in this study and the short-lived climate 'events' of the CES. For example, the CES suggests two interstadial events occurred within the extended last glacial maximum period and evidence from my study also supports the occurrence of two interstadials (phases 3 and 5) within climate period 2. However, there appear to be some discrepancies between the CES and RCES regarding the duration and timing of these interstadials. The first of these two short-lived interstadials of the CES (event 8w) is longer in duration (c. 2.25 kyrs) compared with the first of the two short-lived interstadials of the RCES (phase 3) (c. 600 yrs) and begins earlier than that of the RCES by c. 2.5 kyrs. The second of the two short-lived interstadials of the CES (event 6w) is slightly longer in duration (c. 900 yrs) compared with the second of the two short-lived interstadials of the RCES (c. 600 yrs) and begins earlier than that of the RCES by c. 1.7 kyrs. The late glacial reversal event (2c), within the last glacial-interglacial transitional period of the CES, was also supported by a cool climate phase (phase 8) of similar duration within the RCES which was relatively well synchronised with the associated event in the CES. Possible reasons for the imperfect synchronisation between some of the climate periods and climate phases of the RCES and other records may in part be due to differences in site location, elevation and the climatic-sensitivity of some sites resulting in different climatic conditions at different sites simultaneously and/or differences in the magnitude of climatic signals from site to site. Other factors such as sampling resolution and chronological limitations may also have influenced the apparent temporal and spatial variability of climate.

Recommendations for future work

This study has recognised evidence of climatic signals in tephric loess sequences aged c. 33—9.5 cal ka in the Rotorua region. In order to refine the occurrence and timing of these climatic periods and phases, further detailed work on these tephric loess deposits would be useful. It may be beneficial to undertake additional detailed analysis of those proxies which appeared to result in detailed paleoclimatic records (e.g. MS, loess potassium content and loess grain-size) or which may have the potential for such (e.g. phytolith analysis), at a larger number of sites in the Rotorua region and surrounding areas and/or at a higher resolution. Furthermore, it is likely that analysis of other properties of the loess not measured in this study, such as clay type, may also have the potential to provide detailed records of paleoclimate for the Rotorua region. More tightly constrained ages on the tephras present in these loess deposits may afford better synchronisation between the derived records and other New Zealand records. It may also be possible to obtain a series of AMS-derived ^{14}C ages for these loess deposits which may also assist in improving the chronological resolution when analysed together with tephra ages. Further work on the sources of the tephric loess may aid climatic interpretations from these deposits. Additional phytolith analyses within tephric loess deposits of this age in the Rotorua region are planned.

References

Allan, A. S. R., Baker, J. A., Carter, L., & Wysoczanksi, R. J. (2008). Reconstructing the Quaternary evolution of the world's most active silicic volcanic system: insights from an similar to 1.65 Ma deep ocean tephra record sourced from Taupo Volcanic Zone, New Zealand. *Quaternary Science Reviews, 27*(25-26), 2341-2360.

Alloway, B. V., Stewart, R. B., Neall, V. E., & Vucetich, C. G. (1992). Climate of the last glaciation in New Zealand, based on aerosolic quartz influx in an andesitic terrain. *Quaternary Research, 38*(2), 170-179.

Alloway, B. V., Lowe, D. J., Barrell, D. J. A., Newnham, R. M., Almond, P. C., Augustinus, P. C., Bertler, N. A. N., Carter, L., Litchfield, N. J., McGlone, M. S., Shulmeister, J., Vandergoes, M. J., Williams, P. W., & Members., N. I. (2007). Towards a climate event stratigraphy for New Zealand over the past 30 000 years (NZ-INTIMATE project). *Journal of Quaternary Science, 22*(1), 9-35.

Almond, P. C., & Tonkin, P. J. (1999). Pedogenesis by upbuilding in an extreme leaching and weathering environment, and slow loess accretion, south Westland, New Zealand. *Geoderma, 92*(1-2), 1-36.

Almond, P. C., Moar, N. T., & Lian, O. B. (2001). Reinterpretation of the glacial chronology of South Westland, New Zealand. *New Zealand Journal of Geology and Geophysics, 44*(1), 1-15.

An, Z. S., Kukla, G., Porter, S. C., & Xiao, J. L. (1991). Late Quaternary dust flow on the Chinese loess plateau. *Catena, 18*(2), 125-132.

Augustinus, P., D'Costa, D., Deng, Y. B., Hagg, J., & Shane, P. (2011). A multi-proxy record of changing environments from ca. 30 000 to 9000 cal. a BP: Onepoto maar palaeolake, Auckland, New Zealand. *Journal of Quaternary Science, 26*(4), 389-401.

Barrell, D., Alloway, B. V., Shulmeister, J., & Newnham, R. (2005). Towards a climate event stratigraphy for New Zealand over the past 30,000 years. *Institute of Geological and Nuclear Sciences Science Report* SR2005/7, pp. 1-12+poster.

Barrell, D., Almond, P. C., Lorrey, A., Newnham, R., Vandergoes, M. J., Alloway, B. V., Barrows, T. T., Burge, P., Fink, D., Hyatt, O., Lowe, D. J., Shulmeister, J., Woodward, C. A., & Williams, P. W. (in prep.). The sequence of climatic events in New Zealand over the past 30 000 years - a composite stratotype for regional correlation and comparison. *Quaternary Science Reviews*.

Benny, L. A., Kennedy, N. M., Kirkman, J. H., & Stewart, R. B. (1988). Mineralogical and texural discrimination of loess derived from a tephra near Rotorua, New Zealand. *Australian Journal of Soil Research, 26*(2), 301-312.

Blaauw, M., & Christen, J. A. (2011). Flexible paleoclimate age-depth models using an autoregressive gamma process. *Bayesian Analysis, 6*, 457-474.

Briggs, R. M., Houghton, B. F., McWilliams, M., & Wilson, C. J. N. (2005). Ar-40/Ar-39 ages of silicic volcanic rocks in the Tauranga-Kaimai area, New Zealand: dating the transition between volcanism in the Coromandel Arc and the Taupo Volcanic Zone. *New Zealand Journal of Geology and Geophysics, 48*(3), 459-469.

Carter, J. A. (2000). Phytoliths from loess in Southland, New Zealand. *New Zealand Journal of Botany, 38*(2), 325-332.

Carter, J. A. (2002). Phytolith analysis and paleoenvironmental reconstruction from Lake Poukawa Core, Hawkes Bay, New Zealand. *Global and Planetary Change, 33*(3-4), 257-267.

Carter, J. A. (2007a). *Ancient climate and environmental history from phytolith-occluded carbon.* (Unpublished doctoral dissertation). Victoria University of Wellington, Wellington.

Carter, J. A. (2007b). Phytoliths. In S. A. Elias (Ed.), *Encyclopedia of quaternary science* (Vol. 3): Elsevier.

Carter, J. A., & Lian, O. B. (2000). Palaeoenvironmental reconstruction from last interglacial using phytolith analysis, southeastern North Island, New Zealand. *Journal of Quaternary Science, 15*(7), 733-743.

Carter, R. M. (2008). Climate Swings and Roundabouts. In I. J. Graham (Ed.), *A Continent on the Move: New Zealand Geoscience into the 21st Century*. Wellington, New Zealand: Geological Society of New Zealand.

Cas, R., Porritt, L., Pittari, A., & Hayman, P. (2008). A new approach to kimberlite facies ten-ninology using a revised general approach to the nomenclature of all volcanic rocks and deposits: Descriptive to genetic. *Journal of Volcanology and Geothermal Research, 174*(1-3), 226-240.

Childs, C. W., & Searle, P. L. (1975) Element distributions in loess columns at Claremont, Table Flat and Stewarts Claim, New Zealand. In N. Z. S. Bureau (Series Ed.), *N.Z. Soil Bureau. Scientific report 20*. Lower Hutt: New Zealand Soil Bureau.

Churchman, G. J., & Lowe, D. J. (2012). Alteration, formation, and occurrence of minerals in soils. [Chapter 20]. In P. M. Huang, Y. Li & M. E. Sumner (Eds.), *Handbook of Soil Sciences. 2nd ed. Vol 1: Properties and Processes.* Boca Raton, FL, pp. 20.1-20.72: CRC Press, Taylor & Francis.

Clark, P. U., Dyke, A. S., Shakun, J. D., Carlson, A. E., Clark, J., Wohlfarth, B., Mitrovica, J. X., Hostetler, S. W., & McCabe, A. M. (2009). The Last Glacial Maximum. *Science, 325*(5941), 710-714.

Cole, J. W., Briggs, R. M., & Smith, I. (2008). Progression. In I. J. Graham (Ed.), *A Continent on the Move: New Zealand Geoscience into the 21st Century*. Wellington, New Zealand: Geological Society of New Zealand.

Darragh, M., Cole, J., Nairn, I., & Shane, P. (2006). Pyroclastic stratigraphy and eruption dynamics of the 21.9 ka Okareka and 17.6 ka Rerewhakaaitu eruption episodes from Tarawera Volcano, Okataina Volcanic Centre, New Zealand. *New Zealand Journal of Geology and Geophysics, 49*(3), 309-328.

Dodonov, A. E. (2007). Loess records. In S. A. Elias (Ed.), *Encyclopedia of quaternary science* (Vol. 4). Amsterdam: Elsevier.

Eden, D. N., & Hammond, A. P. (2003). Dust accumulation in the New Zealand region since the last glacial maximum. *Quaternary Science Reviews, 22*(18-19), 2037-2052.

EPICA Community Members. (2006). One-to-one coupling of glacial climate variability in Greenland and Antarctica. *Nature, 444*.

Esler, W. (2010). An introduction to the Rotorua Basin and Okataina Volcanic Centre: an iconoclastic view. In D. Lowe, V. E. Neall, M. Hedley, B. Clothier & A. Mackay (Eds.), *Guidebook for pre-conference North Island New Zealand "Volcanoes to ocean" 26th-30th July, 2010, 19th World Congress of Soil Science: soil solutions for a changing world: Brisbane Australia 1-6 August 2010*. Palmerston North, New Zealand: New Zealand Society of Soil Science.

Froggatt, P. C., & Lowe, D. J. (1990). A review of late Quaternary silicic and some other tephra formations from New Zealand - their stratigraphy, nomenclature, distribution, volume, and age. *New Zealand Journal of Geology and Geophysics, 33*(1), 89-109.

Gonzalez, S., Jones, J. M., & Williams, D. L. (Eds.). (1999). Characterization of tephras using magnetic properties: an example from SE Iceland (Vol. 161). London: The Geological Society of London.

Hajdas, I., Lowe, D. J., Newnham, R. M., & Bonani, G. (2006). Timing of the late-glacial climate reversal in the Southern Hemisphere using high-resolution radiocarbon chronology for Kaipo bog, New Zealand. *Quaternary Research, 65*(2), 340-345.

Hay, M. J. M., Walker, T. W., Adams, A. F. R., & Campbell, A. S. (1976). Potassium status of 6 loessial soils of Canterbury, New Zealand, in relation to rainfall and rate of loess accumulation. *Journal of Soil Science, 27*(2), 227-236.

Heller, F., & Evans, M. E. (1995). Loess Magnetism. *Reviews of Geophysics, 33*(2), 211-240.

Hill, R. B. (1999). *Applying a land systems approach to describe and partition soil and forest variability, southern Mamaku Plateau, part of Kinleith Forest, New Zealand.* (Unpublished doctoral dissertation). Lincoln University, Canterbury.

Hogg, A. G., Lowe, D. J., Palmer, J. G., Boswijk, G., & Bronk Ramsey, C. J. (in press). Revised calender date for the Taupo eruption derived by ^{14}C wiggle-matching using a New Zealand Kauri ^{14}C calibration dataset. *The Holocene*.

Holt, K. A., Wallace, R. C., Neall, V. E., Kohn, B. P., & Lowe, D. J. (2010). Quaternary tephra marker beds and their potential for palaeoenvironmental reconstruction on Chatham Island, east of New Zealand, southwest Pacific Ocean. *Journal of Quaternary Science, 25*(7), 1169-1178.

Howorth, R. (1975). New formations of late Pleistocene tephra from the Okataina Volcanic Centre, New Zealand. *New Zealand Journal of Geology and Geophysics, 18*(5), 683-711.

Iriondo, M. H., & Krohling, D. M. (2007). Non-classical types of loess. *Sedimentary Geology, 202*(3), 352-368.

Jurado-Chichay, Z., & Walker, G. P. L. (2000). Stratigraphy and dispersal of the Mangaone Subgroup pyroclastic deposits, Okataina Volcanic Centre, New Zealand. *Journal of Volcanology and Geothermal Research, 104*(1-4), 319-383.

Kennedy, N. (1994). New Zealand tephro-chronology as a tool in geomorphic history of the c.140 ka Mamaku Ignimbrite plateau and in relating oxygen-isotope stages. *Geomorphology, 9*(2), 97-115.

Kilgour, G. N., & Smith, R. T. (2008). Stratigraphy, dynamics, and eruption impacts of the dual magma Rotorua eruptive episode, Okataina Volcanic Centre, New Zealand. *New Zealand Journal of Geology and Geophysics, 51*(4), 367-378.

Kondo, R., C., C., & Atkinson, I. (1994). *Opal Phytoliths of New Zealand*. Lincoln, New Zealand: Manaaki Whenua Press.

Leonard, G. S., Begg, J. G., & Wilson, C. J. (2010). Geology of the Rotorua area. Institute of Geological & Nuclear Sciences 1:250 000 geological map 5. 1 sheet + 102 p. Lower Hutt, New Zealand: GNS Science.

Litchfield, N. J., & Berryman, K. R. (2005). Correlation of fluvial terraces within the Hikurangi Margin, New Zealand: implications for climate and baselevel controls. *Geomorphology, 68*(3-4), 291-313.

Liu, Q. S., Deng, C. L., Torrent, J., & Zhu, R. X. (2007). Review of recent developments in mineral magnetism of the Chinese loess. *Quaternary Science Reviews, 26*(3-4), 368-385.

Liu, X. M., Hesse, P., Beget, J., & Rolph, T. (2001). Pedogenic destruction of ferrimagnetics in Alaskan loess deposits. *Australian Journal of Soil Research, 39*(1), 99-115.

Lorrey, A., Vandergoes, M. J., Almond, P. C., Renwick, J., Stephens, T., Bostock, H., Mackintosh, A., Newnham, R., Williams, P. W., Ackerley, D., Neil, H., & Fowler, A. M. (in press). Palaeocirculation across New Zealand during the last glacial maximum at c. 21 ka. *Quaternary Science Reviews*.

Lowe, D. J. (2010). Quaternary volcanism, tephras, and tephra-derived soils in New Zealand: an introductory review. In D. J. Lowe, V. E. Neall, M. Hedley, B. Clothier & A. Mackay (Eds.), *Guidebook for pre-conference North Island New Zealand "Volcanoes to ocean" 26th-30th July, 2010, 19th World Congress of Soil Science: soil solutions for a changing world: Brisbane Australia 1-6 August 2010*. Palmerston North, New Zealand: New Zealand Society of Soil Science.

Lowe, D. J. (2011). Tephrochronology and its application: A review. *Quaternary Geochronology, 6*(2), 107-153.

Lowe, D. J., & Green, J. (1992). Lakes. In J. M. Soons & M. J. Selby (Eds.), *Landforms of New Zealand* (pp. 107-143). Auckland: Longman Paul.

Lowe, D. J., & Percival, H. J. (1993). Clay mineralogy of tephras and associated paleosols and soils, and hydrothermal deposits, North Island [New Zealand]. *Review and Guide F1 Field Tour - New Zealand*. Tenth International Clay Conference, Adelaide, Australia, 1-110.

Lowe, D. J., & Briggs, R. M. (1994). Intra-conference Tour Day 2: Hamilton-Rotorua-Hamilton. In D. Lowe (Ed.), *Conference Tour Guides. International Inter-Inqua Field Conference on Tephrochronology, Loess, and Palaeopedology* (pp. 45-71). Hamilton, New Zealand: University of Waikato.

Lowe, D. J., & Tonkin, P. (2010). Unravelling upbuilding pedogenesis in tephra and loess sequences in New Zealand using tephrochronology. Proceedings of the 19th World Congress of Soil Science "Soil Solutions for a Changing World" (1-6 Aug., 2010, Brisbane), Symposium 1.3.2 Geochronological techniques and soil formation, pp. 34-37. Published on DVD and at http://www.iuss.org.

Lowe, D. J., Tonkin, P., Palmer, A., & Palmer, J. (2008a). Dusty Horizons. In I. J. Graham (Ed.), *A Continent on the Move: New Zealand Geoscience into the 21st Century*. Wellington, New Zealand: Geological Society of New Zealand.

Lowe, D. J., Shane, P., Alloway, B. V., & Newnham, R. M. (2008b). Fingerprints and age models for widespread New Zealand tephra marker beds erupted since 30,000 years ago: a framework for NZ-INTIMATE. *Quaternary Science Reviews, 27*(1-2), 95-126.

Lowe, D. J., Neall, V. E., Hedley, M. J., Clothier, B. E., & Mackay, A. D. (2010). Guidebook for Pre-Conference North Island New Zealand 'Volcanoes To Ocean' 26th-30th July, 2010. 19th World Congress of Soil Science, Brisbane. Soil & Earth Sciences Occasional Publication No. 3. Massey University, Palmerston North, New Zealand, ISSN No. 1175-4966

Lowe, D. J., Lanigan, K. L., Esler, W., Pittari, A., & Newnham, R. M. (2011). Using tephrochronology to synchronize and date high-resolution palaeoenvironmental reconstructions derived from tephric loess deposits *18th INQUA Congress*.

Lowe, D. J. (Ed.). (1995). Teaching clays: from ashes to allophane. Proceedings 10th International Clay Conference, Adelaide, Australia (1993): CSIRO Publishing, Melbourne, 19-23.

Maher, B. A. (1998). Magnetic properties of modern soils and Quaternary loessic paleosols: paleoclimatic implications. *Palaeogeography Palaeoclimatology Palaeoecology, 137*(1-2), 25-54.

Maher, B. A., & Thompson, R. (1991). Mineral Magnetic Record of the Chinese Loess and Paleosols. *Geology, 19*(1), 3-6.

Manville, V., & Wilson, C. J. N. (2004). The 26.5 ka Oruanui eruption, New Zealand: a review of the roles of volcanism and climate in the post-eruptive sedimentary response. *New Zealand Journal of Geology and Geophysics, 47*, 525-547.

McCraw. (1975). Quaternary Airfall Deposits of New Zealand. *Bulletin of the Royal Society of New Zealand*, 35-44.

McGlone, M. S. (1983). Holocene pollen diagrams, Lake Rotorua, North Island, New Zealand. *Journal of the Royal Society of New Zealand, 13*(1-2), 53-65.

McGlone, M. S., Howorth, R., & Pullar, W. A. (1984). Late pleistocene stratigraphy, vegetation and climate of the Bay of Plenty and Gisborne regions, New Zealand. *New Zealand Journal of Geology and Geophysics, 27*(3), 327-350.

McLaren, R., & Cameron, K. (2008). *Soil Science: Sustainable production and environmental protection*: Oxford University Press.

Milner, D. M., Cole, J. W., & Wood, C. P. (2002). Asymmetric, multiple-block collapse at Rotorua Caldera, Taupo Volcanic Zone, New Zealand. *Bulletin of Volcanology, 64*(2), 134-149.

Milner, D. M., Cole, J. W., & Wood, C. P. (2003). Mamaku Ignimbrite: a caldera-forming ignimbrite erupted from a compositionally zoned magma chamber in Taupo Volcanic Zone, New Zealand. *Journal of Volcanology and Geothermal Research, 122*(3-4), 243-264.

Mix, A. C., Bard, E., & Schneider, R. (2001). Environmental processes of the ice age: land, oceans, glaciers (EPILOG). *Quaternary Science Reviews, 20*(4), 627-657.

Mortimer, N. (2008). Remnants of a Distant Past. In I. J. Graham (Ed.), *A Continent on the Move: New Zealand into the 21st Century*. Wellington, New Zealand: Geological Society of New Zealand.

Murphy, B. P., & Bowman, D. (2009). The carbon and nitrogen isotope composition of Australian grasses in relation to climate. *Functional Ecology, 23*(6), 1040-1049.

Nairn, I. A. (1980). Source, age and eruptive mechanisms of Rotorua Ash. *New Zealand Journal of Geology and Geophysics, 23*(2), 193-207.

Nairn, I. A. (1992). The Te Rere and Okareka eruptive episodes - Okataina-Volcanic-Center, Taupo Volcanic Zone, New Zealand. *New Zealand Journal of Geology and Geophysics, 35*(1), 93-108.

Newnham, R. M., & Lowe, D. J. (2000). Fine-resolution pollen record of late-glacial climate reversal from New Zealand. *Geology, 28*(8), 759-762.

Newnham, R. M., Lowe, D. J., & Green, J. D. (1989). Palynology, Vegetation and Climate of the Waiakato Lowlands, North Island, New Zealand, since c 18,000 years ago. *Journal of the Royal Society of New Zealand, 19*(2), 127-150.

Newnham, R. M., Lowe, D. J., & Williams, P. W. (1999). Quaternary environmental change in New Zealand: a review. *Progress in Physical Geography, 23*(4), 567-610.

Newnham, R. M., Alloway, B. V., & NZ-INTIMATE Members. (2007a). Towards a climate event stratigraphy for New Zealand over the past 30,000 years (the NZ-INTIMATE project). *Quaternary International, 167-168 Supplement*, 304.

Newnham, R. M., Eden, D. N., Lowe, D. J., & Hendy, C. H. (2003). Rerewhakaaitu Tephra, a land-sea marker for the Last Termination in New Zealand, with implications for global climate change. *Quaternary Science Reviews, 22*(2-4), 289-308.

Newnham, R. M., Lowe, D. J., Giles, T., & Alloway, B. V. (2007b). Vegetation and climate of Auckland, New Zealand, since ca.32 000 cal. yr ago: support for an extended LGM. *Journal of Quaternary Science, 22*, 517-534.

Palmer, A. S., & Pillans, B. J. (1996). Record of climatic fluctuations from ca 500 ka loess deposits and paleosols near Wanganui, New Zealand. *Quaternary International, 34-6*, 155-162.

Pecsi, M. (1995). The role of principles and methods in loess-paleosol investigations. *GeoJournal*, 117-131.

Pickett, R. C. (2008). *A tephra-dated record of palaeoenvironmental change since ~ 5,500 years ago from Lake Rotorua, North Island, New Zealand.* (Unpublished master's thesis). University of Waikato, Hamilton.

Piperno, D. (2006). *Phytoliths: a comprehensive guide for archaeologists and paleoecologists*: Altamira Rowman

Price, R., Gamble, J., & Stewart, B. (2008). The Subduction Factory. In I. J. Graham (Ed.), *A Continent on the Move: New Zealand Geoscience into the 21st Century*. Wellington, New Zealand: Geological Society of New Zealand.

Ramsey, C. B. (2009a). Bayesian analysis of radiocarbon dates. *Radiocarbon, 51*(1), 337-360.

Ramsey, C. B. (2009b). Dealing with outliers and offsets in radiocarbon dating. *Radiocarbon, 51*(3), 1023-1045.

Read, N. E. (Ed.). (1974). Soil Groups of New Zealand: Part 1: yellow-brown pumice soils. Wellington, New Zealand: New Zealand Society of Soil Science.

Reimer, P. J., Baillie, M. G. L., Bard, E., Bayliss, A., Beck, J. W., Blackwell, P. G., Ramsey, C. B., Buck, C. E., Burr, G. S., Edwards, R. L., Friedrich, M., Grootes, P. M., Guilderson, T. P., Hajdas, I., Heaton, T. J., Hogg, A. G., Hughen, K. A., Kaiser, K. F., Kromer, B., McCormac, F. G., Manning, S. W., Reimer, R. W., Richards, D. A., Southon, J. R., Talamo, S., Turney, C. S. M., van der Plicht, J., & Weyhenmeye, C. E. (2009). IntCal09 and Marine09 radiocarbon age calibration curves, 0-50,000 years cal BP. *Radiocarbon, 51*(4), 1111-1150.

Rogers, K. (2010). *Detecting environmental change using stable isotopes*. Paper presented at the 7th Quaternary Techniques Shortcourse: techniques of palaeoclimatic and palaeoenvironmental reconstruction, National Isope Centre, GNS Science, Wellington.

Sandiford, A., Horrocks, M., Newnham, R., Ogden, J., & Alloway, B. (2002). Environmental change during the last glacial maximum (c. 25 000-c. 16 500 years BP) at Mt Richmond, Auckland Isthmus, New Zealand. *Journal of the Royal Society of New Zealand, 32*(1), 155-167.

Sheldon, N. D., & Tabor, N. J. (2009). Quantitative paleoenvironmental and paleoclimatic reconstruction using paleosols. *Earth-Science Reviews, 95*, 1-52.

Shulmeister, J., & McGlone, M. (2008). The Last Glaciation. In I. J. Graham (Ed.), *A Continent on the Move: New Zealand Geoscience into the 21st Century*. Wellington, New Zealand: Geological Society of New Zealand.

Singer, M. J., Verosub, K. L., Fine, P., & TenPas, J. (1996). A conceptual model for the enhancement of magnetic susceptibility in soils. *Quaternary International, 34-6*, 243-248.

Smith, V. C., Shane, P., & Smith, I. E. M. (2002). Tephrostratigraphy and geochemical fingerprinting of the Mangaone Subgroup tephra beds, Okataina Volcanic Centre, New Zealand. *New Zealand Journal of Geology and Geophysics, 45*(2).

Smith, V. C., Shane, P., & Nairn, I. A. (2004). Reactivation of a rhyolitic magma body by new rhyolitic intrusion before the 15.8 ka Rotorua eruptive episode: implications for magma storage in the Okataina Volcanic Centre, New Zealand. *Journal of the Geological Society, 161*, 757-772.

Sun, D. H., Su, R. X., Li, Z. J., & Lu, H. Y. (2011). The ultrafine component in Chinese loess and its variation over the past 7.6 Ma: implications for the history of pedogenesis. *Sedimentology, 58*(4), 916-935.

Swap, R. J., Aranibar, J. N., Dowty, P. R., Gilhooly, W. P., & Macko, S. A. (2004). Natural abundance of C-13 and N-15 in C-3 and C-4 vegetation of southern Africa: patterns and implications. *Global Change Biology, 10*, 350-358.

Tang, Y. J., Jia, J. Y., & Xie, X. D. (2003). Records of magnetic properties in Quaternary loess and its paleoclimatic significance: a brief review. *Quaternary International, 108*, 33-50.

Thorn, V. C. (2006). Vegetation reconstruction from soil phytoliths, Tongariro National Park, New Zealand. *New Zealand Journal of Botany, 44*(4), 397-413.

Vandergoes, M. J., Newnham, R. M., Preusser, F., Hendy, C. H., Lowell, T. V., Fitzsimons, S. J., Hogg, A. G., Kasper, H. U., & Schluchter, C. (2005). Regional insolation forcing of late Quaternary climate change in the Southern Hemisphere. *Nature, 436*(7048), 242-245.

Vandergoes, M. J., Hogg, A. G., Lowe, D. J., Newnham, R. M., Denton, G. M., Barrell, D. J. A., Almond, P. C., Allan, A., & Wilson, C. J. N. (2011). *Refining the age of the Kawakawa/Oruanui tephra in New Zealand.* Paper presented at the 18th INQUA Congress, Bern, Switzerland [available on INQUA website: http://www.inqua2011.ch/?a=programme&subnavi=abstract&id=1572]

Verosub, K. L., Fine, P., Singer, M. J., & Tenpas, J. (1993). Pedogenesis and paleoclimate - interpretation of the magnetic-susceptibility record of Chinese loess-paleosol sequences. *Geology, 21*(11), 1011-1014.

Vucetich, & Pullar. (1969). Stratigraphy and chronology of late pleistocene volcanic ash beds in central North Island, New Zealand. *N.Z. Journal of Geology and Geophysics*, 784-837.

Williams, P. W., Neil, H. L., & Zha, J. X. (2010). Age frequency distribution and revised stable isotope curves for New Zealand speleothems: palaeoclimatic implications. *International Journal of Speleology, 39*(2), 99-112.

Wilmshurst, J. M., McGlone, M. S., Leathwick, J. R., & Newnham, R. M. (2007). A pre-deforestation pollen-climate calibration model for New Zealand and quantitative temperature reconstructions for the past 18 000 years BP. *Journal of Quaternary Science, 22*(5), 535-547.

Wilson, C. J., Gravley, D. M., Leonard, G., & Rowland, J. V. (2009). Volcanism in the central Taupo Volcanic Zone, New Zealand: tempo, styles and controls. In T. Thordarson, S. Self, G. Larsen, S. K. Rowland & A. Hoskuldsson (Eds.), *Studies in Volcanology: The Legacy of George Walker* (pp. 225-249). UK: The Geological Society for IAVCEI.

Wilson, C. J. N. (2001a). The 26.5 ka Oruanui eruption, New Zealand: an introduction and overview. *Journal of Volcanology and Geothermal Research, 112*(1-4), 133-174.

Wilson, C. J. N. (2001b). The 26.5 ka Oruanui eruption, New Zealand: an introduction and overview. *Journal of Volcanology and Geothermal Research, 112*(1-4), 133-174.

Wilson, C. J. N., & Leonard, G. (2008). Slumbering Giants. In I. Smith (Ed.), *A Continent on the Move: New Zealand Geoscience into the 21st Century*. Wellington, New Zealand: Geological Society of New Zealand.

Wilson, C. J. N., Rogan, A. M., Smith, I. E. M., Northey, D. J., Nairn, I. A., & Houghton, B. F. (1984). Caldera volcanoes of the Taupo Volcanic Zone, New Zealand. *Journal of Geophysical Research, 89*(NB10), 8463-8484.

Wilson, C. J. N., Houghton, B. F., McWilliams, M. O., Lanphere, M. A., Weaver, S. D., & Briggs, R. M. (1995). Volcanic and structural evolution of Taupo Volcanic Zone, New Zealand: a review. *Journal of Volcanology and Geothermal Research, 68*(1-3), 1-28.

Xiao, J., Porter, S. C., An, Z. S., Kumai, H., & Yoshikawa, S. (1995). Grain-size of quartz as an indicator of winter monsoon strength on the loess plateau of central China during the last 130,000 yr. *Quaternary Research, 43*(1), 22-29.

Xie, Q. Q., Chen, T. H., Xu, H. F., Chen, J., Ji, J. F., Lu, H. Y., & Wang, X. Y. (2009). Quantification of the contribution of pedogenic magnetic minerals to magnetic susceptibility of loess and paleosols on Chinese Loess Plateau: Paleoclimatic implications. *Journal of Geophysical Research-Solid Earth, 114*.

Zhou, L. P., Oldfield, F., Wintle, A. G., Robinson, S. G., & Wang, J. T. (1990). Partly pedogenic origin of magnetic variations in Chinese loess. *Nature, 346*(6286), 737-739.

Appendix 1 – Field site photographs

Dalbeth Rd site

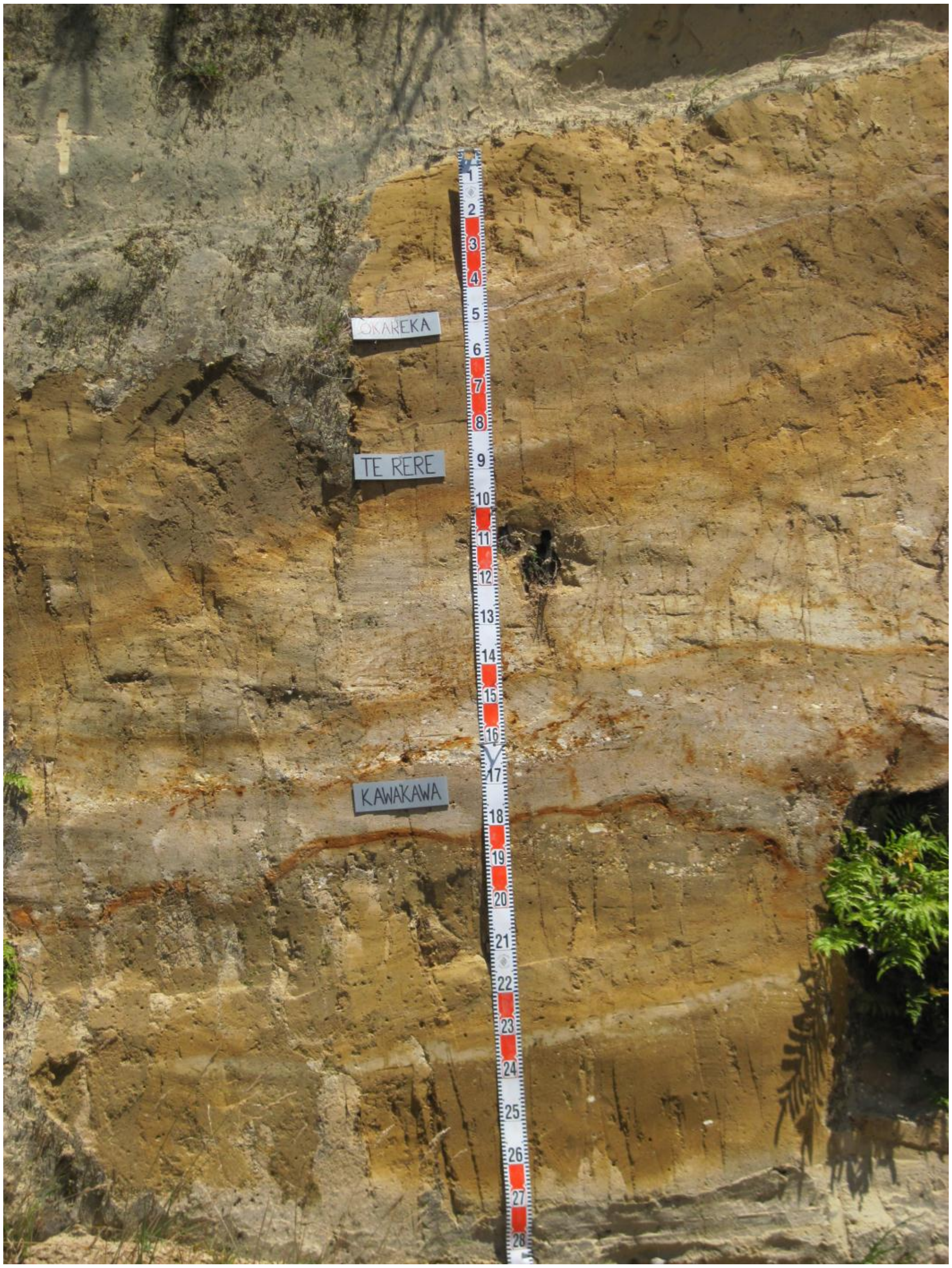

Highlands Rd (stratigraphy uncertain)

Belk Rd

Hamurana Rd

Kaharoa Rd


ROTORUA
REREWHAKAAITU
OKAREKA
TE RERE
ORUANUI IG
?
KAWAKAWA
UNIT L

Glue Pot Rd

Leslie Rd

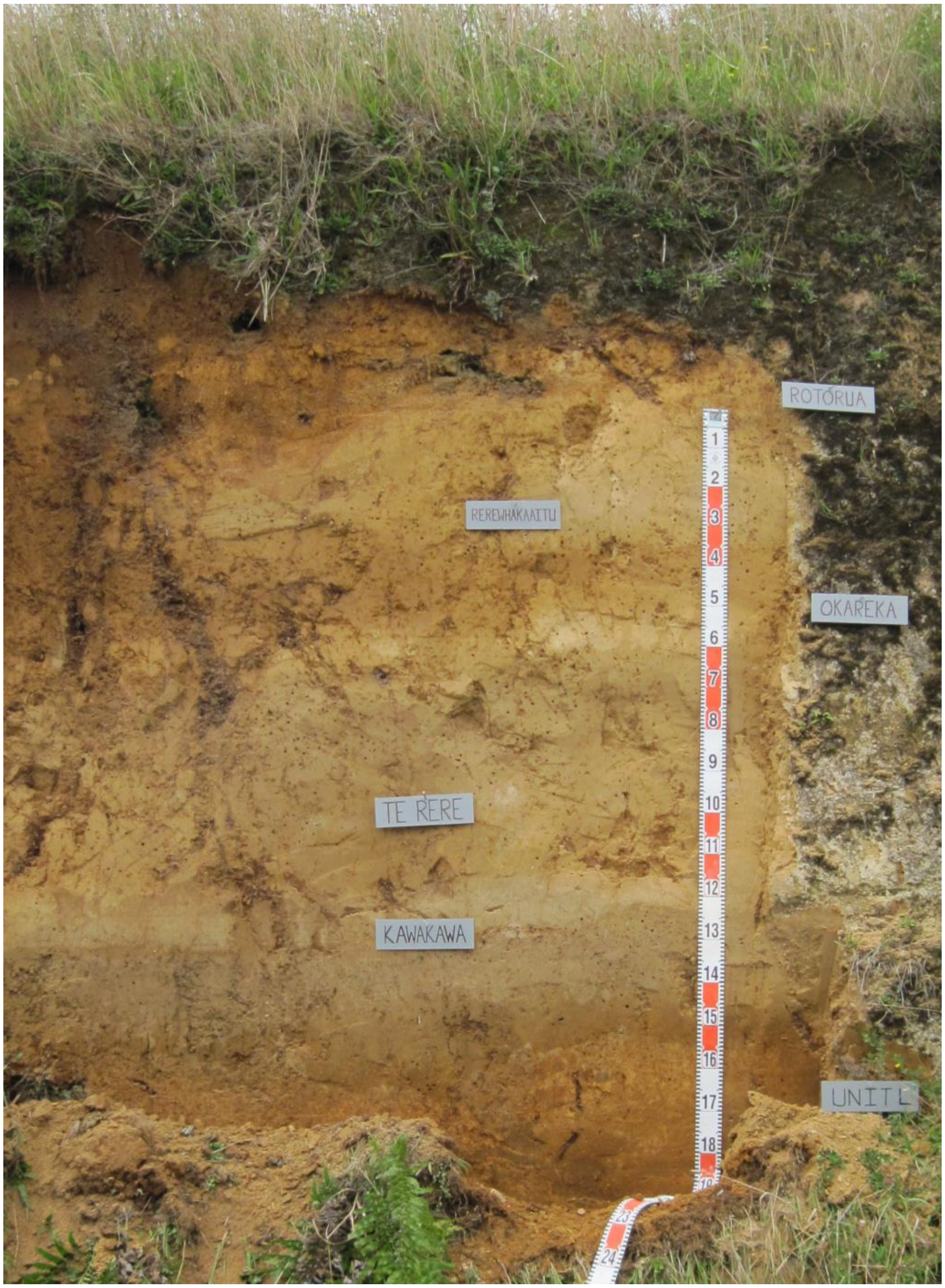

Taumata Rd

Maniatutu Rd (1/2-upper)

Maniatutu Rd (2/2-lower)

Oturoa Rd (1/3-upper)

Oturoa Rd (2/3-mid)

Oturoa Rd (3/3-upper)

Dansey R (1/4-upper)

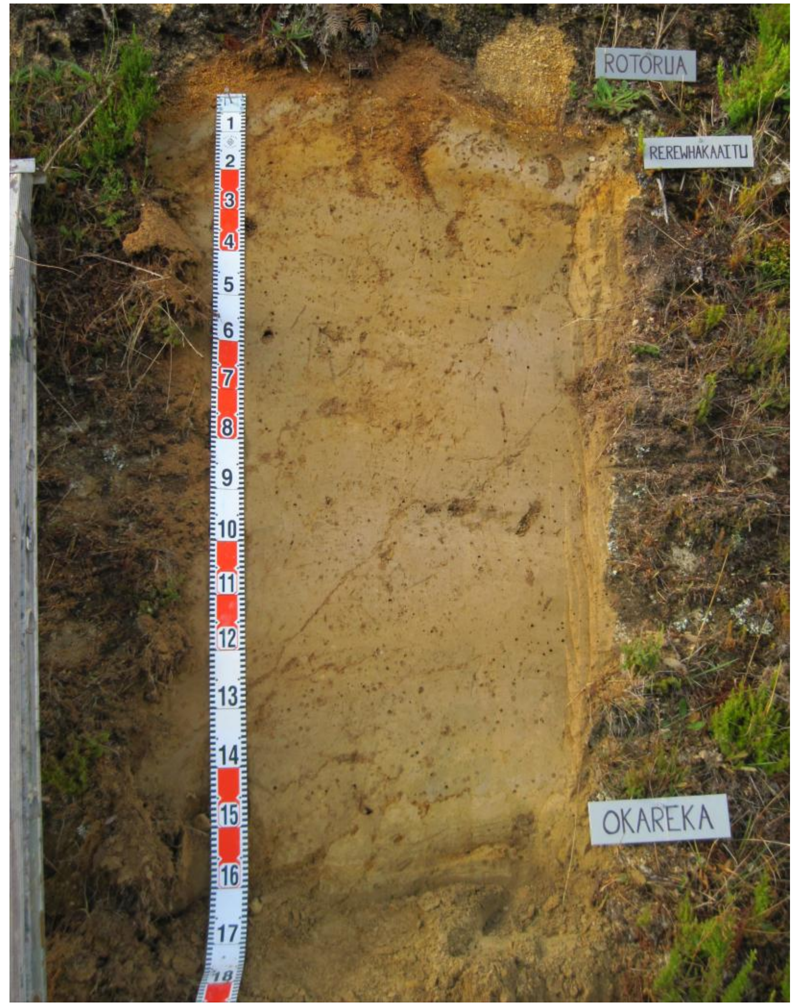

Dansey Rd (2/4-mid)

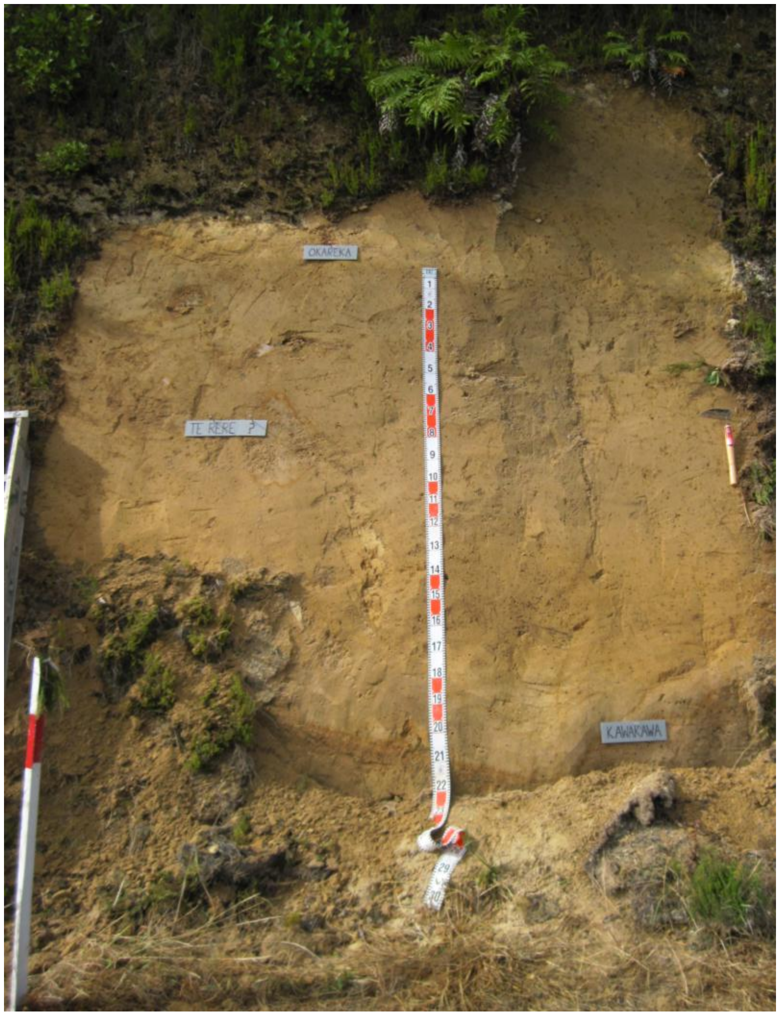

Dansey Rd (3/4-mid)

Dansey Rd (4/4-lower)

Tapapa Rd (1/2-upper)

Tapapa Rd (2/2-lower)

Penny Rd (magnetic susceptibility site)

Penny Rd (stratigraphic description site)

Appendix 2 – Field site stratigraphic logs

Cameron's Quarry site stratigraphic log

Map reference: V15 225 660

Waiohau Tephra?
loess
Rotorua Tephra?
loess
Rerewhakaaitu Tephra?
loess
Okareka Tephra
loess
Te Rere Tephra?
loess
Kawakawa Tephra
loess
Unit L

Stratigraphic Log

Site name: **Belk Road site**

Date: 2011

Map reference: NZMS 260 U15 827 677

Depth (m) | Stratigraphic log | Lithological description

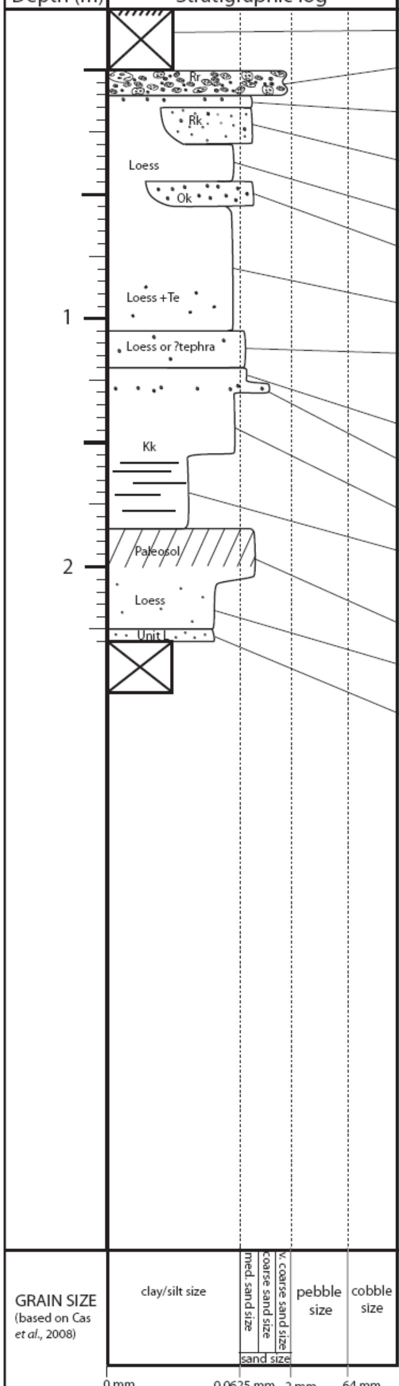

- Post Rotorua material and modern soil (not drawn to scale)
- **Rotorua Tephra.** Bright yellowish brown (10 YR 6/8), massive, very coarse sand texture with white/orange sub-angular pumice lapilli (up to 1-2 mm). Abrupt wavy lower boundary.
- **Loess.** Yellowish brown (10 YR 5/8) massive, medium sand texture with white, sub-angular, very course sand-sized pumice. Diffuse lower boundary.
- **Rerewhakaaitu Tephra (within loess).** Dull yellow orange (10 YR 6/3), discontinuous, massive, medium sand texture with pumice clasts (from above). Diffuse lower boundary.
- **Loess.** Bright yellowish brown (10 YR 6/8) massive, clay/silt texture. Diffuse lower boundary.
- **Okareka Tephra (within loess).** Dull yellow orange (10 YR 6/4), discontinuous, massive, medium sand texture.
- **Loess (with clasts of Te Rere tephra?).** Dull yellow orange (10 YR 6/4) massive, clay/silt texture. Few black obsidian lithics – may correspond to Te Rere tephra.
- **Loess or (?)tephra.** Yellowish brown (2.5 Y 5/6) normally graded, medium sand texture, with few, white, sub-rounded pumice clasts (up to 5 mm). Distinct smooth lower boundary.

Kawakawa Tephra.

- Upper 8 cm: Yellowish brown (10 YR 5/6), massive, mottled, medium sand texture. Distinct convolute lower boundary
- Upper-mid 4 cm: Yellowish brown (10 YR 5/6), normally graded, course sand texture with white, sub-angular pumice clasts (up to 5 mm). Distinct convolute lower boundary.
- Lower-mid 28 cm: Dull yellowish brown (10 YR 5/4), massive, clay/silt texture. Sharp wavy lower boundary.
- Lower 26 cm: Dull yellow orange (10 YR 7/3) & light grey (10 YR 8/2), stratified, clay/silt texture with Mg concretions. Sharp smooth lower boundary.

Loess.

- Upper 20 cm (enhanced soil development) = Yellowish brown (10 YR 5/4) massive, medium sand texture.
- Lower 20 cm = Dull yellow orange (10 YR 6/3), massive, clay/silt texture with some course sand-sized clasts. Diffuse lower boundary.
- **Unit L.** Yellowish brown (10 YR 5/6) pyroclastic texture with some coarse sand-sized clasts within a clay/silt-textured matrix. Very fragile orange pumice clasts and black clasts.

Stratigraphic Log

Site name: **Dalbeth Road site**

Date: 2011

Map reference: NZMS260 U15 880 435

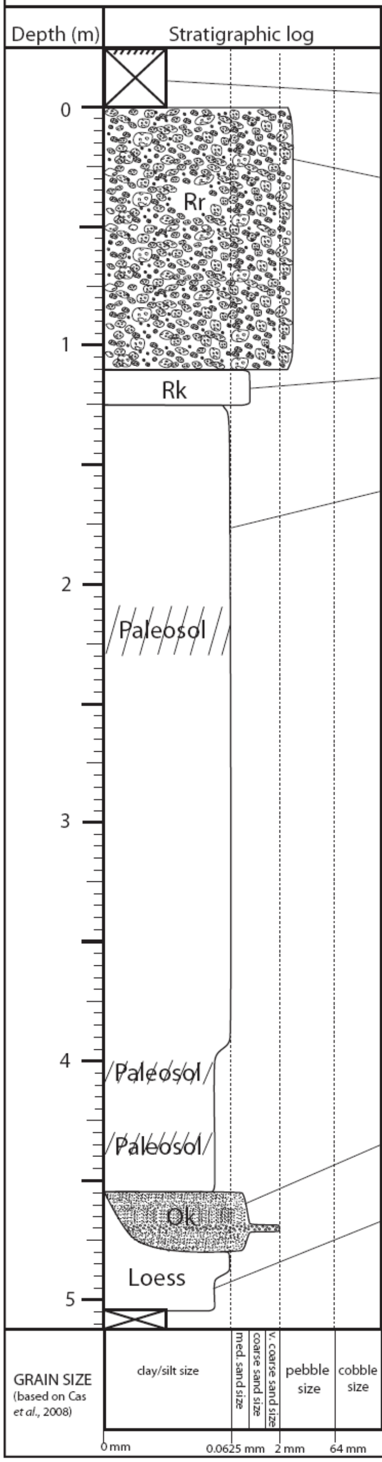

Lithological description

- Post Rotorua material and modern soil (not drawn to scale)

- **Rotorua Tephra.** Bright yellowish brown (10 YR 6/8) shower bedded lapilli (pumice up to 15 mm, black rhyolite lithics approximately 12 mm). Sharp wavy lower boundary.

- **Rerewhakaaitu Tephra/Loess?** Dull yellowish brown (10 YR 5/4) & Yellowish brown (10 YR 5/8) massive, firm, discontinuous, medium sand texture. Diffuse lower boundary.

- **Sand dune/loess.**
  Upper 85 cm: Dull yellow orange (10 YR 6/4) massive, soft, clay/silt texture. Diffuse lower boundary.
  20 cm (paleosol?): Dull yellow orange (10 YR 6/3) massive, slightly mottled (Dull yellowish brown (10 YR 5/4)) clay/silt texture. Diffuse lower boundary.
  50 cm: Dull yellowish brown (10 YR 5/3) massive, slightly mottled (Dull yellowish brown (10 YR 5/4)) clay/silt texture. Very diffuse lower boundary.
  40 cm: Dull yellow orange (10 YR 6/3) massive, mottled (Brown (10 YR 4/4)) clay/silt texture. Very diffuse lower boundary.
  75 cm: Dull yellowish brown (10 YR 5/3) massive, clay/silt texture. Very diffuse lower boundary.
  5 cm: Dull yellowish brown (10 YR 5/4) massive, clay/silt texture. Diffuse, slightly occluded lower boundary.
  10 cm (paleosol): Dull yellowish brown (10 YR 5/3) massive, clay/silt texture. Diffuse, slightly occluded lower boundary.
  20 cm: Dull yellowish brown (10 YR 5/4) massive, clay/silt texture. Occluded lower boundary.
  10 cm (paleosol): Dull yellowish brown (10 YR 5/4) massive, mottled (Brown (10 YR 4/4)), clay/silt texture. Very diffuse lower boundary.
  Lower 15 cm: Dull yellowish brown (10 YR 5/4) massive, slightly mottled, clay/silt texture. Very diffuse lower boundary.

- **Okareka Tephra.** Dull yellow orange (10 YR 6/3) & dull yellow orange (10 YR 6/4) discontinuous, stratified unit (upper 17 cm= medium sand texture, mid 3 cm = very coarse sand texture, lower 5 cm = medium sand texture) with pumice lapilli. Occluded lower boundary.

- **Loess.**
  Upper 10 cm: Dull yellowish brown (10 YR 5/4) massive, clay/silt texture. Occluded lower boundary.
  Lower 20 cm: Dull yellow orange (10 YR 6/3) massive, vaugly mottled, clay/silt texture with Mg concretions.

Note: Kawakawa Tephra was observed few metres furtheralong the road from the sire of this stratigraphic column

Stratigraphic Log

Site name: **Danseys Road site**

Date: 2010

Map reference: NZMS260 U15 855 408

Depth (m)	Stratigraphic log	Lithological description

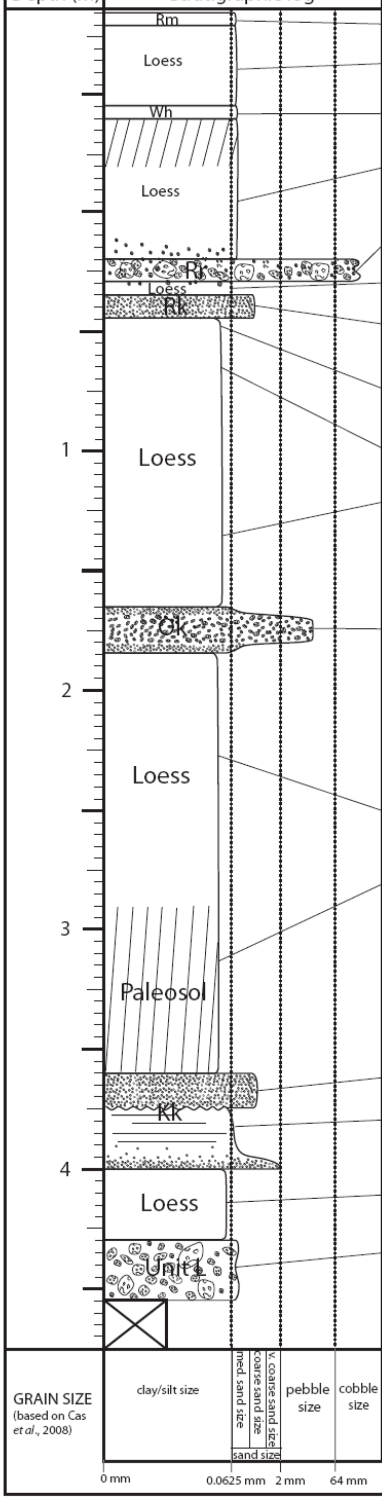

Rotoma Tephra (podolized) (not to scale)

Loess.

Waiohau Tephra (not to scale)

Loess. Including upper paleosol and mixing with Rr at base

Rotorua Tephra (not to scale). Bright brown (7.5YR 5/8) hard, angular to sub-rounded, white, pebble to cobble-sized pumice clasts, and black lithics.

Loess. Yellowish brown (10YR 5/8) clay/silt texture with pebble-sized pumice clasts. Crystal rich. Indistinct occluded upper boundary.

Rerewhakaaitu Tephra. Greyish yellow brown (10YR 6/2), medium sand texture. Crystal rich. Charcoal present. Indistinct wavy upper boundary.

Loess.
Upper 5 cm: Bright yellowish brown (10YR 6/8), clay/silt texture. Crystal rich. Distinct wavy upper boundary.

Middle 25 cm: Olive brown (2.5Y 4/6), clay/silt texture. Crystal rich.

Lower 95 cm: Dull yellowish brown (10YR 5/4), clay/silt texture. Crystal rich.

Okareaka Tephra. Dull yellow orange (10YR 6/4) clay/silt-textured base and top separated by pebble-sized bed. Hard angular white (2-5 mm) pumice clasts present. Few crystals. Indistinct wavy upper boundary.

Loess.
Upper 80 cm: Dull yellowish brown (10YR 5/4), clay/silt texture. Crystal rich. Abrupt wavy upper boundary.

Lower 95 cm: Brown (10YR 4/6), clay/silt texture. Crystal rich. Diffuse boundary with above loess unit.

Kawakawa Tephra.
Upper: Dull yellowish brown (10YR 5/4) mottled, medium sand texture with few hard, rounded, white pumice clasts (approx. 2 mm). Few crystals. Indistinct convelute upper boundary.
Lower: Dull Yellowish brown (10YR 5/3) stratified, clay/silt texture with very course sand-sized base. Few crystals. Mg concreations present. Abrupt irregular and discontinuous upper boundary

Loess. Olive brown (2.5Y 4/6), massive, clay/silt texture. Abrupt wavy upper boundary.

Unit L. Yellowish brown (10YR 5/8), rounded orange pebble-sized (5-20 mm) pumice clasts within clay/silt-sized maxtrix. Crystal rich. Diffuse wavey upper boundary.

Stratigraphic Log

Site name: **Glue Pot Road site**

Date: 2011

Map reference: NZMS260 U15 876 661

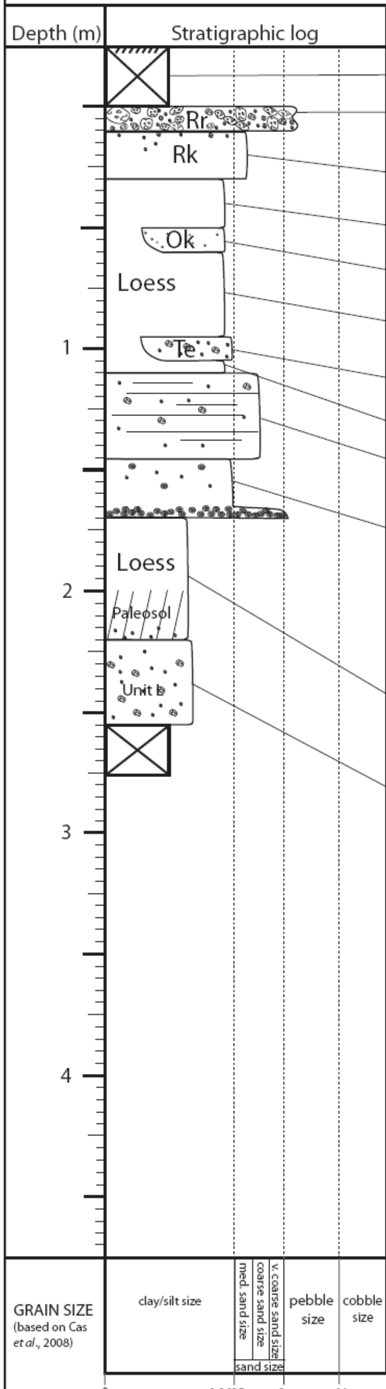

Lithological description

- Post Rotorua material and modern soil (not drawn to scale)
- **Rotorua Tephra.** Yellowish brown (10 YR 5/8) massive, pebble texture, with orange, sub-rounded pumice lapilli up to 3 mm). Indistinct irregular lower boundary.
- **Rerewhakaaitu Tephra.** Dull yellow orange (10 YR 6/4) massive, medium sand texture (with some Rotorua Tephra mixed down). Diffuse lower boundary.
- **Loess.** Brown (10 YR 4/6) massive, clay/silt texture. Occluded abrupt lower boundary.
- **Okareka Tephra.** Bright yellowish brown (10 YR 6/6) discontinuous, massive, clay/silt texture. Sharp occluded lower boundary.
- **Loess.** Dull yellowish brown (10 YR 5/4) massive, clay/silt texture with mottles. Very diffuse lower boundary.
- **Te Rere Tephra** within loess. Pumice (up to 2 mm) and lithic (sharp, up to 8 mm) clasts within clay/silt-sized matrix.
- **Loess.** Dull yellowish brown (10 YR 5/4) massive, clay/silt texture.
- **Reworked sediment** (Kawakawa Tephra?). Dull yellow orange (10 YR 6/4) bedded, coarse sand texture with few pumice lapilli and titanomagnetite skeins. Abrupt convolute lower boundary.
- **Kawakawa Tephra.**
  Upper 15 cm: Dull yellow orange (10 YR 6/4), massive, clay/silt texture with few pumice lapilli and accretionary lapilli (up to 1 cm). Abrupt irregular lower boundary.
  5 cm: Dull yellow orange (10 YR 7/3) massive, clay/silt texture with sand-sized clasts and Mg concretions. Abrupt smooth lower boundary.
  Lower 5 cm: Dull yellow orange (10 YR 6/4) clast-supported accretionary lapilli (up to 3 mm) bed. Abrupt wavy lower boundary.
- **Loess.**
  Upper 30 cm: Dull yellow orange (10 YR 6/3) massive, clay/silt texture. Diffuse lower boundary.
  20 cm (paleosol): Brown (10 YR 4/6) massive, clay/silt texture, with few pumice clasts from Unit L below. Diffuse lower boundary.
- **Unit L.** Orange (7.5 YR 6/8) pyroclastic texture with lapilli (soft, orange, pumice lapilli approximately 6 mm and black lithics approximately 2 mm) in a clay/silt-sized matrix.

Stratigraphic Log

Site name: **Hamurana Road site**

Date: 2011

Map reference: NZMS260 U15 997 468

Depth (m)	Stratigraphic log	Lithological description

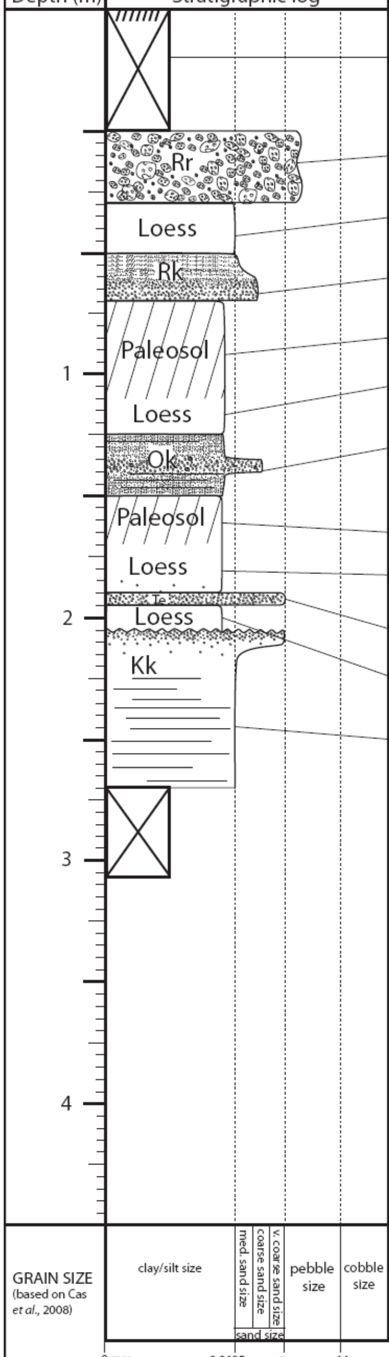

- Post Rotorua material and modern soil (not drawn to scale)
- **Rotorua Tephra.** Bright yellow brown (10YR 6/8) hard sub-rounded orange pebble-sized pumice clasts.
- **Loess.** Bright yellowish brown (2.5Y 7/6) mottled, clay/silt texture. Wavy sharp upper boundary.

Rerewhakaaitu Tephra.
- Lower 10 cm: Bright yellowish brown (10YR 6/8) normally graded sand. Some crystals. Abrupt smooth upper boundary.

Loess.
- **Upper 40 cm:** (paleosol) Olive brown (2.5Y 4/6), clay/silt texture. Abrupt wavy upper boundary.
- **Lower 15 cm:** Bright yellowish brown (2.5Y 6/6), clay/silt texture. Diffuse wavy upper boundary.

- **Okareka tephra.** Light yellow (2.5Y 7/4) clay/silt-sized base (lower 12 cm) and top (upper 10 cm) separated by a coarse sand-sized bed (middle 3 cm). Few orange and white pumice clasts present. Crystal rich. Distinct smooth upper boundary.

Loess.
- **Upper 20cm:** (paleosol) Brown (10YR 4/6), clay/silt texture. Few crystals. Sharp convolute upper boundary.
- **Lower 20 cm:** Yellowish brown (10YR 5/6) mottled, clay/silt texture, white pebble–sized pumice clasts present. Few crystals. Distinct wavy upper boundary.

- **Te Rere Tephra.** Yellowish brown (10YR 5/8), very coarse sand with white pebble-sized pumice clasts present. Crystal rich. Distinct wavy upper boundary.
- **Loess.** Yellowish brown (10YR 5/6) clay/silt texture. Few crystals. Indistinct wavy upper boundary.
- **Kawakawa Tephra.** Dull yellow brown (10YR 6/3) stratified clay/silt-sized base with very coarse sand-sized top (upper 15 cm), showing 'lava lamping'-type deformation/erosion. Many crystals. Mg concretions present. Abrupt irregular upper boundary.

Stratigraphic Log

Site name: Highlands Road site

Date: 2011

Map reference: NZMS 260 U16 011 229

Depth (m) | Stratigraphic log | Lithological description | Sample Number

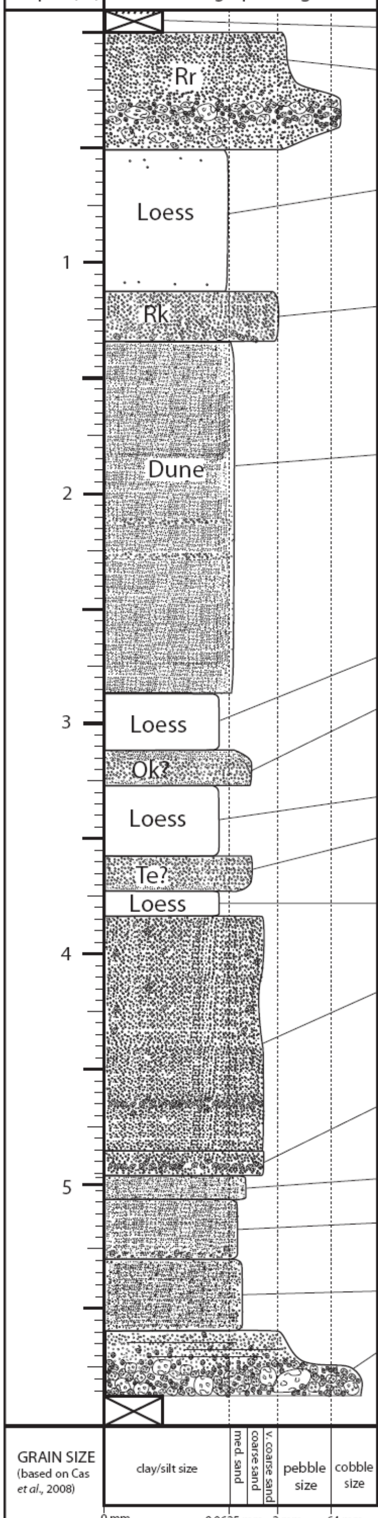

- Post Rotorua material and modern soil (not drawn to scale)
- **Rotorua Tephra.** Bright yellowish brown (10YR 6/8) moderate stratification, upper 30 cm pebble-sized, mid 10 cm pebble-sized and cobble-sized pumice clasts (white/yellow, hard, sub-rounded, up to 30 mm), lower 10 cm sand-sized with cobble-sized clasts. Black, obsidian lithics (up to 12 mm) present in mid 10 cm. Wavy distinct lower boundary.
- **'Loess'.** Yellowish brown (10YR 5/8), massive, clay/silt texture with few white pumice clasts (approx. 3mm) reworked down (approx 200mm) from overlying Rotorua Tephra, also pumice clasts reworked up from underlying Te Rere Tephra. Indistinct smooth lower boundary.
- **Rerewhakaaitu Tephra.** Light yellow (2.5 Y 7/4) vague normal grading, upper 20 cm very coarse sand-sized, lower 2 cm coarse sand-sized with pumice lapilli (white, up to 12 mm). Indistinct smooth lower boundary.
- **Sand dune.**
  Upper 50 cm yellowish brown (10YR 5/6)
  Lower 150 cm (max thickness of dune is 250 cm) Dull yellow (2.5Y 6/4) vague bedding, clay/silt to medium sand texture with coarse ash beds. Sharp convolute lower boundary.
- **'Loess'.** Yellowish brown (10YR 5/6) mottled, clay/silt texture. Indistinct lower boundary over 100 mm
- **Okareka Tephra?**
  Upper approx 10 cm: Dull yellow orange (10YR 6/4) clay/silt texture, Mg concreations, accretionary lapilli present (Looks similar to Kawakawa Tephra).
  Lower approx 5 cm: Light grey (10YR 8/2) coarse sand texture. Sharp lower boundary
- **Loess.** Dull yellowish brown (10YR 5/4) massive, clay/silt texture, indistinct lower boundary
- **Te Rere Tephra?** Top: Dull yellow orange (10YR 6/4), mid: Bright yellowish brown (10YR 7/6), lower: Light yellow orange (10YR 8/4). Upper approx 10 cm: sand texture, lower approx 5 cm: clay/silt texture. Sharp lower boundary.
- **Loess.** Dull yellow brown (10YR 5/4) clay/silt texture with sparse pumice clasts (up to 5 mm). Indistinct lower boundary over 100 mm.
- **Oruanui Ignimbrite?**
  Upper aprrox. 25 cm: pale yellow brown, upper-mid aprrox. 20 cm: pale grey, lower-mid aprrox. 5 cm: dark grey, lower aprrox. 30 cm: light grey . Coarse to very coarse sand texture with pumice concentration zones and pumice clasts (5-80 mm). Abrupt, irregular lower boundary.
- **Oruanui Ignimbrite (?).**
  Dark grey, matrix-supported pumice (up to 50 mm) beds, 20 mm iron pan at top, indistinct lower boundary.
- **Sand (?).** Dark greybrown, massive, medium sand texture, with sparse pumice clasts (up to 5 mm) indistinct lower boundary.
- **Unknown tephra (Awakeri?).** Yellow brown upper, pale grey lower, well stratified unit (clay/silt texture separated by 50 mm thick sand-sized bed), sparse pumice clasts (up to 4 mm). Indistinct lower boundary.
- **Sand(?).** Yellow brown, massive, sand texture, sparse pumice clasts. Inistinct lower boundary.
- **Reworked Earthquake Flat Ignimbrite (fluvial?) sediment.** Pale grey, well bedded at top, poorly bedded lower, sand, pebble and cobble-size clasts, lithics (up to 100 mm) containing biotite and hornblende crystals.

Stratigraphic Log

Site name: **Kaharoa Road site**

Date: 2011

GPS reference: NZMS260 U15 011 543

Depth (m)	Stratigraphic log	Lithological description

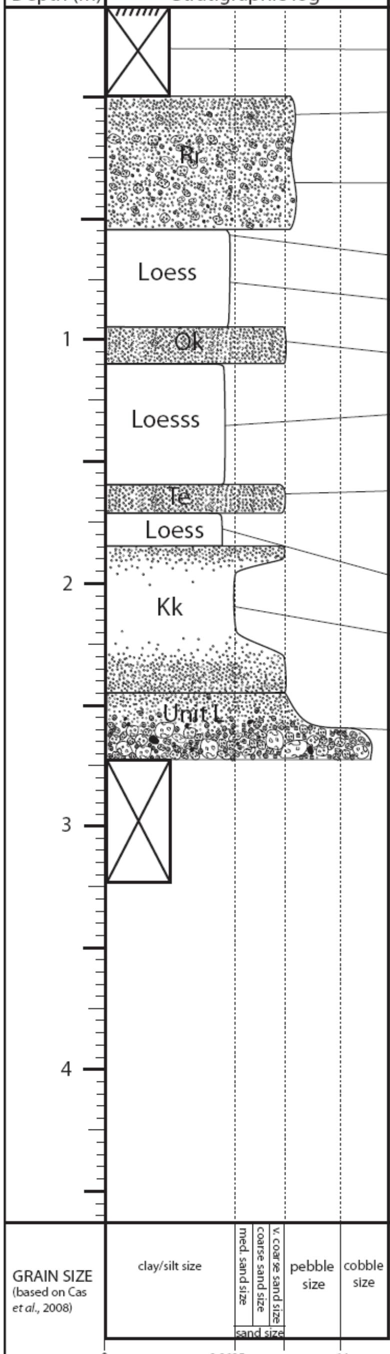

Post Rotorua material and modern soil (*not drawn to scale*)

Rotorua Tephra.
Upper 15 cm: Brown (10YR 4/6) massive, pebble-sized texture with few white, hard, sub-angular pumice lapilli (approx. 3mm). Many crystals. Abrupt smooth upper boundary.
Lower 40 cm:Bright yellowish brown (10YR 6/8) massive, very coarse sand texture with many white pumice lapilli. Few crystals.

Loess.
Upper 5 cm: Bright yellowish brown (10YR 6/6) massive, clay/silt texture with few white pumice (approx. 1mm). Few crystals. Indistinct smooth upper boundary.
Lower 35 cm: Dull yellowish orange (10YR 6/4) massive, clay/silt texture with slight mottling. Few very small crystals. Diffuse smooth upper boundary.

Okareka Tephra. Bright yellowish brown (10YR 6/6) massive, very coarse sand texture. Few crystals. Indisticnt smooth upper boundary.

Loess. Bright yellowish brown (10 YR 6/6) (slightly darker in upper 10 cm) massive, clay/silt texture with very few white, hard pumice lapilli (2-5 mm) in lower 10 cm. Few very small crystals. Diffuse smooth upper boundary.

Te Rere Tephra. Bright yellowish brown (10YR 7/6) very coarse sand texture with matrix-supported lapilli clasts. Many white, hard, rounded pumice clasts (1-6 mm), few black lithic clasts (3-8 mm). Few crystals. Vague inverse grading. Diffuse wavy upper boundary.

Loess. Yellowish brown (10YR 5/6) massive, clay/silt texture with few black crystals (approx. 1 mm). Indistinct wavy upper boundary.

Kawakawa Tephra. Yellowish brown (10YR 5/6) mottled, upper 10 cm and lower 15 cm very coarse sand texture with a 35 cm thick , clay/silt-sized middle bed. Few white pumice lapilli in upper approx. 10 cm, few soft, orange pumice lapilli in lower approx. 20 cm. Few crystals. Indistinct smooth upper boundary.

Unit L. Orange (7.5YR 6/8), Upper 10 cm: paler colour, very coarse sand texture with few lapilli clasts. Lower portion: pebble-textured matrix with clast-supported cobble-sized clasts. Pumice clasts (up to cobble-sized) are soft, weathered to orange on outside, yellowish white inside. Includes hard, black lithic clasts (pebble to cobble-sized). Unit fines upward. Abrupt wavy upper boundary.

Stratigraphic Log

Site name: **Leslie Road site**

Date: 2011

Map reference: NZMS 260 T15 688 453

Depth (m)	Stratigraphic log	Lithological description

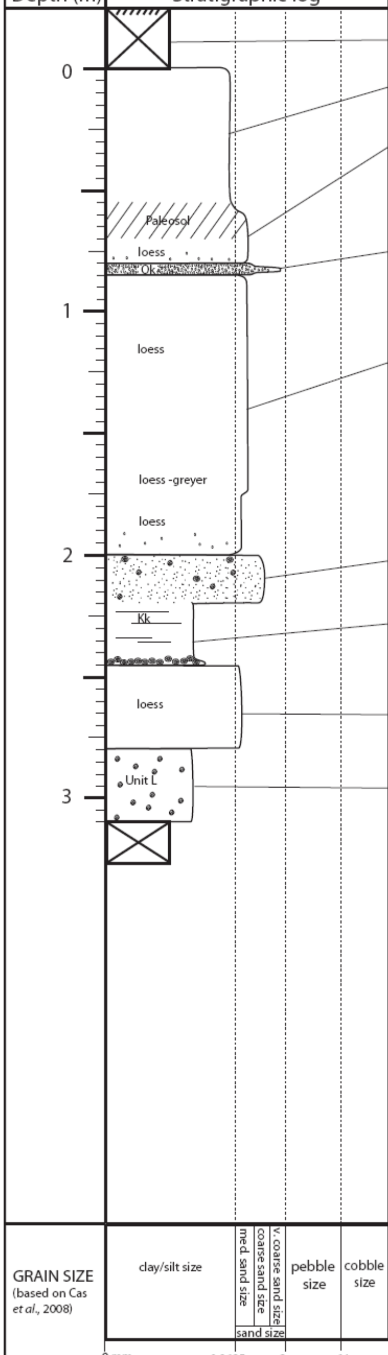

- Post-Ok material and modern soil (not drawn to scale)
- **Post Ok material.** Bright yellowish brown (10 YR 6/8) massive, mottled (greyish yellow brown (10 YR 6/2)), clay/silt texture. Indistinct lower boundary.
- **Loess.**
  Upper 15 cm (enhanced soil development)= Dull yellowish brown (10 YR 5/4) massive, medium sand texture, with many Mg concretions (approx. 1 mm). Indistinct occluded lower boundary.
  Lower 7 cm= Dull yellow orange (10 YR 6/4) massive, medium sand texture, with few white ash-sized (1 mm) pumice. Many root pseudomorphs. Abrupt wavy lower boundary.
- **Okareka Tephra.** Stratified unit, with sharp wavy lower boundary.
  Upper 4 cm= Dull yellow orange (10 YR 7/4) medium sand texture
  Mid 2 cm= Bright yellowish brown (10 YR 6/6) very coarse sand texture
  Lower 2 cm= Light yellow (2.5 Y 7/4) medium sand texture
- **Loess.**
  Upper 80 cm= Dull yellow orange (10 YR 6/4) massive, medium sand texture with many root pseudomorphs, few Mg concretions. Diffuse lower boundary.
  Mid 10 cm= Dull yellow orange (10 YR 7/2) massive, mottled, medium sand texture with few Mg concretions. Diffuse lower boundary.
  Lower 25 cm= Dull yellowish brown (10 YR 5/4) massive, medium sand texture with few white pumice clats (max 8 mm). Root pseudomorphs present and few Mg concretions. Indisitinct occluded lower boundary.

Kawakawa Tephra

- Upper 20 cm (Oruanui Ig?) = Dull yellow orange (10 YR 6/3) massive, coarse sand texture with few pumice lapilli (upper approximately 5 cm), few indistinct accretionary lapilli (approx. 8 mm diameter). Sharp wavy lower boundary.
- Lower 27 cm= Dull yellow orange (10 YR 7/3) weakly stratified, clay/silt texture, with lapilli basal unit (approx. 5 cm thick) composed of accretionary lapilli (approx. 5 mm diameter). Mg concretions present. Sharp smooth lower boundary.
- **Loess.** Dull yellow orange (10 YR 6/3) massive, medium coarse sand with few Mg concretions. Distinct occluded lower boundary.
- **Unit L.** Yellowish brown (10 YR 5/6) massive, clay/silt texture with indistinct creamy coloured pumice up to 1 cm, some iron formation present. Indistinct wavy lower boundary.

Stratigraphic Log

Site name: **Maniatutu Road site**

Date: 2011

Map reference: NZMS 260 U15 078 496

Depth (m)	Stratigraphic log	Lithological description

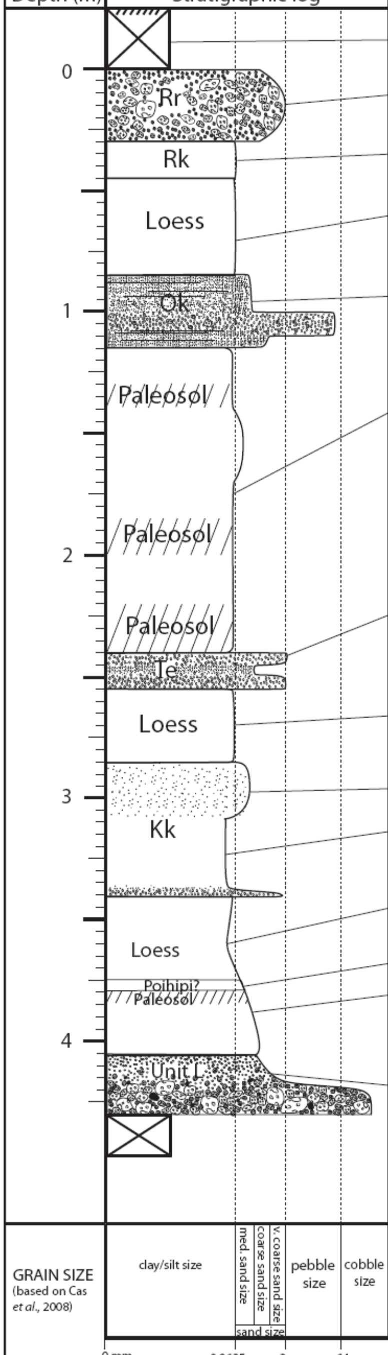

- Post Rotorua material and modern soil (not drawn to scale)

- **Rotorua Tephra.** Bright yellowish orange (2.5 Y 7/6) bedded, pumice clasts up to 3 mm, dark rhyolite lithics up to 2 mm. Indistinct lower boundary.

- **Rerewhakaaitu Tephra (or loess?).** Yellowish brown (10 YR 5/6) massive, clay/silt texture with biotite. Indistinct lower boundary.

- **Loess.** Yellowish brown (10 YR 5/8) massive, clay/silt texture with root pseudomorphs. Diffuse lower boundary.

- **Okareka Tephra.** Light yellow & Bright yellowish brown (2.5 Y 7/4) & (10 YR 7/6) stratified unit (upper 15 cm= medium sand texture, mid 10 cm= sand/pebble texture, lower 5 cm= coarse sand texture with pumice clasts up to 3 mm and dark rhyolite. Occluded smooth lower boundary.

Loess.
Upper 15 cm= Dull yellow orange (10 YR 6/4) massive, clay/silt texture. Indistinct lower boundary.
- 10 cm= (paleosol) bright yellowish brown (10 YR 6/6) massive, clay/silt texture. Diffuse lower boundary.
30 cm = Bright yellowish brown (10 YR 6/6) massive, clay/silt texture. Very diffuse lower boundary.
15 cm = Dull yellow orange (10 YR 6/4) massive, firm, clay/silt texture. Very diffuse lower boundary.
15 cm = (paleosol) Bright yellowish brown (10 YR 6/6) massive, clay/silt texture. Very diffuse lower boundary.
20 cm = dull yellow orange (10 YR 6/4) massive, soft, clay/silt texture. Diffuse lower boundary.
Lower 20 cm = (paleosol) Bright yellosish brown (10 YR 6/6) massive, clay/silt texture. Distinct lower boundary.

- **Te Rere Tephra.** Bedded unit with low vesicularity pumice, black lithics up to 4 cm. Occluded abrupt lower boundary.
Upper 7 cm = Bright yellowish brown (10 YR 7/6) very coarse sand texture and lapilli
Mid 6 cm = Dull yellow, coarse sand texture
Lower 2 cm = Light yellow orange, very coarse sand texture

- **Loess.** Yellowish brown (10 YR 5/8) massive, clay/silt texture, unit is of irregular thickness. Occluded lower boundary.

Kawakawa Tephra
- Upper 25 cm = Greyish yellow brown (10 YR 6/2) & … (10 YR 6/6) massive, mottled, medium sand texture. Abrupt irregular lower boundary.
- Lower 30 cm = Dull yellow orange (10 YR 6/4) clay/silt texture with basal layer of very coarse sand sized clasts (3 cm thick), vague stratification and small scale mottling, possible accretionary lapilli (approximately 4 mm). Sharp smooth lower boundary.

- **Loess.**
Upper 35 cm = Dull yellow orange (10 YR 7/3) massive, clay/silt texture with leisegang banding in upper 10 cm. Indistinct lower boundary.
- **Poihipi Tephra?**
- **Loess.**
Upper 5 cm = (paleosol) = Dull yellowish brown (10 YR 5/4) massive, mottled, clay/silt texture with few pumice clats (up to 2 mm). Unit of irregular thickness. Wavy diffuse lower boundary.
Lower 20 cm = Dull yellow orange (10 YR 6/4) massive, coarse sand texture with few pumice lapilli. Diffuse lower boundary.
- **Unit L**
Upper 15 cm Dull yellow orange (10 YR 7/4) massive, medium sand texture with dull orange/yellow pumice clasts (up to 10 mm). Indistinct lower boundary.
Lower (at least) 10 cm = yellow orange (10 YR 7/8) massive unit with soft white cobble-sized pumice (up to 2.5 cm) within a medium sand-sized matrix (pyroclastic texture).

Stratigraphic Log

Site name: **Oturoa Road site** Date: 2011

Map reference: NZMS 260 U15 893 462

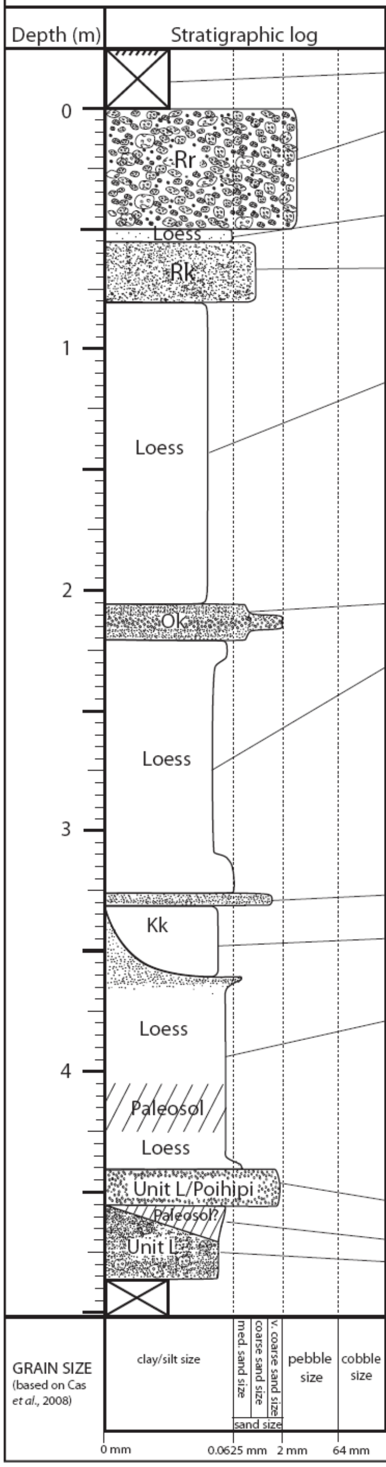

Lithological description

- Post Rotorua material and modern soil (not drawn to scale)
- **Rotorua Tephra.** Yellow orange (10 YR 7/8), massive lapilli unit with orange (when weathered) hard, sub-angular pumice lapilli (3-5 mm) and black lithics (approximately 2 mm). Abrupt smooth lower boundary.
- **Loess.** Brown (10 YR 4/6) massive, clay/silt texture with few pumice lapilli. Indistinct wavy lower boundary.
- **Rerewhakaaitu Tephra.**
  Upper 5 cm = Dull yellow orange (10 YR 6/3) massive, coarse sand texture. Indistinct convolute lower boundary.
  Lower 20 cm = Bright yellowish brown (10 YR 6/3) massive , coarse sand texture with rare white pumice lapilli. Diffuse wavy lower boundary.
- **Loess.**
  Upper 15 cm = Dull yellowish brown (10 YR 5/4), massive, clay/silt texture. Diffuse wavy lower boundary.
  20 cm = Yellowish brown (10 YR 5/6), massive clay/silt texture. Diffuse wavy lower boundary.
  20 cm = Dull yellowish brown (10 YR 5/4), massive clay/silt texture. Diffuse lower boundary.
  20 cm = Dull yellowish brown (10 YR 5/4) matrix with brown (10 YR 4/4) mottles, massive, clay/silt texture Diffuse lower boundary.
  15 cm = Dull yellowish brown (10 YR 5/4), massive, clay/silt texture. Diffuse lower boundary.
  20 cm = Yellowish brown (10 YR 5/6), massive, clay/silt texture. Diffuse lower boundary.
  15 cm = Dull yellowish brown (10 YR 5/4), massive, mottled, clay/silt texture. Diffuse lower boundary.
- **Okareka Tephra.** Dull yellow orange (2.5 Y 6/4), stratified unit with rare pumice lapilli. Occluded wavy lower boundary.
- **Loess.**
  Upper 10 cm = Dull yellow orange (10 YR 6/4), massive, mottledclay/silt texture.
  30 cm = Dull yellow orange (10 YR 6/4), massive, clay/silt texture. Very diffuse lower boundary.
  20 cm = Dull yellow orange (10 YR 6/3), massive, clay/silt texture. Diffuse lower boundary.
  10 cm = Yellowish brown (10 YR 5/6), massive, clay/silt texture. Very diffuse lower boundary.
  20 cm = Dull yellow orange (10 YR 6/3), massive, clay/silt texture. Convolute lower boundary.
  15 cm = yellowish brown (10 YR 5/6), massive, clay/silt texture. Very irregular lower boundary.

Kawakawa Tephra.

- Upper 5 cm = Dull yellow orange (10 YR 5/3), massive, mottled?, coarse sand texture with few pumice lapilli (up to 5 mm). Abrupt very irregular lower boundary.
- Lower 30 cm = Dull yellow orange (10 YR 6/4) & (10 YR 7/3), discontinuous, vaguely stratified, clay/silt texture with Mg concretions. Abrupt smooth lower boundary.

Loess.

- Upper 5 cm = Dull yellowish brown (10 YR 5/4), massive, medium sand texture, with few reworked orange pumice clasts (up to 5 mm). Indistinct lower boundary.
  40 cm = Dull yellow orange (10 YR 6/4), massive, clay/silt texture. Diffuse lower boundary.
  20 cm = (Paleosol) Dull yellowish brown (10 YR 5/4), massive, soft, clay/silt texture. Diffuse lower boundary.
  15 cm = Yellowish brown (10 YR 5/6), massive, mottled, clay/silt texture. Indistinct lower boundary

Unit L

- Upper 15 cm (Poihipi Tephra?) Dull yellow orange (10 YR 6/4) of very coarse sand texture with orange pumice clasts (up to 15 mm).
- Possible paleosol wedge
- Lower (at least) 30 cm = Bright yellowish brown (10 YR 6/8)(variable colour), pyroclastic unit with clay/silt-sized matrix and soft, orange pumice lapilli (up to 20 mm).

Stratigraphic Log

Site name: **Penny Road site**

Date: 2011

Map reference: NZMS260 U15 966 498

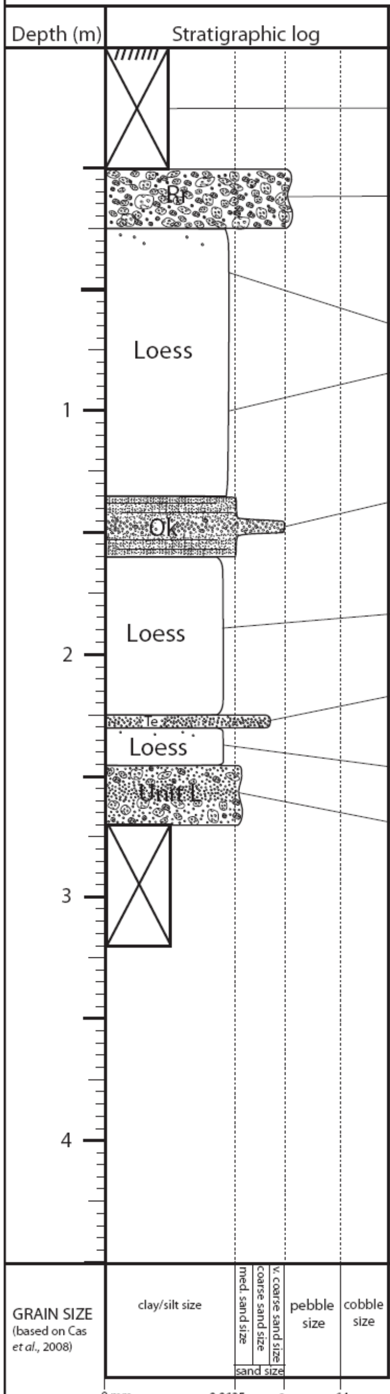

Lithological description

- Post Rotorua material and modern soil (not drawn to scale)
- **Rotorua Tephra.** Yellow orange (10YR 7/8) massive, clast-supported pumice lapilli (3-10 mm, hard, sub-rounded, weathered orange on outside, white inside), unit appears faulted/disrupted.

'Loess'.

- **Upper 35 cm:** Yellowish brown (2.5Y 5/6) massive, clay/silt-sized with soft, orange pumice lapilli in upper 10 cm. Distinct wavy upper boundary.
- **Lower 75 cm:** Dull yellow orange (10YR 6/4) massive, clay/silt texture.
- **Okareka Tephra.** Light yellow (2.5Y 7/4) stratified unit, upper 10 cm clay/silt-sized, mid 3 cm very coarse sand-sized, lower 12 cm bedded clay/silt and sand. Few crystals. Abrupt wavy upper boundary.
- **Loess.** Dull yellow orange (10YR 6/4) massive, clay/silt-sized, mottled in lower portion. Few crystals. Sharp occluded upper boundary**.**
- **Te Rere Tephra:** Bright yellowish brown (10YR 6/6,) vague reverse grading, coarse sand-sized matrix with white, sub-rounded pumice lapilli (1-5mm) and black lithic clasts (1 & 5 mm). Indistinct smooth upper boundary.
- **Loess:** Yellowish brown (10YR 5/8) massive, clay/silt-sized with few black (approx 1 mm) clasts. Distinct wavy upper boundary.
- **Unit L (reworked-fluvial?):**
Matrix-supported soft, orange pumice lapilli (2-5 mm) in bedded sand matrix. Many crystals. Distinct wavy upper boundary.

Note: Kk was observed further a long the road from the site of this stratigraphic column

Stratigraphic Log

Site name: **Tapapa Road site**

Date: 2011

Map reference: NZMS260 T15 524 634

Depth (m) | Stratigraphic log | Lithological description

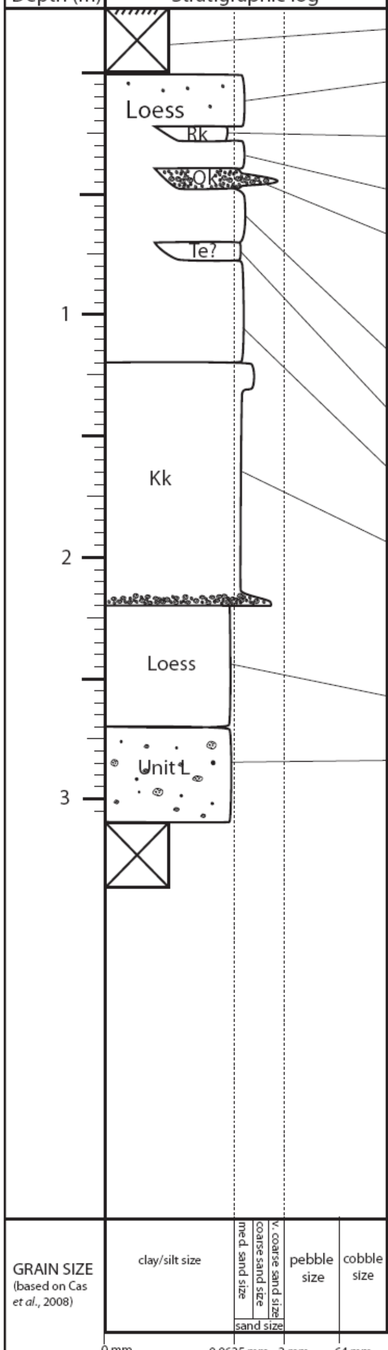

- Rotorua tephra material, post-Rotorua tephra material and modern soil (not drawn to scale)
- **Loess.** Yellowish brown (10 YR 5/6) massive, medium sand-sized with few white pumice (up to 3 mm). Distinct lower boundary where Rerewharkaitu Tephra is present
- **Rerewhakaitu Tephra within loess (?).** Dull yellow orange (10 YR 6/3) discontinuous, massive, clay/silt-sized. Distinct lower boundary where Rerewharkaitu tephra is present.
- **Loess.** Yellowish brown (10 YR 5/6) massive, medium sand-sized. Abrupt wavy lower boundary.
- **Okareka Tephra.** Discontinuous, stratified unit with pumice up to 2mm. Sharp irregular lower boundary.
  Upper: Light yellow (2.5 Y 7/3) medium sand-sized
  Mid: Bright yellowish brown (10 YR 6/8) very coarse sand-sized
  Lower: Light yellow (2.5 Y 7/3) medium sand-sized
- **Loess.** Dull yellow orange (10 YR 6/4) massive, mottled, medium sand-sized. Distinct lower boundary where Te Rere tephra is present.
- **Te Rere Tephra (?).** Greyish yellow brown (10 YR 6/2) massive, medium sand-sized, some iron staining. Indistinct wavy lower boundary where Te Rere Tephra is present.
- **Loess.** Dull yellowish brown (10 YR 5/4) massive, mottled (Dull yellow orange (10 YR 6/4)), medium sand-sized. Distinct occluded lower boundary.
- **Kawakawa Tephra.**
  Upper 10 cm (Oruanui Ig?) = Dull yellow orange (10 YR 6/4) massive, medium sand-sized. Distinct irregular lower boundary.
  Lower 90 cm = dull yellow orange (10 YR 7/3) pyroclastic texture, medium sand-sized with coarse-very corase sand-sized basal unit (approximately 5 cm thick). Sharp smooth lower boundary.
- **Loess.** Gradational dull yellow orange (10 YR 6/3)-dull yellowish brown (10 YR 5/4) massive with some vertical structures, clay/silt-sized. Very diffuse lower boundary.
- **Unit L.** Dull yellow orange (10 YR 6/4) pyroclastic texture, clay/silt-sized matrix with orange/white pumice clasts (up to 4mm) and black lithics (?) (up to 2 mm).

Stratigraphic Log

Site name: **Taumata Road site** Date: 2011

Map reference: NZMS260 U15 842 635

Depth (m) | Stratigraphic log | Lithological description

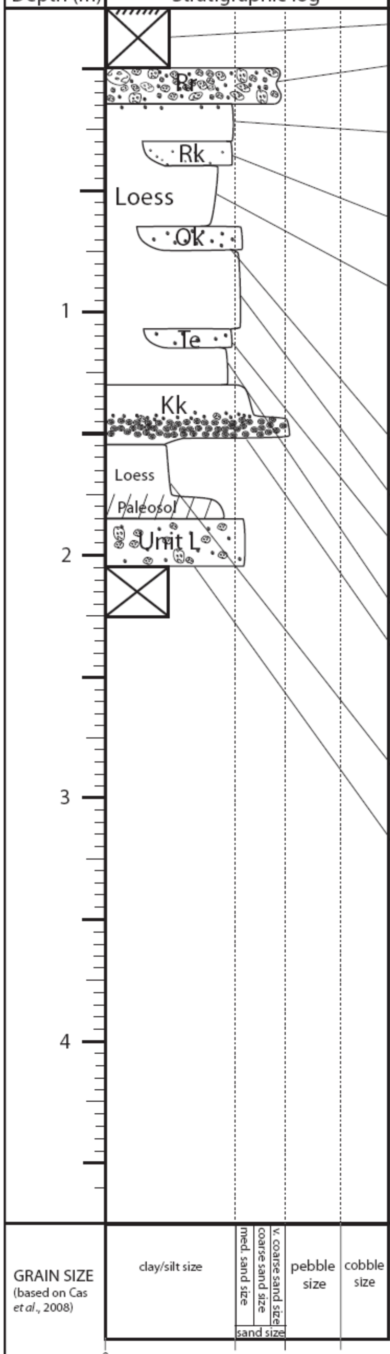

- Post Rotorua material and modern soil (not drawn to scale)
- **Rotorua Tephra.** Bright Yellowish Brown (10 YR 6/8), massive, very coarse sand-sized with few fine lapilli (orange, sub-angular pumice clasts up to 3 mm and lithics up to 2.5 mm). Diffuse convolute lower boundary.
- **Loess.**
  Upper 5 cm = Yellowish Brown (10 YR 5/8), massive, medium sand-sized with some very coarse sand to pebble-sized clasts (pumice clasts up to 2 mm). Diffuse wavy boundary.
  Lower = 10 cm = Yellowish Brown (10 YR 5/6), massive, clay/silt-sized. Diffuse lower boundary.
- **Rerewhakaaitu Tephra (+ loess).**
  Dull yellow orange (10 YR 6/3) (Loess- yellowish brown (10 YR 5/8)), discontinuous, massive, clay/silt-sized. Diffuse lower boundary.
- **Loess.**
  Upper 5 cm: Yellowish brown (10 YR 5/8) massive, clay/silt-sized. Diffuse convolute lower boundary.
  2 cm = Mottled (reddish brown (5 YR 4/8) & dull yellow orange (10 YR 7/3) clay/silt-sized. Convolute lower boundary.
  5 cm: Yellowish brown (10 YR 5/8) massive, clay/silt-sized. Diffuse lower boundary.
  8 cm: Bright yellowish brown (10 YR 6/8) massive, clay/silt-sized. Occluded lower boundary.
- **Okareka Tephra.** Dull yellow orange (10 YR 7/4), discontinuous, massive, medium sand-sized. Occluded lower boundary.
- **Loess.** Mottled (Dull yellow orange (10 YR 6/4) & Dull yellow orange (10 YR 7/2), sand-sized.
- **Te Rere Tephra (+ loess).** Dull yellow orange (10 YR 7/2) (Loess-bright yellowish brown (10 YR 6/8)), massive clay/silt-sized. Occluded lower boundary.
- **Loess.** Yellowish brown (10 YR 5/6) massive, clay/silt-sized. Diffuse lower boundary.
- **Kawakawa Tephra.** Bedded unit of variable thickness.
  Upper 15 cm: Dull yellow orange (10 YR 7/3) medium sand-sized with pumice lapilli (up to 3 mm)
  2 cm: Yellowish brown (10 YR 5/6) very coarse sand to pebble-sized with pumice lapilli (up to 3 mm)
  5 cm: discontinuous, clast-supported accretionary lapilli (up to 4 mm) bed
  3 cm: Dull yellow orange (10 YR 7/3) discontinuous, massive, clay/silt-sized
- **Loess.**
  Upper 22 cm: Dull yellowish brown (10 YR 5/3) clay/silt-sized. Convulute lower boundary.
  Lower 10 cm (paleosol?): Brown (10 YR 4/6) massive, clay/silt-sized.
- **Unit L.** Dull yellow orange (10 YR 6/4) pyroclastic texture with lapilli (soft, orange pumice lapilli up to 1 cm and dark rhyolite lithics up to 3 cm) in medium sand-sized matrix.

Appendix 3 – Phytolith extraction and identification method

Phytolith Extraction Method

(Pers. comm., J.A. Carter, 2011)

This method of phytolith extraction is similar to methods described by Piperno (1988) and Hart (1988).

1) Initial removal of organics by immersion in 27% hydrogen peroxide and heating in a water bath until all visible reaction had ceased.

2) Hydrogen peroxide removal by centrifuging at 5000 rpm for 10 minutes. The supernatant is poured off the sample re- agitated and the procedure repeated three times.

3) Separation of the < 250 micron fraction by wet sieving using a bolting cloth sieve.

4) The disaggregation of phytoliths from the organic and clay complexes is achieved by ultrasonic treatment. A Virsonic Digital 600 is used on the following settings: output control =7; % duty cycle = 70%; time = 5 minutes.

5) Clay sized particles below 5 micron are removed by agitating the sample in 500 ml of distilled water and allowing settling for one hour. The supernatant is carefully poured off and the procedure is repeated until there is no obvious material in the supernatant.

6) Any remnant organic material is removed by digestion using "Schulzes Solution". 50 ml potassium chlorate is added to 250 ml of Nitric Acid to make this highly corrosive cocktail. About 30 ml of the solution is added to the test tubes containing the sample and digestion carried out in a water bath (80°C) in a fume cupboard. Distilled

water is added to the sample and this is centrifuged for 5 minutes at 5000 rpm. This procedure is repeated three times to clean the sample of any remaining solution.

7) The phytoliths are then extracted from the sample. This is achieved using the density contrast between the phytoliths (<2.3) and clastic material (>2.3), which allows the two fractions to be separated using a heavy liquid. A mixture of sodium polytungstate and distilled water is mixed in appropriate proportions to give a liquid with a specific density of 2.3. The heavy liquid is then added to test tubes containing the samples and agitated. These are then centrifuged for 15 minutes at 2000 rpm. The light fraction (containing the phytoliths) is pipetted off into clean test tubes and distilled water added to reduce the density of the liquid.

8) These are centrifuged at 5000 rpm for 5 minutes, the supernatant poured off and the process repeated five times.

9) Test tubes are re-filled with distilled water and re-agitated. A small sample from the top of the supernatant is then pipetted onto a microscope coverslip, allowed to dry and then glued to a microscope slide.
(*Note: sample may need to be diluted with distilled water if the sample contains excessive amounts of phytoliths*)

Phytolith Identification and Counting Method

1) Phytolith slides are analysed using non-polarising binocular microscopes.

2) Aprroximatly 300 phytoliths per slide are identified and counted.

Appendix 4 – Results from δ13C and δ15N analysis

SAMPLE	ug N/55mg	Delta 15N	ugC/55mg	Delta 13C
D1	12	3.08	236	-25.67
D4	17	5.68	338	-25.06
D5	18	6.07	370	-24.73
D6	20	5.41	405	-24.70
D7	19	5.81	423	-24.68
D8	16	6.30	346	-24.56
D9	14	6.15	277	-24.69
D10	15	6.30	304	-24.55
D11	13	6.29	257	-24.68
D12	13	6.54	264	-24.47
D13	13	6.03	218	-24.39
D14	13	6.94	250	-24.47
D15	12	6.53	239	-24.25
D16	13	9.07	263	-24.18
D17	14	5.93	285	-24.25
D18	12	7.57	202	-23.76
D19	11	5.87	175	-23.80
D20	9	6.75	142	-23.69
D21	9	7.27	144	-23.41
D22	11	6.03	166	-23.41
D23	8	6.86	118	-22.80
D24	8	4.78	122	-23.30
D25	7	16.56	97	-23.71
D26	6	13.01	80	-22.95
D27	6	11.06	81	-23.05
D28	6	5.68	93	-23.18
D33	9	3.43	155	-24.95
D34	6	5.03	98	-23.62
D35	6	5.01	86	-23.81
D36	6	6.82	88	-23.84
D37	6	6.53	81	-23.61
D38	7	7.36	99	-24.28
D39	7	5.86	97	-24.06
D40	7	5.64	108	-23.65
D41	8	5.78	110	-23.34
D42	8	12.65	107	-23.36
D43	7	8.27	106	-23.22
D44	9	5.92	114	-23.25
D45	8	12.84	103	-23.46
D46	8	6.51	100	-23.05
D47	9	13.29	104	-23.18
D48	8	4.92	109	-24.07
D49	8	5.39	91	-23.23

D50	7	6.04	84	-23.23
D51	9	6.02	96	-23.20
D52	9	4.30	112	-23.69
D53	10	6.17	108	-23.24
D54	9	5.99	110	-23.25
D55	10	5.15	130	-24.06
D56	12	4.30	152	-24.20
D57	9	4.46	120	-23.62
D58	9	3.31	105	-23.19
D59	8	2.86	105	-23.50
D60	10	3.33	129	-23.44
D61	11	3.85	128	-23.05
D62	11	28.79	133	-23.19
D63	14	4.04	183	-23.48
D64	14	5.29	180	-23.46
D65	13	3.57	172	-22.96
D66	12	3.24	147	-22.79
D67	11	5.33	162	-22.69
D68	8	2.58	115	-23.16
D73	9	5.13	113	-24.21
D74	8	5.12	110	-24.57
D75	7	4.55	104	-24.72
D76	8	4.57	112	-24.60
D77	7	4.88	120	-24.97
D78	8	11.39	134	-24.67
D79	8	4.37	138	-24.69
D80	7	4.51	129	-24.69
D81	8	4.07	135	-24.56
optimum level of nitrogen for δ15N analysis is between 100-300ug				
optimum level of carbon for δ13C analysis is between 800-1500ug				

Appendix 5 – Results from XRF major element analysis

Major element concentrations through loess column (between Unit L Tephra and Rorotrua Tephra) at Dansey Rd site, Rotorua

Element	Na2O	MgO	Al2O3	SiO2	P2O5	K2O	CaO	TiO2	MnO	Fe2O3	Approx age (yrs)
Dimension	wt %	wt %	wt %	wt %	wt %	wt %	wt %	wt %	wt %	wt %	
BHVO-2 Standard	2.22	7.23	13.5	49.9	0.27	0.52	11.4	2.73		12.3	
BHVO-2 16/8/11	3.00	6.83	15.77	51.92	0.25	0.53	11.28	2.76	0.18	12.92	
BHVO-2 17/8/11	3.22	6.75	15.66	51.44	0.25	0.53	11.16	2.74	0.18	12.88	
BHVO-2 18/8/11	3.23	6.81	15.83	51.85	0.25	0.53	11.23	2.76	0.18	12.91	
BHVO-2 22/8/11	3.25	6.88	15.66	51.54	0.25	0.53	11.12	2.73	0.18	12.72	
D1	3.16	0.19	12.58	80.07	0.06	2.27	0.84	0.24	0.05	1.96	15,557
D4A	3.49	0.17	15.52	76.12	0.07	2.50	0.71	0.27	0.04	2.49	17,599
D5A	3.65	0.15	16.76	77.42	0.07	2.69	0.56	0.27	0.04	2.70	17,769
D6B	3.35	0.13	18.69	74.63	0.08	2.64	0.52	0.25	0.03	2.71	17,939
D7A	3.25	0.12	18.56	73.65	0.08	2.67	0.49	0.25	0.03	2.65	18,109
D8	3.35	0.11	18.22	76.88	0.07	2.79	0.53	0.25	0.03	2.44	18,279
D9	3.50	0.12	16.86	79.49	0.07	2.95	0.53	0.24	0.03	2.45	18,449
D10	3.22	0.13	17.15	77.01	0.06	2.90	0.52	0.24	0.03	2.44	18,619
D11	3.20	0.13	16.74	77.39	0.05	2.96	0.52	0.23	0.03	2.30	18,789
D12	3.30	0.12	16.57	79.11	0.07	2.99	0.53	0.22	0.03	2.16	18,959
D13	3.42	0.15	15.61	79.67	0.06	3.02	0.53	0.23	0.03	2.44	19,129
D14	3.22	0.14	17.31	78.28	0.07	2.93	0.54	0.23	0.03	2.42	19,299
D15	3.26	0.14	18.25	77.12	0.07	2.90	0.56	0.22	0.04	2.31	19,469
D16	3.28	0.15	19.11	76.39	0.08	2.88	0.59	0.23	0.03	2.36	19,639
D17	3.18	0.15	19.31	75.34	0.08	2.83	0.60	0.22	0.04	2.34	19,809
D18	3.33	0.17	18.78	76.30	0.08	2.90	0.61	0.22	0.05	2.32	19,979
D19	3.45	0.19	18.09	77.81	0.07	2.98	0.63	0.22	0.05	2.25	20,149
D20	3.38	0.18	17.27	76.89	0.06	2.99	0.67	0.22	0.04	2.32	20,319
D21	3.13	0.18	18.35	75.91	0.07	2.91	0.68	0.23	0.06	2.46	20,490
D22	3.32	0.19	19.01	75.79	0.07	2.88	0.68	0.26	0.07	2.61	20,660
D23	2.89	0.23	19.43	74.43	0.08	2.81	0.75	0.28	0.06	2.78	20,830
D24	3.18	0.24	19.64	74.34	0.08	2.79	0.77	0.29	0.06	2.87	21,000
D25	3.42	0.25	18.99	75.76	0.07	2.84	0.78	0.27	0.06	2.74	21,170
D26	3.49	0.22	17.61	77.52	0.07	2.95	0.79	0.24	0.05	2.38	21,340
D27	3.43	0.28	17.82	76.30	0.07	2.87	0.90	0.24	0.05	2.30	21,510
D28	3.41	0.32	18.34	71.49	0.07	2.70	1.17	0.25	0.08	2.11	21,680
D33	3.69	0.32	17.64	75.69	0.07	2.89	0.94	0.25	0.09	2.50	21,850
D34	3.48	0.25	18.68	75.70	0.07	2.85	0.81	0.26	0.05	2.55	21,950
D35	3.67	0.22	18.08	76.62	0.06	2.90	0.74	0.25	0.05	2.49	22,050
D36	3.72	0.19	17.91	77.57	0.07	2.95	0.71	0.25	0.05	2.47	22,150

D37	3.74	0.22	17.42	78.27	0.07	2.97	0.73	0.24	0.06	2.43	22,250
D38	3.85	0.16	17.68	78.14	0.07	2.98	0.71	0.24	0.05	2.44	22,350
D39	3.76	0.16	18.47	77.76	0.07	2.95	0.72	0.24	0.04	2.43	22,450
D40	3.66	0.19	18.39	77.51	0.07	2.95	0.71	0.25	0.04	2.45	22,549
D41	3.47	0.20	18.94	76.70	0.08	2.91	0.68	0.24	0.04	2.47	22,649
D42	3.70	0.20	19.57	76.46	0.08	2.84	0.69	0.24	0.05	2.46	22,749
D43	3.63	0.20	19.90	75.28	0.08	2.80	0.70	0.24	0.04	2.47	22,849
D44	2.92	0.19	19.10	74.95	0.07	2.83	0.72	0.24	0.05	2.48	22,949
D45	2.99	0.22	18.89	74.84	0.06	2.83	0.71	0.25	0.07	2.51	22,949
D46	3.04	0.22	18.57	75.19	0.06	2.86	0.71	0.25	0.06	2.50	23,049
D47	3.05	0.24	18.46	75.35	0.06	2.86	0.71	0.24	0.05	2.46	23,149
D48	3.09	0.23	18.33	75.76	0.06	2.89	0.71	0.25	0.04	2.49	23,249
D49	3.11	0.24	18.44	76.30	0.06	2.88	0.71	0.25	0.04	2.53	23,349
D50	3.07	0.23	18.53	75.85	0.06	2.86	0.71	0.26	0.04	2.56	23,449
D51	3.06	0.23	18.92	76.08	0.06	2.84	0.71	0.26	0.04	2.59	23,549
D52	3.08	0.21	18.93	74.92	0.06	2.79	0.71	0.26	0.04	2.59	23,649
D53	3.02	0.23	19.34	74.51	0.06	2.76	0.71	0.25	0.04	2.53	23,748
D54	2.86	0.23	19.52	74.18	0.06	2.73	0.73	0.25	0.04	2.49	23,848
D55	2.88	0.22	19.62	73.75	0.05	2.68	0.75	0.26	0.04	2.52	23,948
D56	2.86	0.24	19.92	73.80	0.05	2.66	0.74	0.25	0.04	2.55	24,048
D57	2.93	0.28	20.28	73.65	0.07	2.59	0.78	0.27	0.04	2.59	24,148
D58	2.97	0.27	20.78	72.48	0.07	2.51	0.82	0.26	0.05	2.61	24,248
D59	2.79	0.30	20.83	72.14	0.07	2.50	0.82	0.28	0.05	2.71	24,348
D60	2.78	0.29	21.39	71.54	0.08	2.47	0.81	0.28	0.05	2.79	24,448
D61	2.79	0.38	21.32	70.94	0.08	2.48	0.84	0.29	0.05	2.86	24,548
D62	2.83	0.39	21.12	71.25	0.08	2.48	0.86	0.28	0.06	2.81	24,648
D63	2.54	0.32	20.71	70.25	0.08	2.47	0.85	0.28	0.09	2.78	24,748
D64	2.56	0.36	20.37	69.27	0.08	2.44	0.86	0.28	0.08	2.79	24,848
D65	2.62	0.37	20.43	70.32	0.08	2.47	0.92	0.28	0.08	2.78	24,947
D66	2.51	0.46	20.52	69.85	0.07	2.38	0.99	0.28	0.07	2.81	25,047
D67	2.70	0.56	20.41	69.86	0.07	2.33	1.17	0.28	0.07	2.89	25,147
D68	2.80	0.66	19.38	70.08	0.07	2.38	1.34	0.31	0.07	3.03	25,247
D73	2.36	0.28	24.02	70.46	0.07	2.27	0.66	0.33	0.10	3.16	25,447
D74	2.50	0.25	22.34	72.42	0.07	2.47	0.58	0.34	0.06	3.20	26,253
D75	2.67	0.24	22.12	73.11	0.07	2.46	0.57	0.34	0.05	3.23	27,059
D76	2.67	0.17	22.02	72.60	0.07	2.44	0.59	0.35	0.04	3.21	27,865
D77	2.65	0.18	22.17	73.03	0.07	2.45	0.61	0.36	0.04	3.25	28,671
D78	2.66	0.20	22.16	72.13	0.07	2.41	0.64	0.39	0.05	3.53	29,476
D79	2.83	0.23	22.61	71.28	0.07	2.30	0.67	0.43	0.04	3.85	30,282
D80	2.70	0.27	23.81	69.54	0.07	2.08	0.78	0.48	0.05	4.36	31,088
D81	2.63	0.24	25.10	68.26	0.07	1.82	0.99	0.51	0.05	4.39	31,894